1A-SUB--94-60

Accelerator System Model (ASM) User Manual with Physics and Engineering Model Documentation

ASM Version 1.0

July 1993

MASTER

ASM Version 1.0 is a joint project of

G. H. Gillespie Associates, Inc. P.O. Box 2961 Del Mar, CA 92014

Attn: George H. Gillespie

and

The Accelerator Technology Division of the Los Alamos National Laboratory P. O. Box 1663 Los Alamos, NM 87545

Attn: Robert A. Jameson M/S H811

This documentation has been prepared by G. H. Gillespie Associates, Inc. as part of the work completed under Subcontract/Contract Numbers 9-XV3-4570E-1/W-7405-ENG-36

DISTRIBUTION OF THIS DOCUMENT IS UNLIMITED

1

Table of Contents

Chapter and Subject	Page
1. Introduction	3
ASM Overview	4
Accelerator Model Summary	4
2. Getting Started	6
Installing ASM	7
The ASM Application Screen	7
Building a Model and Inputting Parameters	8
Running ASM	11
3. ASM Interface Description, Definitions and Functions	12
The Menu Bar	13
The Palette Bar	16
The Document Window	17
- Global Parameter Pane	18
- Model Space Pane	18
- Work Space Pane	21
Piece Windows and Data Tables	23
Data Structures and Data Flow	25
4. ASM Commands and Output	28
The Commands Menu	29
ASM Output	29
Test Vector Use	31
5. User Preferences and Scaling	33
The Preferences Menu	34
ASM User Options	36
Use of Scaling Options	37
6. Analysis Tools	38
Beam and Engineering Vector Graphs	39
Output Correlation	40
Parameter Variation	41
7. Customizing ASM	42
Appendix: ASM Physics and Engineering Model Descriptions	46

DISCLAIMER

Portions of this document may be illegible in electronic image products. Images are produced from the best available original document.

1. Introduction

The Accelerator System Model (ASM) is a computer program developed to model proton radiofrequency accelerators and to carry out system level trade studies. The ASM FORTRAN subroutines are incorporated into an intuitive graphical user interface which provides for the "construction" of the accelerator in a window on the computer screen. The interface is based on the Shell for Particle Accelerator Related Codes (SPARC) software technology written for the Macintosh operating system in the C programming language. This User Manual describes the operation and use of the ASM application within the SPARC interface. The Appendix provides a detailed description of the physics and engineering models used in ASM. ASM Version 1.0 is joint project of G. H. Gillespie Associates, Inc. and the Accelerator Technology (AT) Division of the Los Alamos National Laboratory. Neither the ASM Version 1.0 software nor this ASM Documentation may be reproduced without the expressed written consent of both the Los Alamos National Laboratory and G. H. Gillespie Associates, Inc.

ASM Overview

The Accelerator System Model (ASM) is a computer program for developing designs, at the conceptual level, for ion radiofrequency linear accelerators (RF linacs). The computer model consists of two basic parts: (1) the graphical user interface (GUI) and (2) the mathematical accelerator models. The user primarily interacts with ASM through the GUI and Sections 2-6 of this User Manual describe the use of the ASM GUI. accelerator models used in ASM are described in the Appendix to the ASM User Manual. The algorithms used for the mathematical accelerator model are written in FORTRAN and users may modify the source code, recompile using a third party compiler and relink with the GUI object code. This allows the user to add his own accelerator modeling algorithms and develop a custom version of ASM. A brief description of how to create a custom ASM is given in Section 7 of this User Manual. The remainder of this introduction provides a brief description of the ASM accelerator model.

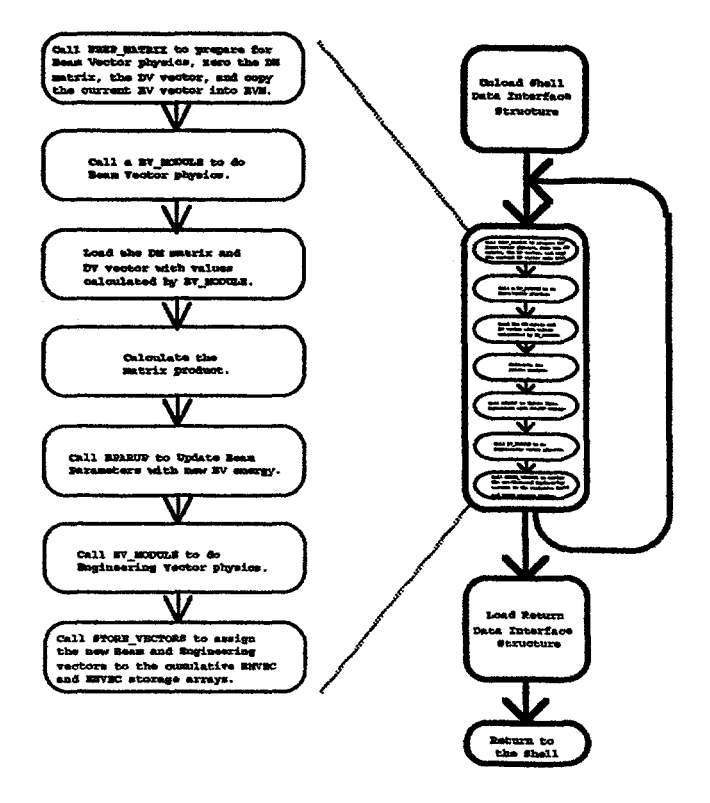
The Accelerator System Model (ASM) is a conceptual design tool for modeling RF linacs. ASM includes an intuitive user interface coupled with a FORTRAN program describing the accelerator model algorithms.

Accelerator Model Summary

The accelerator modeling used in ASM might be described as a collection of expert "rules of thumb" used by accelerator scientists in the development of the design of RF linac components. Some of these rules, primarily those which provide user guidance on input parameters at the component level, have incorporated into the GUI part of ASM. The major part of the modeling, however, is contained in the FORTRAN part of ASM. The FORTRAN modeling includes two descriptions of the accelerator and its components, a beam physics model and an engineering The ASM beam physics uses a root-meansquare (RMS) description of beam properties (e.g. envelope equations), with heuristic treatments of emittance growth and particle loss incorporated. engineering model provides a summary of the physical characteristics of individual components.

The ASM FORTRAN program includes models of both the beam physics and the physical characteristics of the beam line components.

A modular approach has been used for ASM accelerator modeling. Each major component, i.e. an ion source or a radiofrequency quadrupole (RFQ), composes an ASM module. On the FORTRAN side of ASM each module is describe by a group of subroutines which, except for input (I) from the preceding module and output (O) to following module, are essentially independent. The subroutines are called iteratively based upon the sequence of components set up by the user on the GUI side of ASM. This is illustrated in Figure 1.1 below. A common I/O structure is maintained for each module so that modules may be interchanged or rearranged.



Accelerator components are treated as separate modules in ASM. Each module has a common I/O format and a separate set of FORTRAN subroutines. The Beam Vector (BV) is used to describe the beam at each point in the beam line. The Engineering Vector (EV) is used to describe the physical characteristics of each component. The BV and EV are output for each module.

Figure 1.1 Schematic of ASM FORTRAN execution

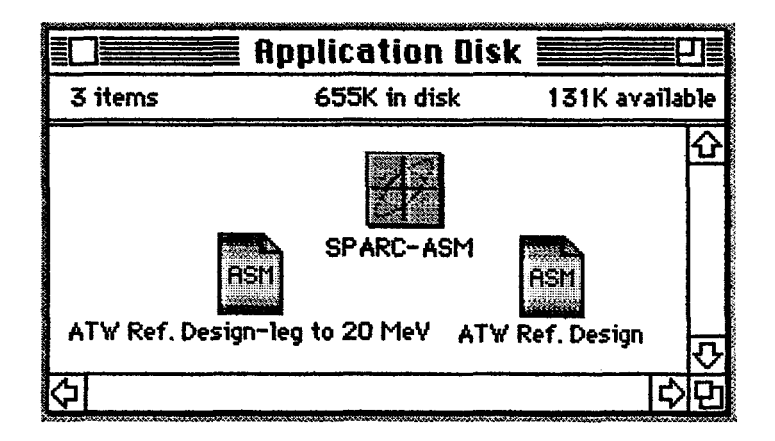
The RMS beam properties are contained in a vector called the Beam Vector (BV). The physical characteristics of the accelerator components are contained in another vector called the Engineering Vector (EV). The BV and EV are outputs from each module. The inputs to each module include the preceding module BV together with user input parameters from the ASM GUI.

2. Getting Started

This section is intended to provide users with a brief introduction to ASM that will get them up and running quickly. It covers the basic installation of the ASM application and provides an overview of the use of the ASM software.

Installing ASM

The ASM software is contained on three 3.5 inch diskettes. The application diskette contains the SPARC-ASM application and example files. ASM may be run directly from the Application Disk floppy (disk must be unlocked), but this is not recommended. ASM will need to write files to the folder (directory) from which it is run and it is recommended that ASM be installed on your computer's hard drive.



Installation is simple. Drag the SPARC-ASM icon to a folder on your computer's hard drive Install the examples the same way.

Figure 2.1 ASM Application Disk

To install the ASM application and example files, first create a folder (select New Folder command under the Macintosh finder's File menu) on your hard drive. Assign this folder a name such as "ASM Folder." Insert the ASM Application Disk into your computer's floppy disk drive. Using your computer's mouse, select and drag the SPARC-ASM application icon, and any example file icons on the diskette, to the assigned folder. That's all there is to installing the ASM application.

The SPARC Object Code Disk and FORTRAN Source Code Disk are not needed to run the ASM application. They are required if you intend to modify the FORTRAN source code and created your own custom application. That is discussed in Section 7 of this User Manual.

The ASM Application Screen

The ASM application may be opened by double clicking on either the ASM application icon or one of the example files. The figure below illustrates the ASM screen after double clicking on the application icon. The principal parts of the ASM application screen are indicated: the Menu Bar, the Palette Bar floating window, and the ASM Document Window.

Double clicking on the SPARC-ASM icon brings up the application screen.

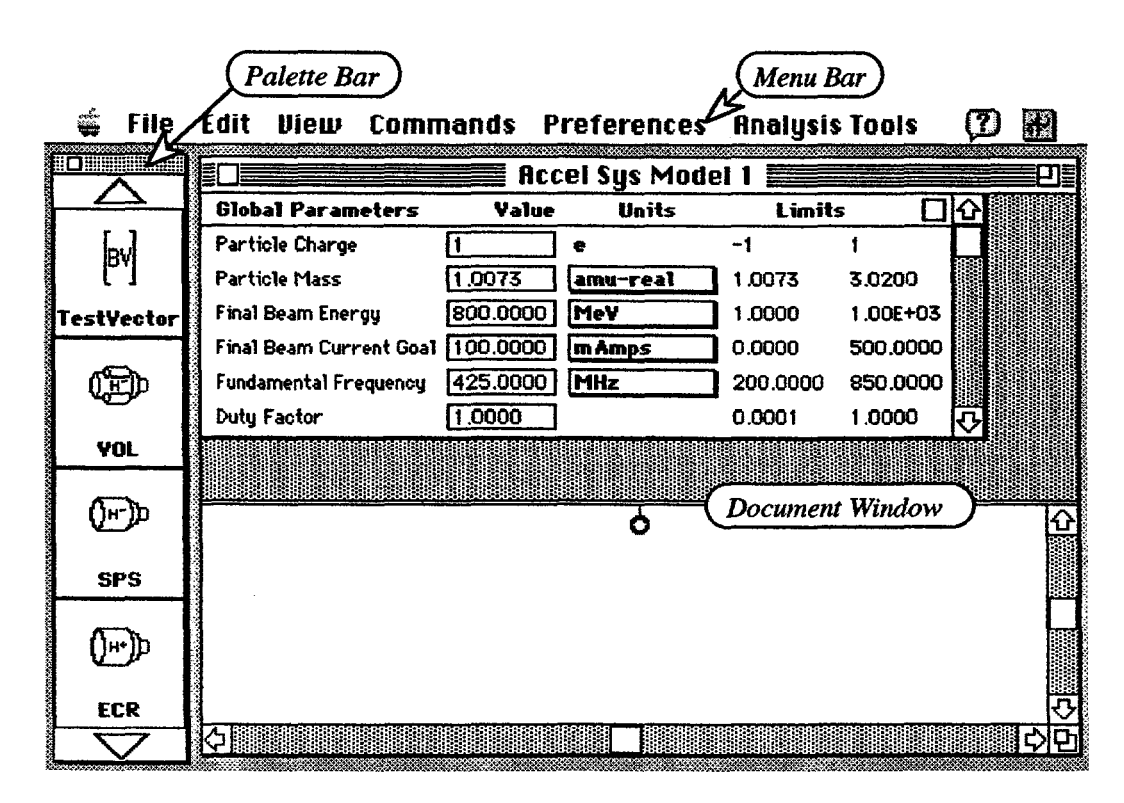


Figure 2.2 ASM Application Screen

There is one Menu Bar and one Palette Bar for the ASM application, but up to six (6) Document Windows may be open at any one time in the application. The next few pages describe the basic functions of the different parts of the ASM application.

Building a Model and Inputting Parameters

ASM uses three sets of user input parameters. The user inputs are grouped by:

- Global Parameters
- Piece Parameters
- User Preferences

The Global Parameters are set in the scrollable Global Parameter Pane of each Document Window. The first step in building an accelerator system model is to review the set of Global Parameters and make changes as necessary.

The second step is to "build" a graphic image for the accelerator to be modeled. An accelerator model is built by selecting and dragging the beam line components from the Palette Bar to the Model Space Pane of the basic Document Window. The figure below shows an example of a Document Window with an accelerator model built on the Model Pane.

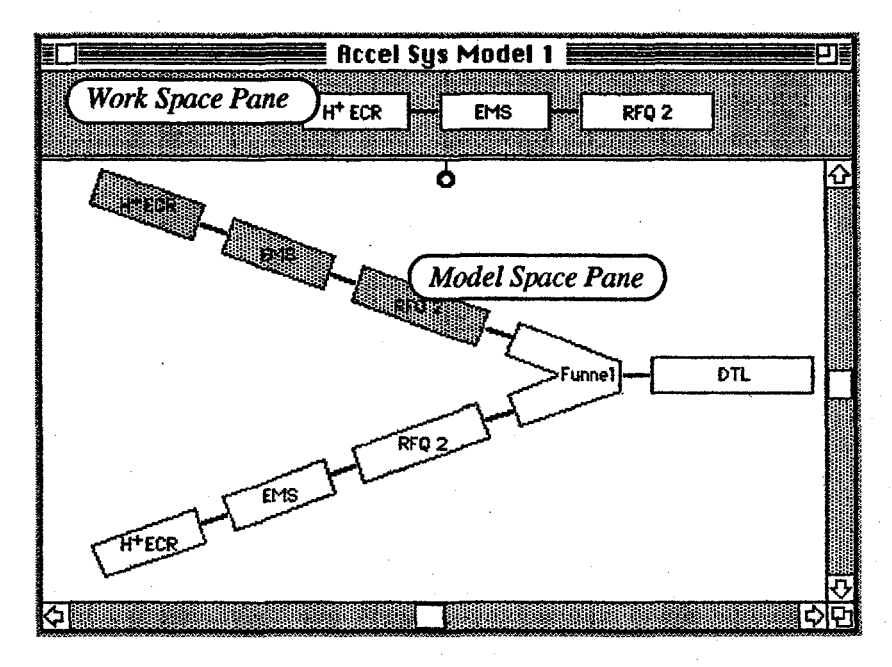


Figure 2.3 Beam Lines on Model Space Pane and Work Space Pane of ASM Document Window

An accelerator model is built by dragging icons to the Model Space Pane of a Document Window. Groups of components may also be placed in the Work Space Pane. The Global Parameter Pane may be closed to provide more area for the Model and Work Space Panes.

In this example, the Global Parameter Pane has been closed (using close box to right of "Limits" in the Document Window, Figure 2.2) and the Work Space Pane shade has been raised (using pull ring in center of Document Window, Figure 2.2) in order to provide more room to view the Model Space Pane.

Scroll the Palette Bar in order to access all the beam line components available in ASM. Selection, dragging and dropping a component on the Model Space will result in that component being attached to the end of the accelerator model nearest the drop point. Components may be inserted into the beam line by selecting and dragging the component to a connection point. Connection points are identified by the black lines between each component. Positive feedback, a flashing of the connection line, indicates that a valid insertion point has been located by the mouse cursor. Releasing the mouse button (dropping the component) while the connection line is flashing will insert the component at the indicated location.

The Piece Parameters define all inputs for each component of the beam line. Double clicking on an individual piece, such as the "ECR" component in the example above, opens a Piece Window. The Piece Parameters are input via this Window.

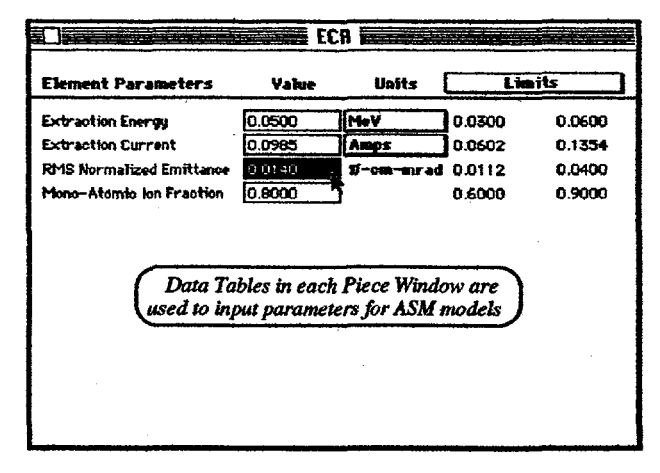


Figure 2.4 Piece Window for the ECR Source Model

Model parameters are input using the Data Tables in each Piece Window. Users are provided with options for units and guidance limits for each Piece Parameter. Any value for a parameter may be used the guidance limits are "sofi", but are used to alert the user if his set of input parameters may have impractical consequences.

Running ASM

Execution of ASM is accomplished from the pull down Commands Menu shown. Figure 2.5 illustrates the mouse selection of the Run ASM command, one of two commands available in ASM Version 1.0. The selected command is executed after the mouse button is released.



Figure 2.5 Executing ASM FORTRAN Program

The Run ASM command executes the ASM FORTRAN as described in the Accelerator Model Summary of the Introduction (Section 1) to this User Manual. An output window is automatically displayed after completion of the FORTRAN execution. The user has different options available for the output display (see Section 4) An example output is illustrated later in Figure 4.2.

The Evaluate Constraints command calls an interface (C language) routine which examines the configuration of the beam line. This is implemented as a demonstration command in ASM Version 1.0 and is discussed in the Appendix.

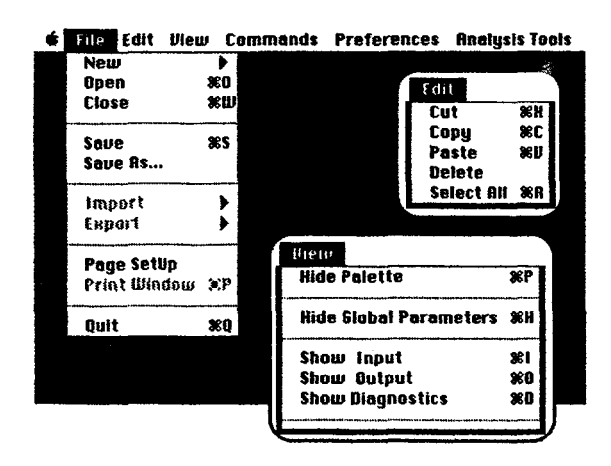
Running the ASM FORTRAN is straightforward. Simply select the Run ASM option from the Commands pull down menu.

3. ASM Interface Description, Definitions and Functions

This section provides a description of the ASM user interface and defines terms used to refer to different parts of the interface. Familiarity with the preceding section "Getting Started" is assumed. This section also provides an overview of the data structures and on the transfer of data between the interface and ASM FORTRAN. A description of the functions of each part of the ASM interface is given in this section.

Menu Bar

The ASM interface has seven (7) pull down menus in the Menu Bar. Several of these also have submenus, but only one of the menus or submenus may be accessed at a time. The first menu is the standard Apple (4) menu whose functions are established by the configuration of your operating system. This menu contains only one command which is controlled by the interface. This is the About ASM command which brings up a dialog box with information about the ASM application. Figure 3.1 below illustrates three of the pull down menus available: File, Edit and View. These are discussed further below. The Commands, Preferences, and Analysis Tools menus are discussed in later Sections.



The File, Edit and View Menus are similar to those of other Macintosh applications.

Figure 3.1 ASM File, Edit and View Menus

The second menu is the File menu and has ten (10) The New command creates a new commands. Document Window. The Open command is used to open a previously saved model (defined by a Document Window). The <u>Close</u> command is used to close the currently active window. The Save and Save As... commands are for saving the current model as defined by the active Document Window. The Import and Export commands are not used with ASM. The Page Setup and Print Window commands control the printing of output. The final command is Ouit which closes all windows and quits the application.

The File commands are similar to other applications and follow the standard Macintosh guidelines. Many bring up standard Macintosh dialogs for defining file names, file desktop locations (directories), etc. Commands which cannot be undertaken at any given time (the Print Window command in the above Figure) are dimmed and not accessible to the user. Users unfamiliar with the Macintosh operating system should consult their Macintosh documentation for additional information.

The third menu is the <u>Edit</u> menu. This menu has five (5) commands. These commands also follow the standard Macintosh guidelines. The <u>Cut</u> command removes (cuts) any selected components from the Document Window, without changing the parameters, and places them on the clipboard for future pasting to the current Document Window or to another Document Window. Information from certain text windows, such as the Diagnostics file window, can also be cut to the clipboard. The <u>Copy</u> command is used to copy selected components, or text information, to the clipboard for future pasting. PICT images of the ASM model in the Document Window are also be copied to the Macintosh clipboard using this command and may be pasted into

other application's documents. This can be used to

provide a graphic for a word processing document.

The <u>Paste</u> command places the current contents of the clipboard (if valid ASM model data) on the Work Space of the Document Window. See the discussion of the Document Window for additional information. If text data is on the clipboard it can be pasted into certain text windows of ASM. The <u>Delete</u> command deletes any selected components from the Document Window, or deletes any selected text data, but does not place them on the clipboard. Deleted data is permanently removed. The <u>Select All</u> command is used to select the entire group of components on the Model Space of the Document Window, or all of the information in a text window, for subsequent execution of Copy, Cut, Paste or Delete.

File commands allow the user to save and load ASM files and control printer functions.

Edit commands can be used to copy and paste beam line components within, and between, Document Windows. Graphic images of the components as well as text data may also be copied and pasted to other applications such as word processors.

The fourth menu discussed here is the View menu. This menu has between four (4) and ten (10) commands depending upon how many Document Windows are open. The first is the Hide(Show) Palette command. This command allows the user to hide (and then show again) the Palette Bar floating window. The second command is the Hide(Show) Global Parameters. command lets the user hide (or show) the Global Parameter Pane of the currently active Document Window. The Hide Palette and Hide Global Parameters commands are useful for increasing the Model Space and Work Space area available for a Document Window. The next three commands, Show Input, Show Output and Show Diagnostics allow the user to view ASM text files for the current Document Window. The rest of the menu consists of the names of all the open ASM Document Windows, with a check mark by the current active window. By selecting one of these commands the user makes that Document Window, who's name is selected, come to the front of the screen and it then becomes the active document. As discussed above (and further below) several commands result in operations determined by the currently active Document Window. Only one Document Window is active at a time and it can be identified by the check mark in this menu.

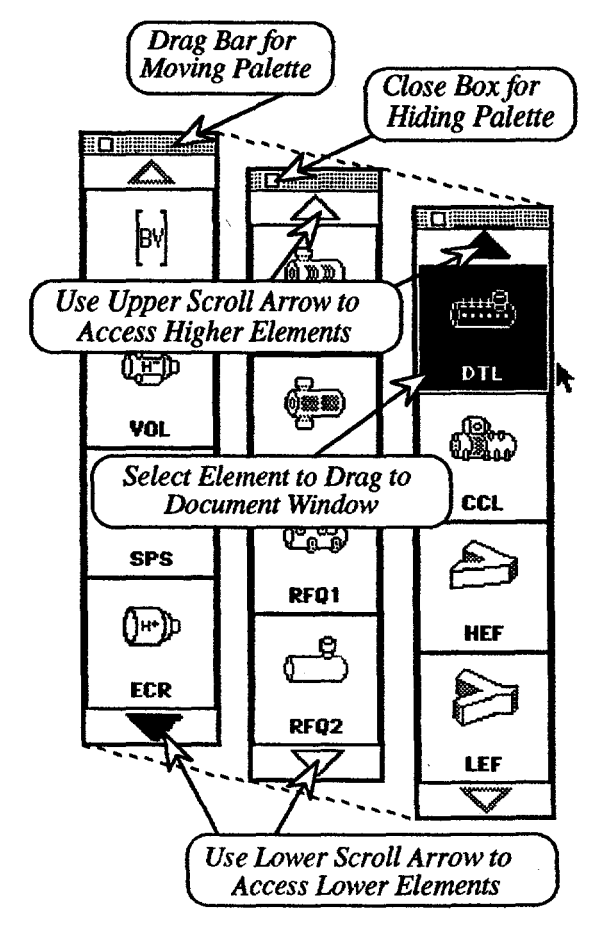
The View Menu is used to configure parts of the ASM interface screen and to access different ASM output files.

While the functions of the File, Edit and View menus are very similar to other Macintosh applications, the Commands, Preferences and Analysis Tools menus are unique to ASM. These are discussed separately in this User Manual.

Other ASM menus are discussed in Sections 4, 5 and 6 of the User Manual.

Palette Bar

The <u>Palette Bar</u> consists of an icon display, two scroll arrows, a drag bar and a close box. The Palette Bar is a floating window (the window will "float" to the top position if a Document Window is placed over it) which contains icons for each of the accelerator modules available in ASM.



The Palette Bar contains icons for all accelerator models available in ASM. Icons are selected from the palette and dragged to a Document Window to "build" an accelerator. Different model elements are accessed by scrolling.

Figure 3.2 ASM Palette in Different Scroll Positions.

The Palette Bar also contains an icon for a Test Vector. Only four icons are displayed at one time on the Palette Bar; other element icons are accessed by scrolling. Figure 3.2 illustrates several different scroll positions. Icons are selected from the Palette Bar and dragged to either the Model Space Pane or the Work Space Pane of the Document Window, discussed next.

Document Window

The <u>Document Window</u> is divided into three (3) areas called panes. These three panes are the <u>Global Parameter</u> Pane, the <u>Model Space</u> Pane and the <u>Work Space</u> Pane. A Document Window showing these three panes is illustrated in Figure 3.3.

Document Windows are the primary ASM window for each accelerator model. Up to 6 Document Windows, each with a different model, may be open at any one time.

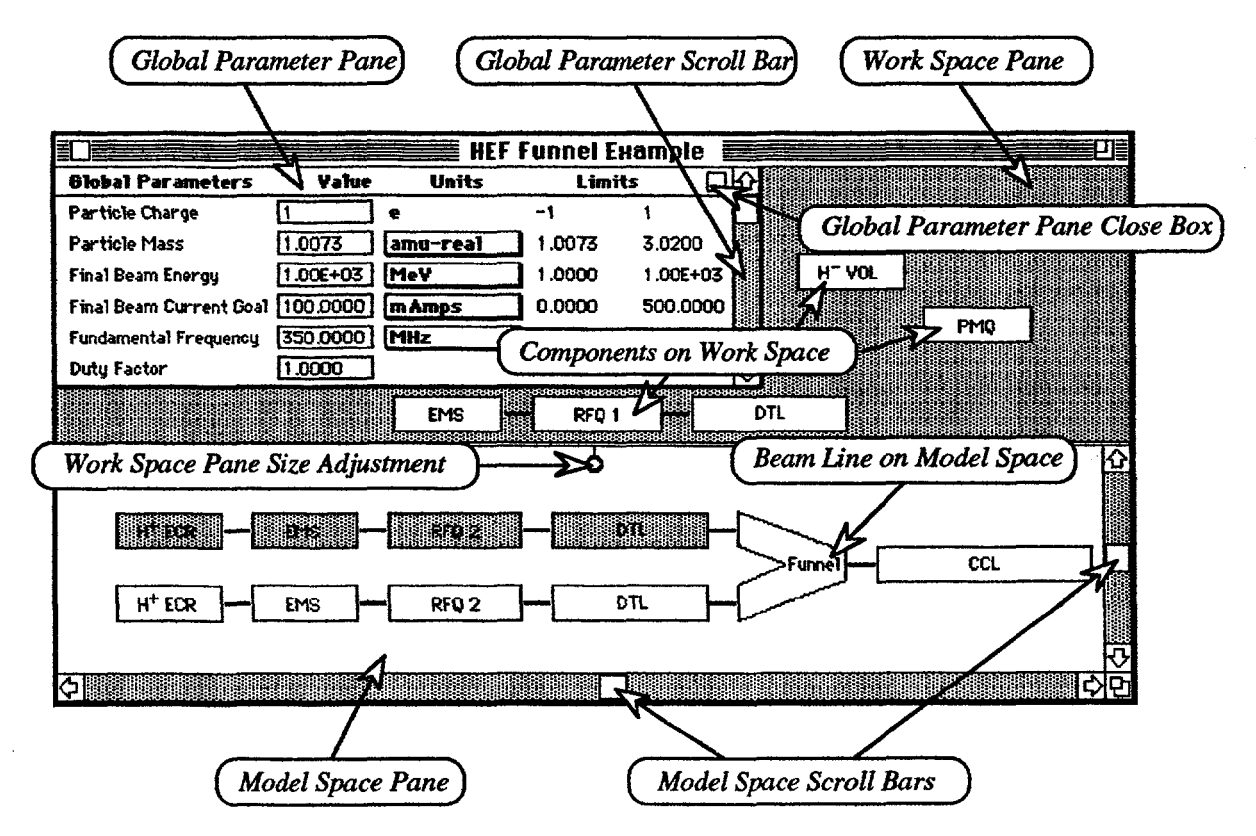


Figure 3.3 Document Window Panes

An important feature of ASM is that multiple Document Windows, up to six (6), may be open at any one time. The user can set up multiple ASM problems, including the ability to exchange beam line elements or groups of elements between them, and run ASM for any of the models.

Document Window - Global Parameter Pane

The Global Parameter Pane consists of the header region, the close box, the scroll bar and the parameters. The header region is at the top of the pane and displays the title of the Global Parameters and the other fields which include the current Value, the Units, and the Limits (lower and upper). The close box, located in the upper right corner of the pane, hides the Global Parameter Pane from view. It is the same as selecting the Hide Global Parameters from the View menu (Figure 3.1). To view the Global Parameter Pane, once hidden, the user must select the Show Global Parameters from the View menu. The scroll bar on the Global Parameter Pane controls the position of the The parameters and other fields are displayed as a Data Table. Data Tables are used for most ASM input parameters and are discussed in a separate subsection later.

Global Parameters are the top level ASM user inputs.

Document Window - Model Space Pane

The Model Space Pane of the Document Window is where the components are placed to construct a beam line model. Components for the model are "dragged" to the Document Window from the Palette Bar. Components may be placed on either the Model Space or the Work Space (discussed below). The first component that is "dragged" to the Model Space may be placed anywhere on the Model Space. Once the first component is placed, the following components "snap" on to the end closest to where the component was "let go" when the mouse button was released. The Model Space Pane will automatically scroll to the end to which the component is placed if this end is not visible in the window. When funnel elements are place on the beam line, ASM automatically generates the necessary beam line "legs" and displays them on the Model Space.

An accelerator system to be modeled is built on the Model Space Pane of a Document Window. Components are selected from the Palette Bar and dropped on the Model Space.

Components may also be placed at <u>connection points</u> which will insert the component in between two other components. Connection points are the solid lines between components of the beam line on the Model Space Pane. For a component insertion, the arrow cursor of the mouse must be placed directly on the connection point. The *connection point will flash* while the cursor is correctly located on it. Releasing the mouse button then inserts the component in the beam line model at that point. Note that there can never be "loose" components in the Model Space. All components are either inserted at connection points or snapped to an end.

Components may be inserted into the beam line at connection points between components on the Model Space.

The two scroll bars on the Model Pane control the positioning of the model with respect to the window, and can be adjusted by the user. The Model Space Pane is large and can accommodate a large number of accelerator components. In building a large model by starting at one end of the beam line, it may be advantageous to scroll to the corresponding end of the Model Space Pane, rather than starting near the center of the Model Space.

The components assembled on the Model Space constitute the accelerator model whose data will be used in running the ASM FORTRAN. This model may be saved at anytime using the appropriate commands from the File menu.

A component or group of components may be selected and copied, cut or deleted using the appropriate commands from the Edit menu. These actions are very similar to the standard Copy, Cut and Delete actions of many other applications. The keyboard equivalents of the Edit menu commands are the Macintosh standards for these commands. The <u>Delete</u> action removes the selected components from the beamline model - information associated with the components is <u>permanently lost</u>.

Components in the beam line on the Model Space may be copied, cut or deleted using the Edit menu commands or their keyboard equivalents.

The Copy action makes a copy of the components and associated information (parameter settings) and stores it. The complete information is stored on an ASM internal "clipboard" and the components may be later pasted onto any ASM Document Window (they will appear on the Work Space Pane). The original components and the data associated with them are unaffected and remain on the Model Space. A graphic image (PICT file) of the selected beam line component(s) is also placed on the Finder Clipboard. This image may then be pasted into other Macintosh applications, for example, in order to prepare a figure for publication.

The <u>Cut</u> action is similar to the Copy action, except that the original components and associated data are removed from the Model Space. Cut makes a copy of the components and associated information and stores it the same as with Copy. The complete information is on the ASM internal clipboard and the components may be pasted onto any ASM Document Window. A graphic image of the selected beamline component(s) is also placed on the Finder Clipboard and may be pasted into other Macintosh applications.

A component or a group of components may be selected and dragged from the Model Space to the Work Space Pane (discussed below). This action creates copies of the component(s) selected for placement on the Work Space. The original components and the data associated with them are unaffected and remain on the Model Space. To move a component or group of components from one position in the beam line to another position, first drag and drop the desired component(s) onto the Work Space and then delete those component(s) from the Model Space beam line. Next. select the component(s) on the Work Space and insert them at the desired connection point in the beam line on the Model Space. This is one example of how the Model Space Pane and Work Space Pane can be used in conjunction to accomplish certain tasks. The Work Space Pane is discussed next.

The Copy and Cut functions follow standard Macintosh guidelines. Beam line information of components is retained on an internal ASM clipboard and a graphic image is placed on the Finder Clipboard for use in other applications.

Components may be moved within the beam line by using the Model Space and Work Space together.

Document Window - Work Space Pane

The Work Space Pane consists of the Work Space "window shade" and a Pull Ring. The Work Space window shade is not scrollable, but it can be raised or lowered, like a window shade, by dragging the Pull Ring. Double clicking the Ring will retract the shade completely. Additional Work Space may be accessed by "hiding" the Global Parameters. This may be done from the close box in the upper right hand corner of the Global Parameter Pane (Figure 3.3), or by selecting the Hide Global Parameters from the View menu (Figure 3.1).

Components may be placed on the Work Space either by dragging them from the Palette Bar or the Model Space. When a component, or a group of components from the Model Space, is dragged to the Work Space it can be placed anywhere on the Work Space. Components are not grouped on the Work Space unless they were grouped prior to being placed on the Work Space. No component is snapped to, or inserted into, a model structure when placed on the Work Space. A group of components placed on the Work Space will remain in their original configuration (i.e. same order in line) and cannot be separated. (Of course they can be dragged to the Model Space, a subset selected, and then that subset placed on the Work Space.) A component or a group of components may also be copied, cut or deleted from the Work Space with the same result as in the case of the Model Space (discussed above). There is one internal ASM clipboard so that any existing data on it will be erased when either Copy or Cut is executed.

If components or groups of components have been previously copied or cut, from either the Work Space or the Model Space, they may be placed on the Work Space by pasting them from the internal MacTrace clipboard. The Paste action is similar to that of other applications. However, the Work Space is the only location to which a previously cut or copied component, or group of components, will be pasted.

Piece Windows and Data Tables

Data input for the components of the beam line is accomplished via the Piece Windows. Piece Windows are accessed by "double clicking" the mouse button while the cursor is on the desired beam line component. Figure 3.4 below illustrates the Piece Window for one of the radiofrequency quadrupole accelerator models (RFQ2) available in ASM.

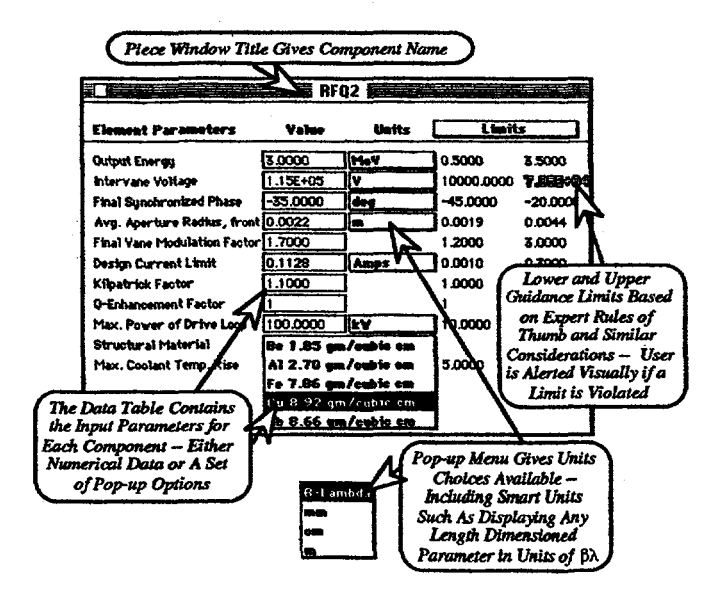


Figure 3.4 RFQ2 Piece Window and input Data Table

Each Piece Window consists of a Title Bar with close box and a Data Table. The Data Table includes four fields of data: (1) a description of the Element Parameters, (2) a Value field for data entry of the numerical parameters, or options using pop-up menus, (3) a Units field which provides options through pop-up menus and (4) a Limits field which gives lower and upper limits based on a expert system set of knowledge based rules. These rules are discussed in the Appendix.

More than one component on the beam line may be selected at any one time. Double clicking on a selection of components will open all the Piece Windows for the selected components.

Several features of the Piece Window Data Table are illustrated in Figure 3.4. All numerical data is entered into a "box" in the Value field. Default values have been defined for all parameters and these are entered into the ASM data structure (discussed below) when a component icon is placed on the Model Space. When the user changes any number in the Value fields, the new numbers are immediately updated in the data structure.

The user may select different units for the Data Table display by selecting the appropriate option from one of the Units field pop-up menus. All unit conversions are done by the Piece Window and all numbers transferred to the data structure are in the default units, which are the same as the units used by the ASM FORTRAN. Several pop-up menus include "smart units." These are units which scale dynamically with certain Global Parameters and other parameters from Piece Windows. For example, all parameters which have the dimensions of length include " β -Lambda" as a units option. The value of the β , the relativistic velocity parameter of the particle, is determined by the Global Parameter values for the particle energy and mass, while the value of λ is set by the radiofrequency Global Parameter.

The Data Table in each Piece Window also contains lower and upper "limits" for each parameter. These limits are not used to restrict the input, any value may be entered and will be passed to ASM via the SPARC data structure, but they are intended to provide the user with estimates of practical limits. In the example shown in Figure 3.4, the user has been alerted that the intervane potential is inconsistent with the upper limit based on the Kilpatrick factor guidance value of 1.1 (another RFQ2 input), the model fundamental radiofrequency 350 MHz (a Global Parameter, see Figure 3.3) and the average aperture radius, r_o , of 2.2 mm (also an RFQ2 input).

Data Structures and Data Flow

The ASM interface is based on the Shell for Particle Accelerator Related Codes (SPARC) written in the C programming language for the Macintosh computer. It is designed to provide a common Graphical User Interface (GUI) for multiple applications. The ASM physics and engineering algorithms are contained in a FORTRAN code which has been linked with the SPARC interface. This mixed language application uses a specialized data structure developed for transferring data between SPARC and FORTRAN routines. There is a dynamic data exchange which is facilitated with data structures in both C and FORTRAN that are identical in size and reference a common relocatable block of memory. This block of memory is accessed from both the SPARC interface and ASM FORTRAN side of the application and the data transfer is illustrated schematically in Figure 3.5.

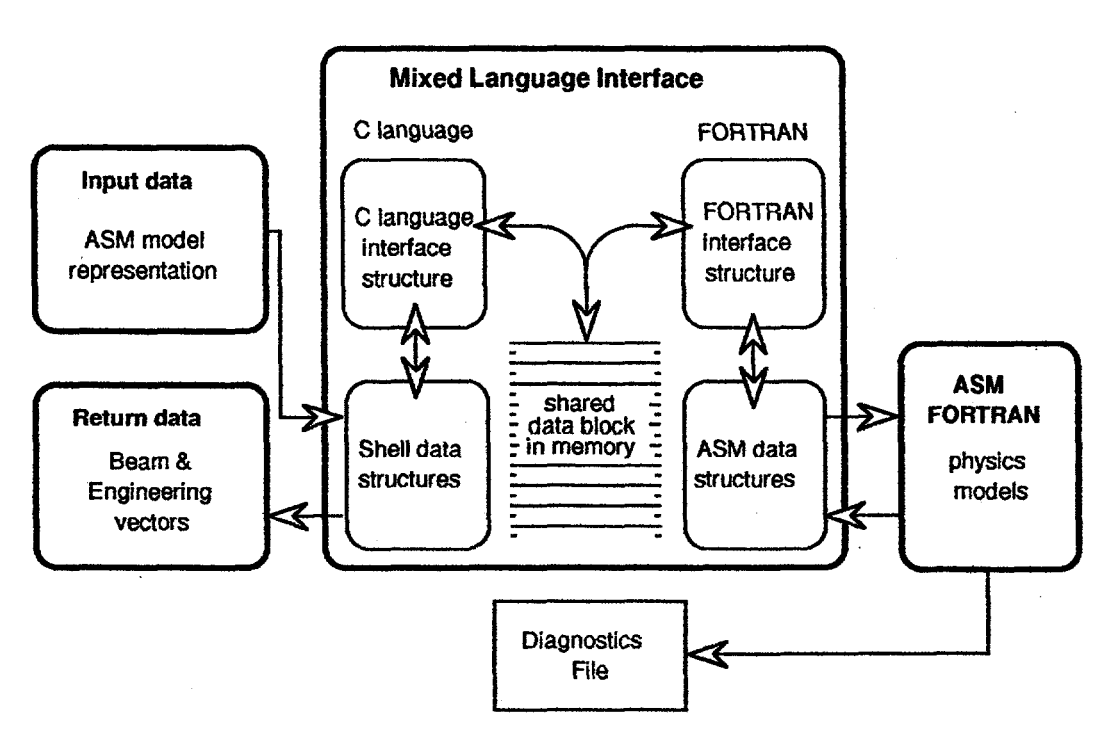


Figure 3.5 ASM mixed language interface and data flow.

As a model beam line is built all data defining the model are stored in Data Tables. The collection of Data Tables is represented in Figure 3.5 by the SPARC Input data (ASM model representation) data structure. Certain actions, such as selection of the Run ASM command from the Commands menu, initiates the interface data transfer process to pass the model data to (or from) the FORTRAN.

Although the data transfer is rapid and transparent to the user it involves a few well defined steps. These are discussed here briefly since an understanding of this data flow is useful in customizing ASM (described in Section 7). The SPARC interface to ASM FORTRAN interface data transfer involves the following steps.

- (1.) ASM model representation data is passed to the C Language Interface Structure which stores data in the shared memory block. The C Language Interface Structure corrects for the different storage schemes of the two languages. The ASM model representation data may be viewed in the text format of an ASM FORTRAN input file by selecting Show Input from the View menu.
- (2.) The ASM applications calls a (SPARC) FORTRAN interface routine, passing a pointer to the shared data block in memory. This defines the FORTRAN Interface Structure.
- (3.) The FORTRAN interface routine assigns data to the ASM FORTRAN common blocks from the FORTRAN Interface Structure.

At this point the original action (i.e. selecting the Run ASM command) that initiated this data transfer is completed. Note that the ASM model representation data is retained in the Data Tables independent of any actions within the ASM that might alter the common block data. During the ASM FORTRAN execution certain diagnostic data is written directly to a disk file. This diagnostic data does not pass through the interface.

- (4.) A FORTRAN interface return data routine assigns data from the ASM output arrays to the shared memory block of the FORTRAN Interface Structure.
- (5.) A pointer to the shared memory block is returned from the FORTRAN Interface Structure to the ASM SPARC shell.
- (6.) The return data is assigned from the shared memory block to the C Interface Structure, correcting for the different storage schemes of the two languages. This return data is used for the output displays of ASM.

All ASM FORTRAN commons are maintained when control returns to the SPARC interface.

4. ASM Commands and Output

Running the ASM FORTRAN is accomplished directly from the ASM interface - the compiled FORTRAN is fully integrated with the interface application. This section discusses the Commands menu and the output from ASM.

The Commands Menu

The <u>Commands</u> pull down menu contains two ASM options illustrated in Figure 4.1: Evaluate Constraints and Run ASM. The Evaluate Constraints command is executed on the SPARC interface side of ASM and does not call FORTRAN. This command checks certain configuration requirements of the accelerator model and their consistency with top level parameter goals set in the Global Parameter Pane. The Run ASM command calls the ASM FORTRAN to compute the Beam Vectors (BV) and Engineering Vectors (EV) for the accelerator model. Other user actions using the Analysis Tools, discussed in Section 5 of the ASM User Manual, also call the ASM FORTRAN.

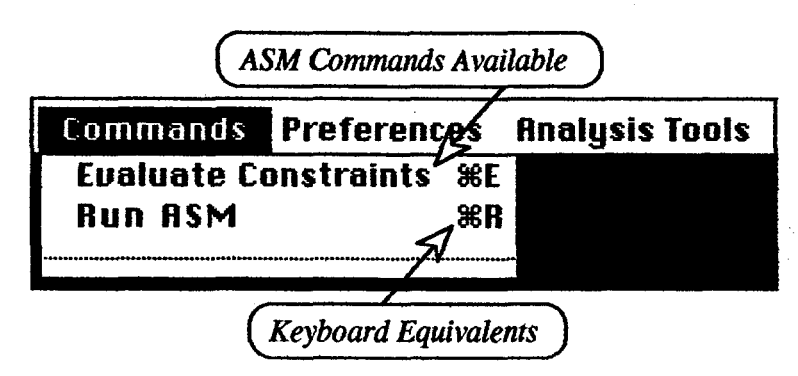


Figure 4.1 ASM Version 1.0 Command Menu

The Evaluate Constraints command has only been implemented in ASM Version 1.0 as a demonstration command in order to illustrate the command's potential utility. The Run ASM command is fully implemented.

ASM Output

This Section discusses the output following the Run ASM command. The Run ASM computes the BV and EV results for the accelerator components and generates three (3) principal output files:

(1.) A text Output file of BV and EV data

- (2.) A Diagnostic file providing detailed output, and
- (3.) A Graphic Output Window.

Data is written to the Diagnostic file directly from the ASM FORTRAN calculations. The user may add output to the Diagnostic file by adding print statements to the FORTRAN source code, recompiling the FORTRAN and linking the recompiled files to the ASM SPARC interface object code. This is discussed further in Section 7 of this User Manual. The Diagnostic file is not automatically displayed. It may be accessed by using the Show Diagnostics option from the View menu (Figure 3.1).

The ASM Graphics Output Window and the BV and EV Output file are written by the SPARC interface. The BV and EV Output Window comes up automatically after completion of the Run ASM command, unless the user has turned off the Always Show Vector Output After Run under the Preferences menu (see User Options in Section 5). If this option is turned off, then the ASM Graphics Output Window will be displayed after execution. The BV and EV Output file may be accessed at any time after a Run ASM command has been executed by using the Show Output option from the View menu (Figure 3.1). An example text Output file of BV and EV data is illustrated in Figure 4.2.

Accelerator System Model

	BEAM VECTORS									
	ENERGY	CURRENT	RADIUS	Transverse Emittance	đР	LONGITUDINA EMITTANCE	L ALPHA TRANSVERSE	ALPHA LONGITUDINA		
	(MeV)	(amp)	(cm)	(cm-mrad)	(MeV/c)	(cm-mrad)	•	•		
ECR	0.05000	0.07880	0.17454	0.01400	0.0000	0.00000	0.0000	0.00000		
EMS	0.05000	0.07880	0.07365	0.01400	0.00000	0.00000	2.50000	0.0000		
RFQ	2.50000	0.07716	0.11487	0.02259	0.18353	0.10943	1.70000	0.04000		
LEF	2.50000	0.15432	0.11487	0.03264	0.18353	0.11914	1.70000	0.04000		
	2.50000	0.15432	0.11487	0.03264	0.18353	0.11914	1.70000	0.04000		
DIL	20.00000	0.15432	0.11487	0.02678	0.19386	0.73708	0.00000	0.00000		
	·			ENGINEERING	VECTORS					
	Length	VOLUME	MASS	POWER	Size(X)	Size(Y)	CONFIDENCE	COST		
	(m)	(m**3)	(Kg)	(MN)	· (m)	(m)	(fraction)	(\$)		
ecr	1.57871	0.31574	2.66e+02	0.01180	0.25000	0.20000	0.90000	0.0		
emb	0.50000	0.09305	2.26e+02	0.04334	0.50300	0.50300	0.90000	0.0		
RFQ	2.02166	0.42716	1.09e+03	0.63954	0.10960	0.76460	0.90000	0.0		
LEF	0.23010	0.00981	7.85e+01	0.07424	0.28658	0.28658	0.75000	0.0		
	0.24961	0.14383	1.22e+02	0.01274	0.42827	0.42827	0.75000	0.0		
DIL	25.77535	17.03449	2.34e+05	3.14287	0.90141	0.90141	0.75000	0.0		
SEV	30.35543	18.02409	2.35+05	3.97965	0.50300	1.66600	2.15087	0.0		

Figure 4.2 Example of ASM Text Output for BV and EV Data.

Test Vector Use

The Test Vector beam line element on the Palette Bar is not an accelerator component but provides a tool for evaluating individual components or groups of components. This vector allows a user specified Beam Vector (BV) to be input to the component appearing to its right on the beam line. The Test Vector may be placed at any connection point in the accelerator model, or at the beginning (left end) of the model. (The Test Vector will have no impact if located at the right end of a model.) The user inputs the desired BV into a Piece Window Data Table just as for any other component. The Test Vector Piece Window is illustrated in Figure 4.3. (Note that the quadratic forms, used for the emittance and other BV elements in the ASM FORTRAN, are not required to be input - the conversion is accomplished by the interface.)

est Beam Vector Parameters	. Value	Units
Beam Energy	0.0500	MeV
Beam Current	0.0788	Amps
RMS Transyerse Dimension	0.2468	em
RMS Normalized Trans. Emittance	0.0140	cm-mrad
Longitudinal Momentum Dispersion	0.0000	MeV/c
RMS Normatized Long. Emittance	0.0000] cm-mrad
Alpha Transverse	0.0000]
Alpha Longitudinal	0.0000.0	

The Test Vector can be used to input a given Beam Vector (BV) at any point in the accelerator model. The Test Vector default inputs corresponds to the BV generated by the ECR ion source module with default input parameters.

Figure 4.3 Test Vector Piece Window

When located in an accelerator model, the BV specified with this element is used for the input to the next beam line component during the Run ASM command. The BV that would normally be input to the component, which would be computed by the ASM FORTRAN, is overwritten at that point in the calculation by the input for the Test Vector. The calculation proceeds normally from that point, with the propagation of the Beam Vector being computed using the Test Vector, rather than using the original BV.

5. User Preferences

ASM provides a number of user options. These options are contained in the Preferences menu and are discussed in this Section.

The Preferences Menu

The <u>Preferences</u> pull down menu contains items: User Definitions, RF System options and ASM Options. The Preferences menu is illustrated in Figure 5.1:.

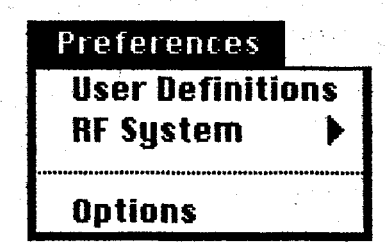


Figure 5.1 ASM Preferences menu

Each item on the Preferences menu offers the user several other choices. The User Definitions selection is to input numerical data for the three Global Parameters which offer the user custom modeling: the accelerator operating temperature regime, the permanent magnet material to be used in the accelerator quadrupoles and the structural material for the accelerator components. Upon selection of the User Definitions option from the Preferences menu, an input window appears on the screen. This window is shown in Figure 5.2.

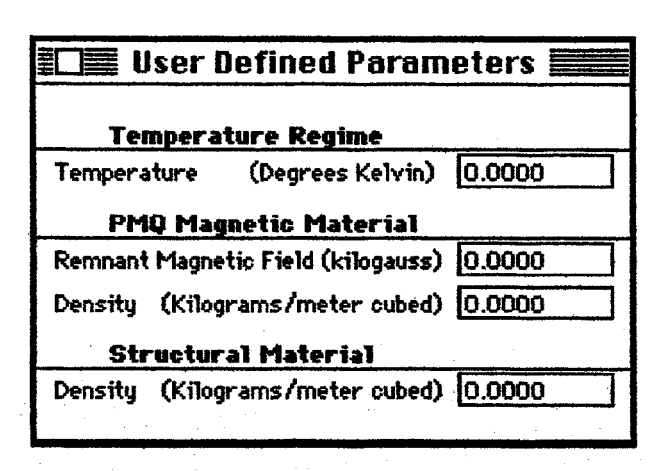


Figure 5.2 ASM User Definable Parameters

The User Defined Parameters are utilized by ASM only for those Global Parameter choices where the user has

selected "user definable" from the pop-up menu. These Global Parameter choices are discussed further in the appendix. The user is alerted in the Preferences menu when he has selected any user definable Global Parameters by a diamond to the left of the User Definitions. In Figure 5.1, the user has not made such a selection (no diamond to left). In Figure 5.3 below a diamond appears on the menu indicating that at least one user definable Global Parameter has been selected.

The second selection on the Preferences menu allows the user to set parameters for the RF power system. A different RF amplifier technology may be used for each frequency. F1 corresponds to the fundamental (lowest) frequency used in the accelerator model (an ASM Global Parameter). F2 through F6 correspond to the second through tenth harmonic of the fundamental, each frequency being a factor of two (2) higher than the preceding one. Funnels in an ASM model result in the doubling of the frequency; the RF settings for higher harmonics are associated with each stage of funneling.

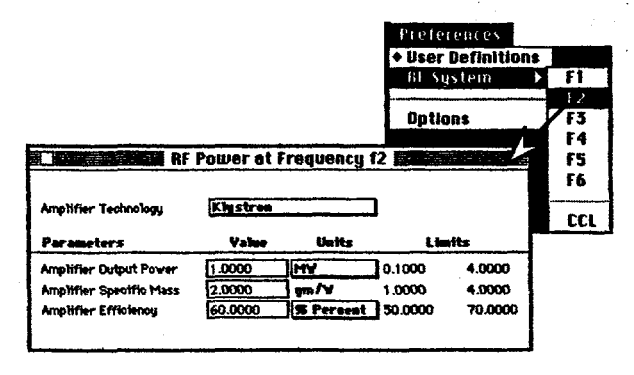


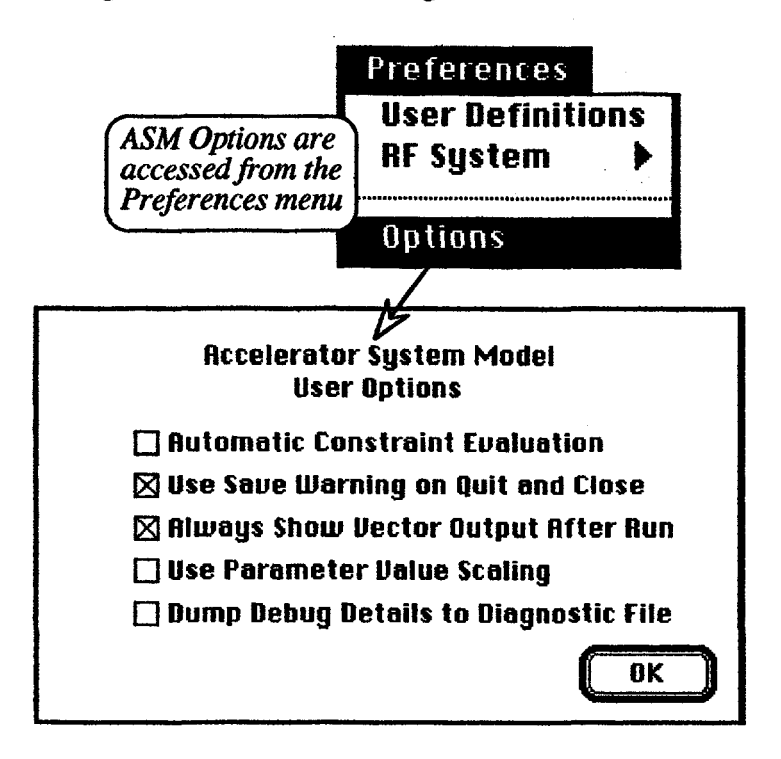
Figure 5.3 Setting RF power system parameters

Default parameters for four RF power amplifier technologies are built into ASM. These options are klystron, klystrode, solid state and magnetron. The pop-up menu at the top of the RF power window is used to select the technology to be used for the frequency selected. The user may input any value for the parameters available, so that the user may effectively define the technology at each frequency.

ASM provides RF power amplifier options for the fundamental frequency and the first five even harmonics to model funneled beam lines. For beam lines without funnels the CCL frequency and RF technology may be set separately.

ASM User Options

Several user options are available. These options are set to default values when ASM is launched, but may be set to the user's preferences by selecting Options from the Preferences pull down menu. This selection brings up the dialog box illustrated in Figure 5.4.



Several user Options are available in ASM under the Preferences pull down menu. These set preferences on command execution, dialog warnings, output windows, and default parameter scaling.

Figure 5.4 ASM User Options

The Automatic Constraint Evaluation option is used to call the Evaluate Constraints command first each time the Run ASM command is executed (see Figure 4.1). The Use Save Warning on Quit and Close option will bring up a dialog asking if the user wants to save the current model(s) whenever a Document Window is closed or the ASM application is closed. The user may have the text Output file (giving the BV and EV data) displayed after executing Run ASM, rather than displaying the Graphics Output Window, by using the third option in Figure 5.4. The Use Parameter Scaling Option is discussed in the next subsection. The last option writes user defined FORTRAN output to the Diagnostics file (see Section 7 for customizing ASM).

Use of Scaling Options

The Use Parameter Value Scaling option turns on the individual Element Parameter scalings, for default values, which the user may select using the Piece Windows for each component in an accelerator model. Individual component scaling options are set using check boxes accessed in the component's Piece Window by selection of the Use Scale Value option from the Limits pop-up menu. An example of setting a scaling option is illustrated in Figure 5.5. Here the user has selected to scale the default value of the vane potential for the RFQ-2 model. This default parameter scaling depends on the average aperture radius, the Kilpatrick factor, and the radiofrequency Global Parameter and is described in the Appendix.

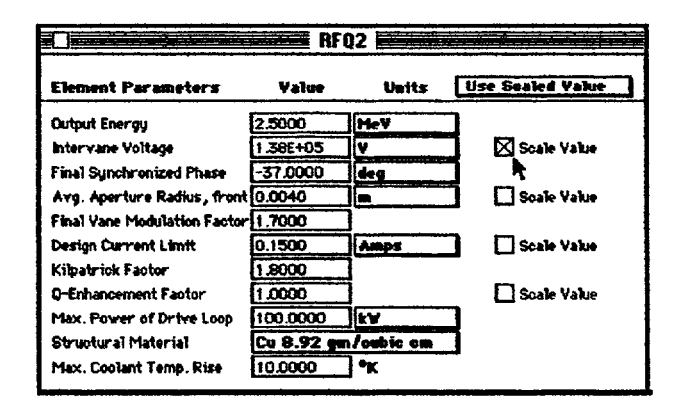


Figure 5.5 Selecting Default Parameter Scaling

In ASM Version 1.0, this Option is used in conjunction with setting defaults. The individual Piece Window(s) containing desired scaled default parameters must be opened in order to have the scaling implemented and the data passed to the FORTRAN. The Scale Value check boxes are accessible only if the Use Parameter Value Scaling option has been selected from the user Preferences. (Otherwise the check box is grayed out.) The user may select this option, check the parameters he or she wishes to scale, and then turn the option off. The Piece Window boxes will be checked and all of the selected scalings will become active again if the Use Parameter Value Scaling option is reselected.

6. Analysis Tools

Several Analysis Tools are available in ASM to aid the user in carrying out parameter variations and in analyzing results. These Tools are discussed in this Section.

Beam and Engineering Vector Graphs

Graphs of any Beam Vector or Engineering Vector element as a function of the component position in the beam line are generated from the pull down menus in the Analysis Tools menu. First the desired graph is selected and then generated using the Run Tools command. Figure 6.1 illustrates the selection of the Beam Current graph and the generation of the graph for the example beam line shown in Figure 2.3.

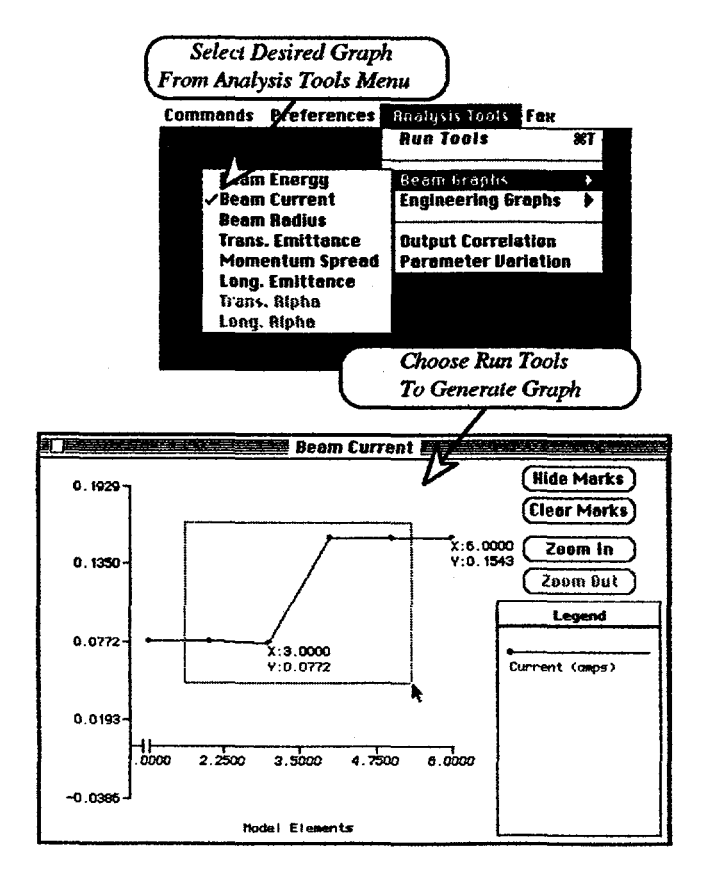


Figure 6.1 Selecting and Generating a Vector Graph

Once a graph has been generated several support functions are available to the user. Specific plotted points used to generate the graphs are displayed by selecting Show Marks. The coordinates of any plotted point are displayed by clicking on the mark for that point. Any region of the graph may be selected to Zoom In on. Unlimited zooms are available.

Graphs of any Beam Vector or Engineering Vector element are easily generated from the Analysis Tools menu.

Once the desired graph is selected, the Run Tools command may be used to generate the graph at any time after a Run ASM command has generated the data to be plotted.

Points used to generate any graph may be displayed and their coordinates shown. An unlimited number of zooms can be used to examine finer details in any graph.

Output Correlations

Graphs of any Beam Vector or Engineering Vector element versus any other Beam Vector or Engineering Vector element may be obtained using the Output Correlation tool. When this option is selected from the Analysis Tool menu a dialog appears for the user to select the Vector elements to be plotted against each other. This dialog is illustrated in Figure 6.2.

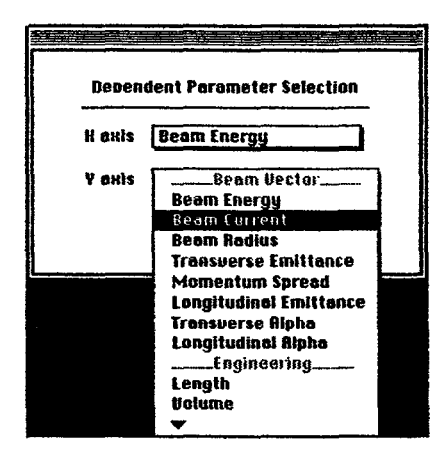


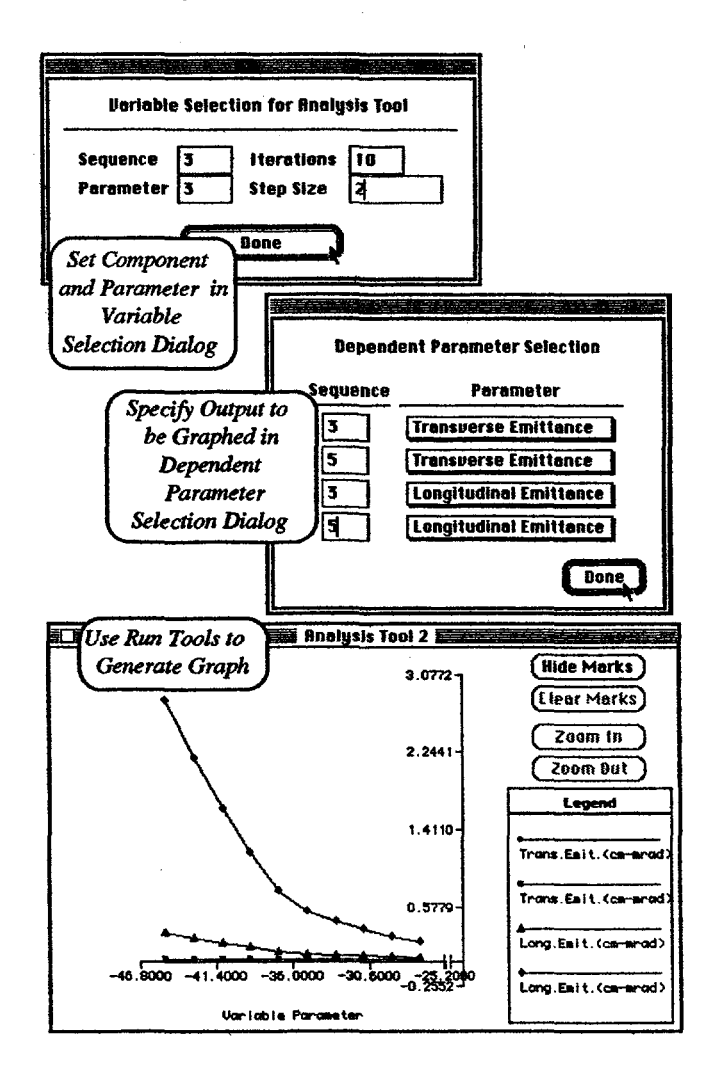
Figure 6.2 Selecting Vector Elements for a Correlation Graph

Once the tool is set up, a check mark appears beside the Output Correlation item on the Analysis Tool menu. Similar to the graphs for Beam and Engineering Vector, the Output Correlation graph may be generated at any time after a Run ASM command has been executed by the Run Tools command.

Parameter Variations

The Parameter Variation tool allows the user to vary any component parameter in a Piece Window and then graph the results for up to four Beam or Engineering Vector outputs. This tool can be used for sensitivity studies or to assist in model optimization. Selection of the Parameter Variation option from the Analysis Tools menu generates two dialogs: one for the parameter to be varied and one for the outputs to be plotted.

Correlation graphs of any two Beam Vector or Engineering Vector elements are also easily generated from the Analysis Tools menu. Once the tool is set up, the Run Tools command is used to generate the graph at any time after a Run ASM command has generated the data. An example of the use of the Parameter Variation tool is illustrated in Figure 6.3.



Graphs displaying the results of parameter variations for up to four elements of the Beam Vector or Engineering Vector are quickly generated from the Analysis Tools menu. Once the Parameter Variation tool is set up, Run Tools calls ASM iteratively to generate the data and display the graph.

Figure 6.3 Generating Graphical Displays of Parameter Variations

All of the support functions for the other Analysis Tools are available for the Parameter Variation graphs. The points used to generate the plots are displayed by selecting Show Marks. The coordinates of any plotted point can be displayed by clicking on the mark for that point. An unlimited number of zooms are available for any region of the graph using Zoom In.

7. Customizing ASM

This section discusses the compilation and linking of the ASM FORTRAN with the SPARC interface object code. This permits the user to customize the application to his particular needs. Users that intend to compile and link a customized version of ASM should be familiar with the Macintosh Programmers Workshop (MPW) version 3.2 and Language Systems FORTRAN compiler version 3.0. The necessary SPARC object code and the ASM FORTRAN source code needed to link with this object code are provided on separate disk from the ASM application. The required FORTRAN compiler may be obtained from Language Systems Corporation. MPW may also be obtained from Language Systems Corporation or directly from Apple Computer Corporation via the Apple Programmers Development Association.

ASM User Manual

A basic knowledge of MPW and Language Systems FORTRAN is assumed. If you are not familiar with the MPW development environment, you might want to work through an example in the MPW manual before attempting to rebuild the SPARC-ASM application. You should make a backup copy of the source code before any modifications. The following is a step by step procedure for setting up a custom application entitled "SPARC-ASM."

- 1. Drag the SLibraries folder (from the Object Code Disk) into the Libraries folder that is inside your MPW folder.
- 2. Create a new folder from which you intend to work. For this discussion let's call it the work folder. This folder may be located anywhere you wish.
- 3. Drag all of the other folders and files from the SPARC Object Code Disk and the FORTRAN Source Code Disk, to the work folder you just created.
- 4. Launch MPW and open the Startup file (located in your MPW folder). Make sure the following commands are in your MPW Startup file; if they are not, then copy and paste them into the Startup file. (If you have not modified the Startup file then these lines will already be there.)

#{MPW} - Directory containing the Macintosh Programmer's Workshop.

Set MPW "{ShellDirectory}"

Export MPW

#{Libraries} - Directory that contains shared libraries.

Set Libraries "{MPW}Libraries:Libraries:"

Export Libraries

#{FLibraries} - Directory that contains FORTRAN libraries.

Set FLibraries "{MPW}Libraries:FLibraries:"

Export FLibraries

5. Copy and paste the following lines into your MPW Startup file, save the MPW Startup file, then quit MPW.

#{SLibraries} - Directory that contains SPARC libraries.

Set SLibraries "{MPW}Libraries:SLibraries:"

Export SLibraries

ASM User Manual

- 6. Returning to your work folder, double click on the LinkInstructions file. This will open the MPW application and make your work folder the default directory.
- 7. Copy and paste the following compilation and link commands to the MPW Worksheet.

```
-o :ASM.f.c:ASMphysics.f.o
FORTRAN : ASM. f : ASMPhysics. f
                                                                            -w -r -u -saveall -sym -mc68882
FORTRAN :ASM.f:SourcePhysics.f
                                      -o :ASM.f.o:SourcePhysics.f.o
                                                                            -w -r -u -saveall -sym -mc68882
FORTRAN : ASM.f:LEBTphysics.f
                                      -o :ASM.f.o:LEBTphysics.f.o
                                                                            -w -r -u -saveall -sym -mc68882
                                      -o :ASM.f.o:RFQphysics.f.o
FORTRAN : ASM.f:RFOphysics.f
                                                                            -w -r -u -saveall -svm -mc68882
FORTRAN : ASM.f:DTLphysics.f
                                       -o :ASM.f.o:DTLphysics.f.o
                                                                            -w -r -u -saveall -sym -mc68882
                                      -o :ASM.f.o:CCIphysics.f.o
FORTRAN : ASM.f: CCLphysics.f
                                                                            -w -r -u -saveall -sym -mc68882
FORTRAN : ASM.f: Funnel Physics.f
                                       -o :ASM.f.o:FunnelPhysics.f.o
                                                                            -w -r -u -saveall -sym -mc68882
Dumlicate ASM.rerc SPARC-ASM
Link -w -t APPL -c SGUI -sym on ô
:SHELL.c.o:Main.c.o :SHELL.c.o:Manus.c.o :SHELL.c.o:Docs.c.o :SHELL.c.o:Palettes.c.o ð
:SHELL.c.o:Pieces.c.o:SHELL.c.o:Tables.c.o:SHELL.c.o:Tape.c.o:SHELL.c.o:Files.c.o\hat{\sigma}
:SHELL.c.o:About.c.o:SHELL.c.o:Dialogs.c.o:SHELL.c.o:Params.c.o
:SHELL.c.o:DEMODummyInterface.c.o :SHELL.c.o:T3DDummyInterface.c.o d
:SHELL.c.o:Graph.c.o :SHELL.c.o:Tools.c.o &
: \lambdaSM.c.o: \lambdaCcel SymModel.c.o : \lambdaSM.c.o: \lambdaSMInterface.c.o : \lambdaSM.c.o: \lambdaSMMenus.c.o \partial
:ASM.c.o:ASMTape.c.o :ASM.c.o:ASMNindows.c.o :ASM.c.o:ASMFiles.c.o d
:ASM.c.o:ASMHotSpots.c.o :ASM.c.o:ASMLimits.c.o :ASM.c.o:ASMTools.c.o ð
:ASM.f.o:ASMInterface.f.o :ASM.f.o:ASMPhysics.f.o 8
:ASM.f.o:SourcePhysics.f.o :ASM.f.o:LEBTphysics.f.o :ASM.f.o:RFQphysics.f.o ∂
:ASM.f.o:DTIphysics.f.o :ASM.f.o:CCLphysics.f.o :ASM.f.o:FunnelPhysics.f.o \theta
* [SIdbraries] *SPARCIdbl.o 8
*{SLibraries}*SPARCLib2.0 8
" [SLibraries] "SPARCLib3.0 &
" [SLibraries] "SPARCLib4.0 @
"{SLibraries}"SPARCIdb5.0 d
* (FLibraries) *IntrinsicLibFPU.o &
* [FLibraries] * FSANELibFPU.o &
* [FLibraries] * FORTRANLib.o &
-o SPARC-ASM
```

The compilation instructions assume you have a the math coprocessor. Remove the -mc68882 compiler directive if you do not have a math coprocessor. The link instructions must also be modified if you do not use a math coprocessor. The FORTRAN FPU libraries should be replaced with the following Libraries:

```
*{FLibraries}*IntrinsicLib.o \hat{\sigma}
*{FLibraries}*FSANELib.o \hat{\sigma}
```

9. Make your modifications to the FORTRAN source files.

ASM User Manual

- 10. After you have made the desired modifications to the source code, select and execute the compile and link commands from the MPW Worksheet, (execute by hitting the "enter" key). Note that any existing ASM application in the work folder named "SPARC-ASM" will be overwritten on link.
- 11. After MPW has completed the compile and link, close your work folder and reopen it in order to set the application icon.
- 12. Now the new application will have the SPARC-ASM icon and it will be ready to run with your FORTRAN modifications.

Appendix:

ASM Physics and Engineering Model Descriptions

ASM Version 1.00 20 July 1993

Accelerator System Model (ASM) Physics and Engineering Model Documentation

ASM Version 1.0

July 1993

George H. Gillespie, Peter K. Van Staagen and Barrey W. Hill

G. H. Gillespie Associates, Inc. P.O. Box 2961 Del Mar, CA 92014

This documentation has been prepared by G. H. Gillespie Associates, Inc. as part of the work completed under Subcontract/Contract Numbers 9-XV3-4570E-1/W-7405-ENG-36

Notice: This document contains technical data whose export may be restricted by the Arms Control Export Act (Title 22, U.S.C., Sec 2751 et seq.) or Executive Order 12470.

Table of Contents

Cr	napter and		Page Sac P
	Sub	section Number and Title	Sec. p
0.	ASM Ov		0. 4
		Introduction	0. 4
		Global Parameters	0. 5
		Parameters Set by Global Pop-Ups	0. 7
		Beam Physics Modeling	0. 9
		Component Engineering Modeling	0. 10
	0.5.	ASM Component Modeling Methodology	0.11
		0.5.1 Beam Vector Representation	0.11
		0.5.2 Engineering Vector Representation	0. 14
	0.6.	ASM System Integration	0. 16
		0.6.1 System Engineering Vector (SEV)	0. 16
		0.6.2 RF Power Subsystem Model	0. 19
		0.6.3 System Configuration Rules	0. 21
		Benchmark Examples	0. 22
		Acknowledgements	0. 25
	0.9.	About the Acronyms and References in this Report	0. 25
1.	Electron	Cyclotron Resonance (ECR) Ion Source Model	1. 1
		ECR Source Model Overview	1. 1
		ECR Model Input	1. 2
	1.2.	ECR Source Beam Vector (BV) Model	1. 6
		ECR Source Engineering Vector (EV) Model	1. 7
		ECR Diagnostic Parameters	1. 12
	1.5.	Interface Parameters To and From Other ASM Models	1. 13
2.	Electron	nagnetic Solenoid (EMS) Low Energy Beam Transport (LEBT) Model	2. 1
		EMS LEBT Model Overview	2. 1
		EMS LEBT Input Data	2. 1
	2.2.	Beam Vector Model for the EMS LEBT	2. 6
		2.2.1 Stripping and Aperture Losses	2. 6
		2.2.2 Beam Transport Equations	2. 8
		2.2.3 R-Matrix Equations	2. 9
		2.2.4 Emittance Growth Modeling	2. 13
	2.3.	EMS LEBT Engineering Vector (EV) Model	2. 18
		2.3.1 LEBT Length Calculation	2. 19
		2.3.3 LEBT Volume Calculation	2. 19
		2.3.3 LEBT Mass Calculation	2. 20
		2.3.4 LEBT Power Calculation	2. 21
		2.3.5 LEBT Transverse Dimensions	2. 23
		2.3.6 EMS LEBT Model Confidence Factor	2. 23

ASM System Model Documentation

Table of Contents (continued)

Chapter and Sub	Subject section Number and Title	Page Sec. p
2.4.	Electromagnetic Solenoid Diagnostic Parameters	2. 24
2.5.	Interface Parameters To and From Other ASM Models	2. 26
2.6.	References for EMS LEBT Model	2. 26
3. Radiofre	equency Quadrupole Two (RFQ-2) Model	3. 1
	Radiofrequency Quadrupole (RFQ-2) Model Overview	3. 1
	RFQ-2 Input Data	3. 1
	Beam Vector Model for RFQ-2	3. 11
	3.2.1 Energy Gain and Beam Current Transmission	3.11
	3.2.2 Transverse Emittance Growth Modeling	3. 13
	3.2.3 Longitudinal Emittance Calculation	3. 15
	3.2.4 Transverse and Longitudinal α Twiss Parameters	3. 18
3.3.	RFQ-2 Engineering Vector (EV) Model	3. 19
	3.3.1 RFQ-2 Length Calculation	3. 19
	3.3.3 RFQ-2 Volume Calculation	3.21
	3.3.3 RFQ-2 Mass Calculation	3.21
	3.3.4 RFQ-2 Power Calculation	3.22
	3.3.5 RFQ-2 Transverse Dimensions	3. 24
	3.3.6 Model Confidence Factor	3.24
3.4.	RFQ-2 Diagnostic Parameters	3.24
3.5.	Interface Parameters To and From Other ASM Models	3.27
3.6.	References for RFQ-2 Model	3. 27
4. ASM El	ectromagnetic Quadrupole (EMQ) Model (for use in TFE routines)	4. 1
	ASM EMQ Model Overview and Formulae	4. 1
	EMQ Engineering Model	4. 5
	References for EMO Model	4. 7

0. ASM Overview

0.0. Introduction

The Accelerator System Model (ASM) is a computer program developed to model proton radiofrequency accelerators and to carry out system level trade studies. The ASM FORTRAN subroutines are incorporated into an intuitive graphical user interface which provides for the "construction" of the accelerator in a window on the computer screen. The interface is based on the Shell for Particle Accelerator Related Codes (SPARC) software technology written for the Macintosh operating system in the C programming language. The User Manual describes the operation and use of the ASM application within the SPARC interface. This report, "Accelerator System Model (ASM) Physics and Engineering Model Documentation," is an appendix to the User Manual and provides a description of the physics and engineering models used in ASM. Not all of the accelerator component models available in ASM Version 1.0 are described here. Those model which were generated, or substantially modified, specifically for this version of ASM are described here. The ASM models available in this version of ASM are summarized in Table 0.1. The models described in this report include the ECR source, EMS LEBT, RFO-2 and TFE.

Table 0.1 Component Models Available in Accelerator System Model (ASM)

Version 1.0 and Reference Documentation.

No.	Accelerator Component	Abbreviation	Description	Reference
0	Test Vector	TV or BV	Used to test other models	[User Manual]
1	Volume Source	VOL	Negative ion volume source	[1]
2	Penning Source	SPS	Negative ion surface plasma sour	rce [1]
3	Electron Cyclotron Source	ECR	Positive ion ECR source	[This Report]
4	Quadrupole LEBT	PMQ	Permanent magnet quadrupole LEBT for negative ions	[1]
5	Solenoid LEBT	EMS	Electromagnetic solenoid LEBT for positive or negative ions	[This Report]
6	Radiofrequency Quadrupole	RFQ-1	RFQ model number 1	[1]
7	Radiofrequency Quadrupole	RFQ-2	RFQ model number 2	[This Report]
8	Drift Tube Linac	DTL	DTL with different goal options	[1]
9	Coupled Cavity Linac	CCL	Side coupled cavity linac	[1]
10	U Shaped Funnel	HEF	Funnel primarily for high energy	[1]
11	Y Shaped Funnel	LEF	Funnel primarily for low energy	[1]
ade long	Quadrupole Lattice	TFE	Lattice for other ASM models	[1, This Report]

as Global Parameters. There are ten user input Global Parameters available in ASM. These parameters, their default units, default values and user guidance limits are summarized below in Table 0.2.

Table 0.2 Global Parameter Inputs for the Accelerator System Model (ASM).

Element Parameters (Symbol)	Default Value*	Default Units	User Guidan Lower	ce Limits Upper
Particle Charge	+1	e	-1	+1
Particle Mass A	+1.0073	amu	1.0073	3.0200
Final Beam Energy E_{final}	+800	MeV	1	1000
Final Beam Current Goa	+100	mA	0	500
Fundamental Frequency f_1	+425	MHz	200	850
Duty Factor df	1	(none)	0.0001	1
Operating Time t_{oper}	24	hours	1 second	365 days
Temperature Regime Q_{eh}	ambient	(none)	ambient, cryogenic, superconduction	ng, user defined
Quad Magnetic Material MM_{linac}	samarium cobalt	(none)	electromagnetic, vario	us PMQ's, user defined
Structural Material SM_{linac}	copper	(none)	beryllium, various met	als, user defined

The input of Global Parameters by the user is accomplished through the Global Parameter Pane of the ASM Document Window. Only six (6) Global Parameters can be viewed at once, the others can be accessed by scrolling the Global Parameter Pane. This is illustrated in Figure 1.

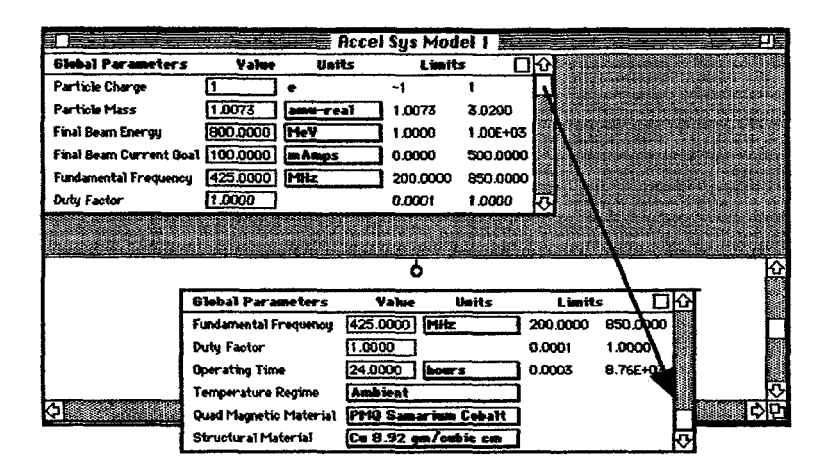


Figure 0-1. Global Parameters are input using the scrollable Global Parameter Pane of the ASM Document Window.

The first seven (7) Global Parameters have numerical inputs and the user guidance limits are soft limits. That is, any value may be input by the user and that value will be used by ASM without adjustment. If a guidance limit is violated, that limit is high-lighted visually to alert the user that there may be impractical consequences of that parameter value, but ASM will still accept the input value. Three (3) Global Parameters have a finite number of input options and the user can only select from the available options. However, all of these parameters have a user definable option.

There are a number of other top-level parameters which are set in the ASM FORTRAN code. These are referred to as FORTRAN data parameters and include parameters such as ΔR_s , the assumed thickness of the linac structural components. These parameters are written to the Diagnostics file.

0.2. Parameters Set by Global Pop-Ups

Three (3) Global Parameters are set by pop-up menus in the ASM interface. These are the last three Global Parameters shown in Table 0.2. Each of these parameters have a finite number of options including a user definable option. The pop-up menus for these Global Parameter options are illustrated Figure 0-2.

Ambient Cryogenic Superconducting User Defined Electromagnetic Quads
PMQ Samarium Cobalt
PMQ Neodynium Iron
PMQ Boron (C.322)
PMQ Boron (C.355)
PMQ Praseodymium
PMQ User Defined

Be 1.85 gm/cubic cm A1 2.70 gm/cubic cm Fe 7.86 gm/cubic cm Cu 8.92 gm/cubic cm Nb 8.66 gm/cubic cm User Defined

Figure 0-2. Options for the Global Parameters of Temperature Regime, Quad Magnetic Material and Structural Material.

The numerical values of certain FORTRAN data parameters are determined by the selection of these Global Parameters. These data parameters are summarized in Table 0.3.

Table 0.3. ASM Pop-Up Global Parameter Selections.

Element Parameters (Symbol)	Parameter Index	Description		AN Data neter(s)
Temperature Regime Q_{eh}	·	Approximate Temperature	Q Enha	ncement
Room Temperature	1	300 K		1
	2	20 K		5
	3 4	4 K User Defined	_	0+4 Specified
Quad Magnetic Material		Quadrupole Type		
MM_{linac}		or Material	B_r (kilogauss)	ρ (kg/m ³)
	0	Electromagnetic	N/A	N/A
	1 (In	Samarium Cobalt ncor-26 HE Sm ₂ Co ₁₇)	10.6	8.3·10+3
	2	Neodymium Iron	10.4	7.55·10+3
	3	Boron (Crumax 322)	11.6	7.55·10 ⁺³
	4	Boron (Crumax 355)	12.3	7.40·10+3
	5	Praseodymium	14.0	$6.8 \cdot 10^{+3}$
	6	User Defined	User Specified	User Specified
Structural Material				
SM_{linac}		Material (Z)	ρ (k	(g/m ³)
	1	Be (3)	1.85	5·10 ⁺³
	2	Al (13)	2.70)·10+3
	3	Fe (26)	7.86	5·10+3
	4	Cu (29)	8.92	2·10+3
	5	Nb (41)		5·10+3
	6	User Defined	User S	Specified

0.3. Beam Physics Modeling

The basic approach to modeling the accelerator beam in ASM involves representing the beam at any place in the accelerator system by a vector. The vector's elements are physical properties of the beam at that point. For example, the beam energy E, current I, and emittance ε can be used to define the beam. This vector is the beam representation vector, or simply the Beam Vector (BV). To increase the sophistication of the beam modeling, one increases the number of elements included in BV, i.e. increases the dimension of the Beam Vector. The fidelity of the computer model depends on the dimensionality, N, of the BV: increasing N increases the fidelity of the model.

A matrix represents each device of the accelerator system (e.g., RFQ, DTL, etc.). This matrix maps the input BV into an output BV by matrix multiplication. In addition to this matrix, the device modeling requires the addition of a column vector which augments the output BV by vector addition. For a particular accelerator component, this matrix and its associated augmentation vector are labeled the device matrix (DM) and the device vector (DV). They define the component's effect on the BV. Independent of the DM or DV's dimensionality, the fidelity of the model also depends on the sophistication used to model a given element in the DM or DV. Sections 1 through 3 describe in detail several of the models used in ASM. The general model equation for each device follows:

$$[BV_o] = [DM] [BV_i] + [DV]$$
 (0.1)

Although ASM uses the matrix formulation, the modeling formalism does not require a matrix representation. For a particular device, any set of formulae mapping the input BV into the output BV will suffice.

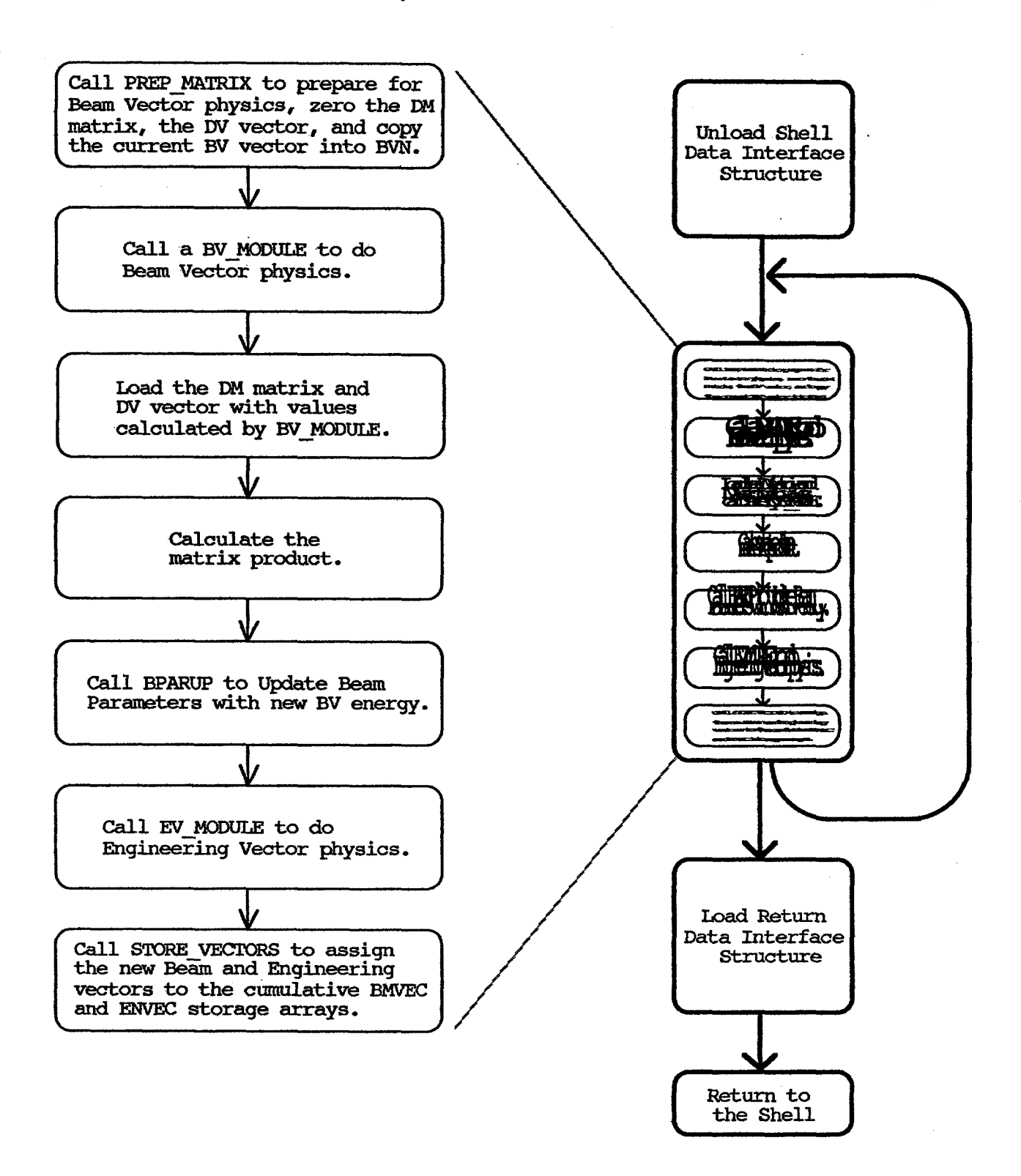
Formally, the flexibility of this approach to accelerator modeling is easy to visualize. One starts by specifying numerical values of the beam vector at any point (BV)_i in the system. By repeated application of the matrix equation,

$$(BV)_{i+1} = (DM)_i (BV)_i + (DV)_i$$
 (0.2)

one can advance the beam to any further position along the system.

The advancement of the BV along the accelerator is carried out when the Run ASM command is executed, that is after the model has been completely defined. These calculations are all done on the FORTRAN side of ASM. Figure 0-3 provides a flow chart of the FORTRAN structure of ASM.

Another advantage of this matrix representation is that the level of sophistication in modeling for a particular device is improved by incorporating additional matrices. For example, the model for a drift-tube linac could be a series of matrices which advance the beam vector tank-by-tank or even cell-by-cell. For further detail, each cell could be represented by a series of matrices. Each series describes the beam transport through the magnetic quadrupoles and drift-tubes, the acceleration gap, and the impulse model for the space charge. In this case, the code would closely resemble linac design codes which use matrix representations to model these elements. In principle, the ASM code can simulate accelerator components in great detail.



0.4 Component Engineering Modeling

In addition to the beam parameters associated with the output (or input) of a particular device model, an auxiliary set of variables are associated with the engineering of the device. This set includes the power required (P) to drive the device, the mass (M) of the device, its transverse dimensions, etc. An Engineering Vector (EV) represents these data for each device, and the total system weight, size, etc., can be computed from these vectors. These data do not directly influence the beam characteristics in the same sense that the DM's and DV's do, but the DM, DV, and EV do depend on common parameters. Thus, constraints imposed on the elements of EV's affect the device matrices and the beam's performance. Conversely, constraints on beam performance or device specifications, limit the EV's elements.

0.5 ASM Component Modeling Methodology

The matrix approach to accelerator modeling described above has one advantage in that it provides a systematic and general method for formulating the mathematical structure that is the same for all components being modeled. This approach provides a standardized format for the representation of any beam line component. The key to the success of this approach lies in the ability to construct matrices which provide a reasonably faithful representation of each device. The remainder of this section describes the methodology used to develop the accelerator scaling model based on the matrix approach.

0.5.1 Beam Vector Representation

A basic assumption use in ASM is that the distribution function of the particles in the beam is essentially Gaussian in each phase-space plane. For example, in the x transverse dimension, this means that the particle distribution f(x,x') is given by

$$f(x,x') = \frac{\beta \gamma}{2\varepsilon_{x,rms}} \exp\left(-\frac{\gamma_{rx}x^2 + 2\alpha_{rx}xx' + \beta_{rx}x'^2}{2\varepsilon_{x,rms}} \pi \beta \gamma\right)$$
(0.3)

Here $\varepsilon_{x,rms}$ is the normalized, root-mean-square, area of the x-x' transverse phase space occupied by the beam. The γ_{Tx} , β_{Tx} , and α_{Tx} are the usual Twiss or Courant-Snyder phase-space ellipse parameters, and β and γ are the standard relativistic velocity (v/c) and energy $(1+E/mc^2)$ parameters.

This form of the distribution function is reasonable for many accelerator beams and has several convenient features. However, one limitation of this parametrization of the beam distribution is that the tails of this distribution are not representative of real beams. Thus, for modeling effects in which the tails of the beam are important, some additional information on the distribution function is needed. In many cases, particles in the tails of the distribution are lost for practical purposes and this particle loss can be treated by using an effective current efficiency factor. The estimates of these losses in Version 1.0 of ASM are primarily based upon the assumption of a Gaussian distribution. For applications of ASM to high average power linacs, of the type required for the

distribution. For applications of ASM to high average power linacs, of the type required for the Accelerator Production of Tritium (APT), the Accelerator Transmutation of Waste (ATW) or Fusion Materials Irradiation Facilities (FMIF), the incorporation of a halo model would be desirable.

Given the beam distribution function specified by form (0.3) in each of the three phase-space planes, the beam's kinetic energy (E), and its average current (I), the specification of the beam is complete. To model any element in the linac system, one specifies the input-output relationship between E, I, $(\varepsilon_{x,ms})$, and the phase-space parameters $(\alpha_{Tx}, \beta_{Tx}, \gamma_{Tx})$ for each plane. Only two of the phase-ellipse parameters appearing in Equation (0.3) are independent, since the identity

$$(\beta_{Tx}\gamma_{Tx} - \alpha_{Tx}^2 = 1) \quad , \tag{0.4}$$

must be satisfied. One choice for the Beam Vector which would completely specify the beam in this representation then, is the eleven dimensional column vector:

$$(BV) = \begin{bmatrix} E \\ I \\ \varepsilon_{x \ rms} \\ \gamma_{Tx} \\ \beta_{Tx} \\ \varepsilon_{y \ rms} \\ \gamma_{Ty} \\ \beta_{Ty} \\ \varepsilon_{z \ rms} \\ \gamma_{Tz} \\ \beta_{Tz} \end{bmatrix}$$

$$(0.5)$$

Although this 11-dimensional representation is not that used in ASM Version 1.0, it is briefly discussed here because it provides the highest level of fidelity for beam modeling that is likely to be considered for ASM. Much of the existing literature is formulated in terms of these, or closely related, variables. For example, it can be used to model the 6-dimensional phase-space matching important for the interface between different accelerator components.

The relationship of the 11-dimensional representation to the general moment representation of a bunched beam is illustrative. The representation given by (0.5) includes the zero moment (total charge) via the current, the first longitudinal velocity moment via the energy, and the second (spatial and velocity) moments for each plane via the emittances and Twiss parameters. It does not include the first transverse (spatial or velocity) moments, the first longitudinal spatial moment, nor

cross-plane moments such as the x-y moment. Compared to a moment representation through second order then, the representation (0.5) neglects those associated primarily with modeling misalignments and correlations (e.g. skew quadrupoles) between the planes. This is consistent with the general ASM approach aimed at modeling nominal, not off-normal, accelerator operation.

The representation for the BV used in ASM is built upon previous experience, beginning in the mid 1980's, in developing linac models using this same methodology. The previous work developed accelerator modeling codes using both 4-dimensional and 6-dimensional BV representations. In addition to the increased dimensionality, there was a continual improvement in the algorithms used to model components. This trend in increased fidelity of the modeling has been extended with ASM, which uses an 8-dimensional representation of the Beam Vector:

$$BV = \begin{bmatrix} E \\ I \\ | < x^{2} > \\ | & \varepsilon_{t,rms}^{2} \\ | < \Delta p^{2} > \\ | & \varepsilon_{l,rms}^{2} \\ | & \alpha_{l} \\ | & \alpha_{l} \end{bmatrix}$$

$$(0.6)$$

There are some changes in variables used in Equation (0.6) as compared to (0.5). Note that quadratic forms for the emittances, $\varepsilon_{t,rms}^2$ and $\varepsilon_{l,rms}^2$, are adopted. These forms are more natural representations for most of the models developed. Rather than using the γ_T and β_T parameters to describe the beam ellipses, the BV uses the parameters α_t and α_p and two other parameters, x^2 and Δp^2 . These latter two, the mean square transverse (horizontal) dimension of the beam and the mean square momentum dispersion, are related to the Twiss parameters and emittances by:

$$x^2 = \beta_{Tx} \varepsilon_{t,rms} \quad , \tag{0.7}$$

and

$$\Delta p^2 = (1 + \alpha_l^2) \, \varepsilon_{l,rms} / \, \beta_{Tz} \quad . \tag{0.8}$$

However, the primary difference between this 8-D representation for the Beam Vector, and the 11-D representation of Equation (0.5), is that the two transverse planes are treated as equal. This is essentially a restriction that the two transverse emittances be equal $(\varepsilon_{x,rms} = \varepsilon_{y,rms} = \varepsilon_{t,rms})$. With this restriction, the 8-D representation is still adequate to model not only cylindrically symmetric beams, but also beams in alternating quadrupole focusing channels. This is possible with the

understanding that the representation of Equation (0.6) is used to describe the beam at points along the accelerator where the beam has spatial symmetry, $x^2 = y^2$, and where the two planes are converging and diverging with equal angles, $\alpha_{Tx} = -\alpha_{Ty}$, so that α_t is used to represent the magnitude of these two transverse Twiss parameters.

The basic equations that use these variables are matched envelope equations with additional information determined from experiments and particle beam simulation codes. These envelope equations and additional information, together with constraints of several different types, form the bulk of the scaling code's "knowledge base."

Sections 1 through 3 of this report outline the derivations of three of the device models used in ASM Version 1.0.

0.5.2 Engineering Vector Representation

In addition to the beam physics model, a parallel description of the engineering parameters for the accelerator components is provided by an Engineering Vector (EV). This vector contains the majority of the engineering oriented parameters of the computer code. The EV elements for each component include: (1) device length, (2) device volume, (3) device weight, (4) device power requirement, (5) the maximum horizontal and (6) vertical dimensions of the component, as measured from the beam axis, (7) a confidence factor for the device as modeled, and (8) a cost estimate for the device. Some of these are straightforward (e.g., the device length) while others have a number of parameters incorporated (e.g., the power requirement which may be d.c. or r.f. and depends on the duty factor, etc.) In order to use the information in the individual EV's, to develop an estimate of the total accelerator power requirement for example, a subroutine of the code combines this information into an overall system EV. The EV is written as:

$$\begin{bmatrix} L \\ V \\ W \\ M \\ P \\ EV = \begin{bmatrix} x \\ x \\ y \\ Conf \\ Cost \end{bmatrix}$$
(0.9)

The confidence factor, Conf, and cost estimate, Cost, require further comment since there are some subjective decisions involved in defining and estimating then. Conf is assigned a value between 0 and 1, with 1 being a "100% confidence model." In general, within a given parameter regime, this parameter represents an estimate of the validity of the beam physics predictions, and engineering parameter estimates, of a particular device. If a given model is used outside of its known parameter regime, this confidence factor tends toward zero. The confidence factor guides the user on how feasible a particular application of the device might be. The guidelines used in

assigning specific numerical values are given in Table 0.4.

There is no cost model for the individual components in ASM Version 1.0. Consequently Cost = 0 for each beam line component. A simplified version of the Lawrence cost model [2] has been included in the System Integration model as an illustration of the capabilities of ASM.

The Test Vector component in ASM, component Type number "0" in Table 0.1, has no engineering associated with it. It is used for evaluating the BV characteristics of a component or group of components in a beam line. All EV parameters for the Test Vector, except *Conf*, are assigned to be zero so that they make no contribution to the summations in the ASM System Integration model. *Conf* is assigned the value of unity, so that the presence of a Test Vector does not degrade the system level confidence factor which is based on a product of individual confidence factors.

Table 0.4. Rationale for Assignment of Device Confidence Factors

Value	Description of Model Confidence
0.95-1.0	Hardware Experience, Data to Support Modeling
0.9-0.95	Good Engineering Design, Sound Physical Principles (SOA*), Modest Extrapolation from POP** Experiment
0.75-0.90	Good Conceptual Design, Sound Physical Principles, Significant Extrapolation From POP Experiment
0.5-0.75	Sound Conceptual Design, No POP Experiment
0.1-0.5	Possible in Principle, but only Vague Conceptual Design
below 0.1	Speculative at Best
0	Outside Validity of Scaling Laws

^{*}SOA - state-of-the-art

Most models in ASM Version 1.0 have confidence factors in the 0.7 to 0.9 range. (As noted above, the Test Vector confidence is set to unity.)

Funnel components are assigned two EVs each. Funnels have two radio frequencies associated with them, and one frequency is associated with each funnel BV. The division of other engineering properties between the two EVs is determined by whether the component is upstream or downstream of the funnel's RF deflector. The first EV for each funnel is for the lower frequency and all upstream components, and the second EV for each funnel is for the higher frequency and all

^{**}POP - proof of principle

0.6 ASM System Integration

ASM contains a set of subroutines for integrating the various EV data, computed for each component, into a system level summary. In Version 1.0, the results of this integration are summarized in a System Engineering Vector (SEV). The SEV is computed each time the Run ASM command is executed and the results are written to the same output file that contains the BV and EV data for each component. The subroutines for the SEV are on the FORTRAN side of ASM and may be modified by the user as desired.

ASM also includes a system level beam line configuration evaluation routine. This routine is executed when the Evaluate Constraints command is executed. A series of rules are examined to check for the overall validity of the order of the components on the beam line and for the self consistency of the model with respect to the Global Parameters. In Version 1.0, these rules are relatively simple, i.e. is an ion source the first component of the beam line and is the ion source type consistent with the particle charge Global Parameter? The routines which do the beam line configuration evaluation are part of the ASM expert system rules and are on the SPARC interface side of ASM.

0.6.1 System Engineering Vector (SEV)

The ASM System Engineering Vector is of the same form as that used for each of the components in an ASM model. This form is given in Equation (0.8). The elements of the individual component EVs are integrated to provide an overall description of the complete accelerator system. This integration depends upon the configuration of the beam line and on other subsystems for the model. For example, the overall length of the accelerator in the absence of funnels is a simple summation of the individual lengths. However, when the beam line contains Y funnels then the length and horizontal extent of the complete system depend upon the angles of the funnel legs. This system integration subroutines are designed to accommodate these variations in providing an overall description.

ASM is designed so that subsystems other than the accelerator beam line can be incorporated into the system model. Subsystems of interest might include the vacuum, cooling or thermal management, and radiofrequency (RF) power subsystems. To date, this capability of ASM has not been fully exploited. However, Version 1.0 contains an basic RF power model as an example of how these subsystems can be incorporated. The RF power model is used in the computation of the overall "wall plug" power given by the fourth element of the SEV.

The first step in computing the SEV is to divide the beam line into segments. Generally, each segment corresponds to one "leg" of the beam line, that is, each section of the beam line defined by a funnel at one end or the other. A segment Engineering Vector is computed for each of these segments. The primary purpose of this division is to provide a basis for breaking up the beam line which can account (1) for the different geometric layouts and (2) for the different RF frequencies. Funnel components themselves have two frequencies associated with them, and there are two EVs computed for each funnel. A funnel component has one EV assigned to each of the upstream and downstream beam line segments. Within each segment the integration of the EV is straightforward. Basically, the physical properties and cost elements are added and the confidence factors are multiplied. Allowance is made for components which have only a DC (i.e. not RF)

power requirement. Specifically for the segment length, volume and mass:

$$L_{seg} = \sum L_i \quad , \tag{0.10}$$

$$V_{seg} = \sum V_i \quad , \tag{0.11}$$

and

$$M_{seg} = \sum M_i \quad . \tag{0.12}$$

The summation in each case runs over the components in that segment of the model, with the understanding that each of the two funnel EV elements are assigned to the appropriate upstream or downstream segment. For the segment power, the total RF power is computed from

$$P_{seg} = \sum P_i$$
 (Type) for Type $\neq 1,2,3,4$, or 5 , (0.13)

and the DC power from

$$P_{DC} = \sum P_i$$
 (Type) for Type = 1,2,3,4, or 5 . (0.14)

In Equations (0.13) and (0.14) the Type number refers to the component numbers given in Table 0.1. In Equation (0.13) the summation runs over the components in the corresponding segment. In Version 1.0 of ASM the summation in Equation (0.14) runs over the entire model. It is implicitly assumed in Version 1.0 of ASM that all DC power components are at the beginning of the accelerator, and are assigned to the first segment.

The transverse dimensions for each segment are taken to be the maximum values of the corresponding horizontal and vertical dimensions of the components in the segment:

$$x_{see} = \text{Max}[x_i] \quad , \tag{0.15}$$

and

$$y_{seg} = \text{Max}[y_i] . (0.16)$$

This assignment for the transverse dimensions, together with the length given by Equation (0.10) provides the dimensions of segment box $(2x_{seg}, 2y_{seg}, L_{seg})$ into which the segment hardware will fit.

The confidence factor for the segment is computed as the product of individual component confidence factors:

$$Conf_{seg} = \prod Conf_i \quad . \tag{0.17}$$

The segment cost is computed as an unweighted sum:

$$Cost_{seg} = \sum Cost_i \quad , \tag{0.18}$$

As noted above, ASM Version 1.0 contains no cost models for individual components so that this summation will be zero. Users may, of course, add cost models to the ASM FORTRAN and, if desired, add a weighted sum or other cost integration model.

The SEV is computed from the individual segment EVs given by (0.10)-(0.18). For each funnel in the beam line there is an additional segment generated (the number of segments is the number of funnels plus one). Each segment contains several "legs." The number of legs in each segment is 2 raised to the power of the number of funnels (or, more correctly, the number of funnel stages) which follow that segment upstream, i.e. the number of funnels between that segment that the high energy end of the accelerator. The total system volume and mass are computed by adding the contribution from all legs:

$$V_{system} = \sum (2)^{n(seg)} V_{seg} , \qquad (0.19)$$

and

$$M_{system} = \sum (2)^{n(seg)} M_{seg} . \qquad (0.20)$$

where n(seg) is the number of funnel stages between the segment and the high energy end of the beam line. The system cost is computed in a similar manner.

The vertical dimension of the system is computed from the maximum vertical size of any segment,

$$y_{system} = Max[y_{seg}] , \qquad (0.21)$$

and the system confidence factor is computed as the product of the segment confidence factors,

$$Conf_{system} = \prod Conf_{seg} . (0.22)$$

The system length and horizontal dimensions are straightforward if no Y funnels are in the beam line and are given by formulas analogous to Equations (0.10) and (0.15). When Y funnels are present the beam line is no longer straight. ASM Version 1.0 computes the system length as the projection of the segments along the axis defined by the last (high energy end) component in the model. The system horizontal dimension is computed as the maximum perpendicular extent of the model, defined as the funnel plane, from this axis. These computations require the cumulative Y (LEF) funnel bend angles, which are given by the sum of the user inputs to LEF funnel components. These calculations are not further described here, but the result is that the SEV elements for the length and transverse dimensions define a box (e.g. building) whose dimensions $(2x_{system}, 2y_{system}, L_{system})$ will enclose the entire accelerator beam line.

The computation of the total system power is discussed in the next subsection.

0.6.2 RF Power Subsystem Model

The RF power subsystem model in Version 1.0 of ASM allows the selection of any of four different amplifier technologies, for frequencies up to six (6) multiples of the fundamental frequency. For each technology option, there are three inputs available to the user: the maximum output power from a single amplifier, the specific mass of the amplifier, and the effective efficiency of the amplifier. A summary of the amplifier technologies, the default values for the input parameters, and the user guidance limits for the parameters is given Table 0.5. The windows to input this data are accessed from the RF Power selection on the Preferences menu (ASM User Manual, Figure 5.3, page 35).

Table 0.5 Summary of Input Parameter for the RF Power Subsystem Model.

Amplifier Technology Parameter - Symbol	Default Value*	Default Units	User Guidance Limits Lower Upp		
Klystron					
Max Tube Power - P _m	+1.0	MW	0.1	4.0	
Specific Mass - M _s	+2.0	gm/W	1.0	4.0	
Efficiency - η	+60	%	50	70	
Klystrode					
Max Tube Power - P _m	+0.25	MW	0.1	0.5	
Specific Mass - M _s	+0.5	gm/W	0.3	1.0	
Efficiency - η	+70	%	60	75	
Solid State					
Max Module Power - P _m	+0.06	MW	0.02	0.1	
Specific Mass - M _s	+1.0	gm/W	0.9	1.2	
Efficiency - η	+50	%	40	60	
Gridded Tube					
Max Tube Power - P _m	+0.06	MW	0.02	0.1	
Specific Mass - M _s	+1.0	gm/W	0.5	2.0	
Efficiency - η	+50	%	40	60	

0.6.3 System Configuration Rules

The Evaluate Constraints command calls a routine on the SPARC interface side of ASM that conducts a top level examination of the current beam line on the Model Space. The examination involves the use of a set of rules which an expert would normally apply in the design of any linac beam line. The rules incorporated into ASM Version 1.0 are relatively basic and are intended to illustrate the capability of this type of command. This initial set of rules is also incomplete and should be viewed with this mind. When the Evaluate Constraints option is selected from the ASM Commands menu, a text report is displayed in a window summarizing the results of the examination. A sample report, for the beam line shown in Section 2 of the ASM User Manual (Figure 2.3, page 9), is shown in Figure 0-3 below.

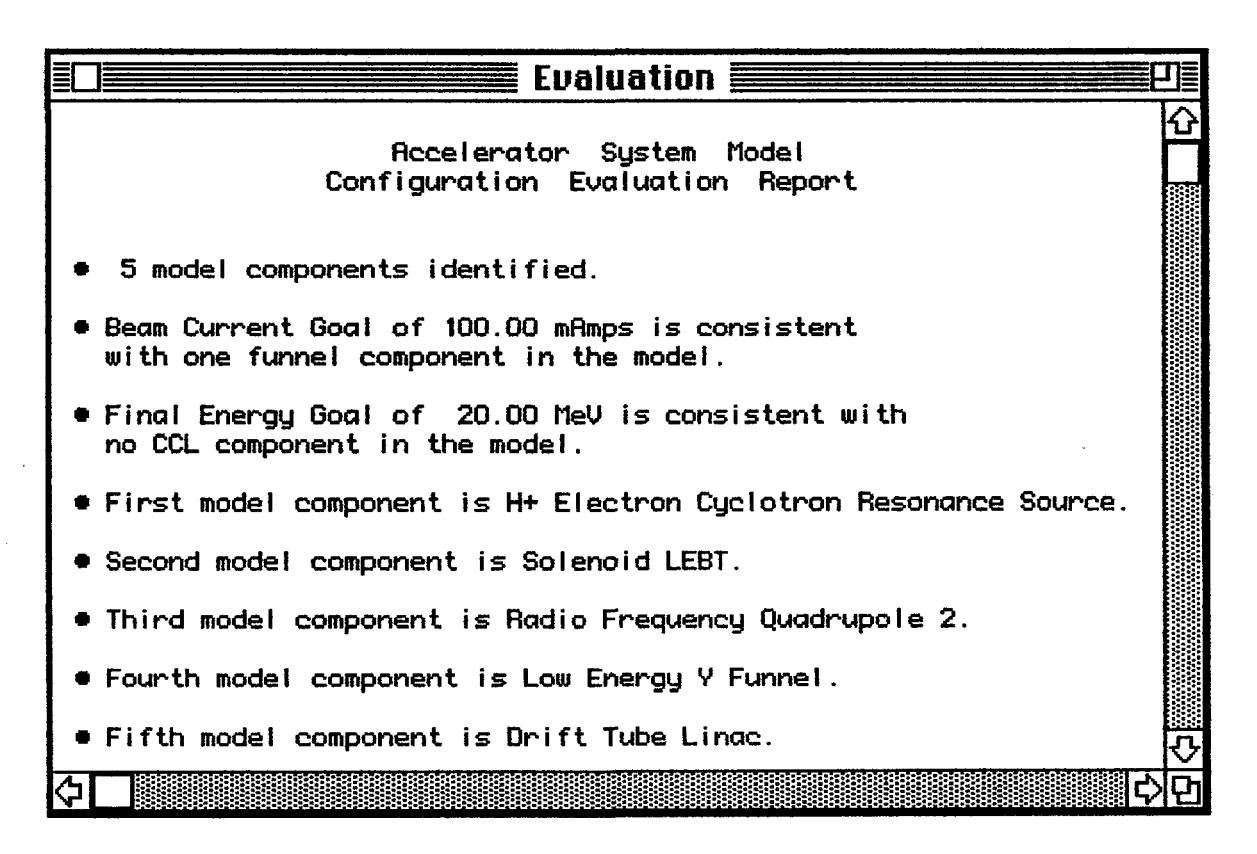


Figure 0-3. Example of Output from the Evaluate Constraints Command.

The configuration rules evaluated in ASM Version 1.0 are summarized in Table 0.6. Again it should be emphasized that the rules incorporated into ASM Version 1.0 are simple and not as complete as one might desire. (The Evaluate Constraints command in ASM Version 1.0 is for demonstration purposes.)

Table 0.6. ASM Component Configuration Rules Used in the Evaluate Constraints Command.

Component	Rule Evaluated Glo	obal Parameter(s) Checked
Ion Source	First Component of Model	N/A
VOL	Negative Ion Beam	Particle Charge
SPS	Negative Ion Beam	Particle Charge
ECR	Positive Ion Beam	Particle Charge
LEBT	Second Component of Model	N/A
PMQ	Negative Ion Beam	Particle Charge
EMS	Any Ion Beam	N/A
RFQ	Third Component of Model	N/A
RFQ-1	•	N/A
RFQ-2		N/A
Funnels	Possible Fourth Component	N/A
HEF	Final Current Over 100 mA	Beam Current
LEF	Final Current Over 100 mA	Beam Current
DTL	Possible Fourth Component	N/A
CCL	Any Possible Component	N/A
HEF	Final Energy Over 100 MeV	Beam Energy

0.7. Benchmark Examples

Several accelerator designs have been used for comparisons with ASM results. In this Section, we present ASM for two systems: (1) a low energy machine, the CRNL RFQ1-1250 beam line, where results are compared to experiment and (2) a high energy design based developed for the accelerator transmutation of waste (ATW).

The comparison for the CRNL RFQ1-1250 beam line is shown in Figure 0-4. The standard ASM format for the Beam Vector and Engineering Vector output is used. The top half of the Figure shows the ASM model results for this beam line. The lower half has the same results displayed, except that experimental data available from the literature are shown in *italics*. Only non-trivial comparison data are used, e.g. the output energy of each component (ECR source, LEBT and RFQ) are identical by model construction.

Accelerator System Model.

				BEAM VE	CIORS			
	ENERGY	CURRENT	RADIUS	TRANSVERSE EMITTANCE	ď₽	LONGITUDINA EMITTANCE		ALPHA LONGETUDENAI
	(MeV)	(sub)	(cm)	(con-micad)	(MeV/c)	(cm-mcad)	-	-
ECR	0.05000	0.05200	0.13274	0.01400	0.00000	0.00000	0.00000	0.00000
ems	0.05000	0.05200	0.07365	0.01400	0.00000	0.00000	2.50000	0.00000
RFQ	1.25000	0.05092	0.08303	0.02174	0.18803	0.07953	1.70000	0.04000
				ENGINEERING	VECTORS			
	LENGIH	VOLUME	MASS	POWER	Size(X)	Size(Y)	CONFIDENCE	COST
	(m)	(m**3)	(Kg)	(MN)	(m)	(m)	(fraction)	(\$)
ECR	1.57871	0.31574	2.66et02	0.00912	0.25000	0.20000	0.90000	0.0
ems	0.46902	0.08799	2.22e+02	0.02136	0.50300	0.50300	0.90000	0.0
RFQ	1.44060	0.18119	1.17e+03	0.16627	0.14056	0.79556	0.90000	0.0
	3.48833	0.58492	1.65e+03	0.16627	0.50300	0.79556	1.72900	0.0
			Results	for Paramete	ers from 1	<i>iterature</i>		
				References 2	253, 485,	486		

	ENERGY	CURRENT	RADIUS	TRANSVERSE EMITTANCE	ď₽	IONGETUDINA EMITTANCE		ALPHA LONGFIUDINA
	(MeV)	(amp)	(cm)	(cm-mrad)	(MeV/c)	(cm-mcad)	-	-
ECR -	0.05000	0.048	0.13274	<0.012	0.00000	0.00000	0.00000	0.00000
EMS	0.05000	0.048	0.07365	0.01400	0.00000	0.00000	2.50000	0.00000
RFQ	1.25000	0.037	0.08303	<0.045*	1.26**	0.07953	1.70000	0.04000

ENGINEERING VECTORS

	LENGIH (m)	VOLUME (te**3)	MASS (Kg)	POWER (MW)	Size(X) (m)	Size(Y) (M)	CONFIDENCE (fraction)	COST (\$)
ECR	1.57871	0.31574	2.66e+02	0.00912	0.25000	0.20000	0.90000	0.0
EMS	1.0	0.08799	2.22e+02	0.02136	0.50300	0.50300	0.90000	0.0
RFQ	1.4688	0.18119	1.17e+03	0.179*	0.14056	0.79556	0.90000	0.0
			*.135 + +	0.044				
	3.48833	0.58492	1.65eH03	0.16627	0.50300	0.79556	1.72900	0.0

Figure 0-4. Comparison of ASM Beam and Engineering Vector Output (top) for the CRNL RFQ1-1250 Beam Line with Selected Experimental Results (italics).

0.8. Acknowledgements

The authors are indebted to a number of individuals who have contributed to the development of the physics and engineering models incorporated into ASM. John L. Orthel and Lawrence A. Wright provided major contributions to the development of models for the LSDC and ODIN computer codes. These included versions of the volume ion source, electromagnetic solenoid LEBT, funnel, and CCL algorithms now included in ASM. Conversations with several scientists at LANL have yielded additional insight into the development requirements of the both the physics and engineering models and the graphical user interface. We specifically acknowledge fruitful discussions with George Lawrence, Robert Jameson and Don Liska. James Gillespie and Aaron Sutton deserve recognition for their contributions to the graphical output displays utilized in ASM.

0.9. About the Acronyms and References Used in This Report

References are given at the end of each major Section of this report. Only two references are cited in this Overview Section. These are:

- [1] "Physics and Engineering Models for the Beam Generator Subsystem of the ODIN 2 NPB Platform Scaling Code," George. H. Gillespie, Barrey W. Hill, John L. Orthel and Lawrence A. Wright, G. H. Gillespie Associates, Inc. Report No. GHGA-91-254-R, September 1991.
- [2] "Scaling and Optimization in High-Intensity Linear Accelerators," R. A. Jameson, P. J. Tallerico, W. E. Fox, N. Bultman, T. H. Larkin, R. L. Martineau and S. J. Black, Los Alamos National Laboratory Report No. LA-CP-91-272, July 1991.

With the exception of Section 4., references in other Sections are not numbered in order, but utilize a database reference number. These references are included in a computer literature database on linear accelerators maintained by G. H. Gillespie Associates, Inc. The complete citation for each reference is included at the end of each Section in which it is used.

A fairly large number of acronyms are in common use within the linear accelerator community. They are used through out this report. We have added a few additional ones in the course of this work as well. Table 0.7 attempts to summarize the acronyms and abbreviations used in this report.

Table 0.7. List of Abbreviations and Acronyms Used in the ASM Documentation.

Acronym	Description (identification if ASM specific)
ANL	Argonne National Laboratory
ASM	accelerator system model (what this ASM documentation is all about)
ATS	accelerator test stand, a LANL accelerator
BEAR	beam experiment aboard a rocket
BV	beam vector
CCL	coupled cavity linac (ASM side-coupled CCL model)
CRNL	Chalk River Nuclear Laboratories, Canada
CW	continuous wave
CWDD	continuous wave deuterium demonstrator, a GAC accelerator at ANI
DM	device matrix
DTL	drift tube linac (ASM DTL model)
DV	device vector
ECR	electron cyclotron resonance (ASM ion source model)
EMS	electromagnetic solenoid (ASM LEBT model)
EV	engineering vector
GAC	Grumman Aerospace Corporation
GTA	ground test accelerator, a LANL accelerator
HEBT	high energy beam transport
HEF	high energy funnel (ASM U-funnel model)
ITEP	Institute for Theoretical and Experimental Physics, Russia
LBL	Lawrence Berkeley Laboratory
LANL	Los Alamos National Laboratory
LEBT	low energy beam transport
LEF	low energy funnel (ASM Y-funnel model)
linac	linear accelerator
LLNL	Lawrence Livermore National Laboratory

Table 0.7. List of Abbreviations and Acronyms (continued).

Acronym	Description (identification if ASM specific)				
MDAC	McDonnel Douglas				
NPB	neutral particle beam				
NPBSE	neutral particle beam space experiment				
PMQ	permanent magnet quadrupole (ASM LEBT model)				
PMQTFE	permanent magnet quadrupole transverse focusing element				
POP	proof-of-principle				
rf, RF	radiofrequency				
RFD	radiofrequency deflector				
RFQ	radiofrequency quadrupole				
RFQ-1	radiofrequency quadrupole one (ASM RFQ model number 1)				
RFQ-2	radiofrequency quadrupole two (ASM RFQ model number 2)				
RGDTL	ramped gradient drift tube linac				
RMS	root mean square				
SAS	small angle source, see SPS also				
SOA	state-of-the-art				
SPARC	shell for particle accelerator related codes (ASM interface)				
SPS	surface plasma source (ASM ion source model)				
SSC	superconducting super collider				
TBF	two beam funnel				
TFE	transverse focusing element				
THR	two hole rebuncher				
VCR	vane coupling ring				
VOL	volume source (ASM ion source model)				

H⁺ ECR

1. Electron Cycloton Resonance (ECR) Ion Source Model

1.0 ECR Source Model Overview.

The Chalk River National Laboratories' high-current ion source [484] is used as the basis for the ECR proton (H⁺) source model in ASM. The beam dynamics (i.e. Beam Vector) model for the ECR source has been developed from the extraction data reported in Reference [483], supplemented with additional data received directly from CRNL [484a]. The engineering model of the source (i.e. Engineering Vector) is based upon descriptions provided in several references. The ECR ion source concept used for this modeling is shown in Figure 1-1.

The ECR source model provides:

- User inputs for extracted beam energy, current, emittance and proton fraction,
- Guidance limits for current and emittance based on perveance scaling,
- Key source design parameters and compares them to practical limits:

Extracted beam perveance
Extraction aspect ratio (aperture to gap)
Plasma (extraction) electrode aperture radius
Extraction gap distance
Extraction current density

- Reliable prediction of the Beam Vector when user inputs are within guidance limits,
- Engineering Vector for a CW ECR source which produces the predicted Beam Vector.

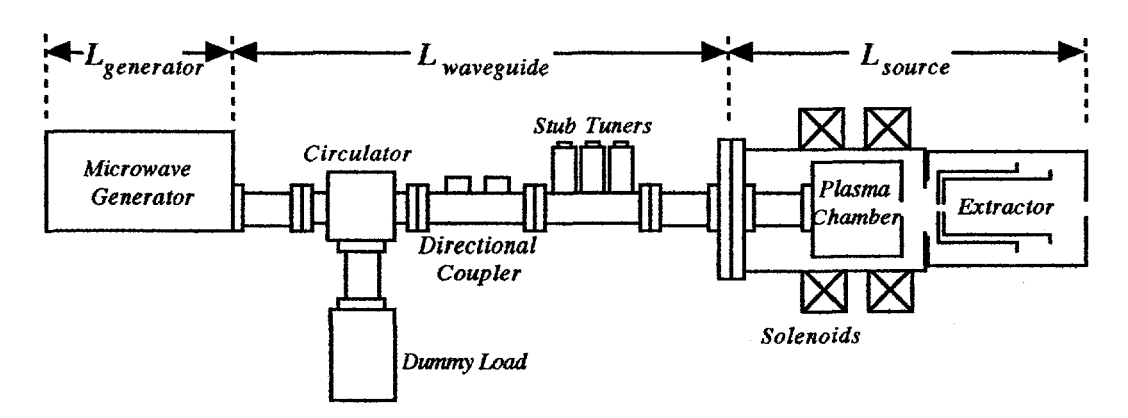


Figure 1-1. ECR ion source concept [484] used for developing the ASM model. Dimensions and major components included in size, mass and power estimates are indicated.

1.1 ECR Model Input.

Data input for the ECR source is accomplished using the Piece Data Window for the ECR source, accessed by double clicking an ECR Piece Icon on either the Model Pane or the Workspace Pane of an ASM Document Window. Table 1.1 summarizes the Piece Data input for the ECR ion source. Figure 1-2 shows the Piece Window used to input this data. The remainder of Section 1.1 describes the expert rules used to assist the user in setting up the input for this component and provides the formulas used to compute certain ECR source model parameters. Section 1.2 describes how these inputs and their diagnostic parameters are used in modeling the Beam Vector for the ECR source. Section 1.3 describes the modeling of the Engineering Vector for the ECR source. Section 1.4 summarizes the ECR source model diagnostic parameters which are output to the ASM Diagnostics file.

Table 1.1. Piece Data Inputs for the ECR Ion Source Model.

Element Parameters	Default	Default	User Guidance Limits		
(Symbol)	Value*	Units	Lower	Upper	
Extraction Energy E_{ext}	0.05	MeV	0.03	0.06	
Extraction Current I_{ext}	0.0985*	Amps	$6.32(q/A_{eff})(E_{ext})^{3/2}$	$14.2(q/A_{eff})(E_{ext})^{3/2}$	
RMS Normalized Emittance ϵ_{rms}	0.014*	π-cm-mrad	$[a+bP_{ext}]/(A)^{1/2}$	0.04	
Mono-atomic Ion Fraction R_{proton}	0.8	(none)	0.6	0.9	

^{*}Indicates a Piece Parameter whose default input can be scaled from Global Parameters and user preferences.

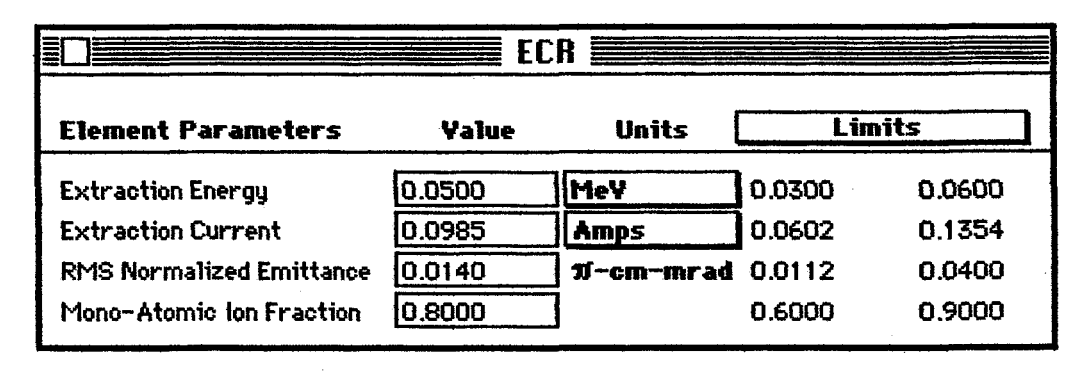


Figure 1-2. Piece Window for ECR ion source parameter input.

The default input value for the extraction energy of the source, E_{ext} , is taken to be 50 keV. The lower and upper user guidance limits are set at 30 and 60 keV, respectively. These correspond to the range of extraction voltage used for a series of experimental studies on the performance of the Chalk River ECR source. The mono-atomic ion fraction, denoted as R_{proton} although it may also refer to the D⁺ component for a deuterium source, has default and limit values also based on the range studied in that experimental work.

The user is assisted in inputing the other data by the use of several rules-of-thumb for the design of a high-current low-emittance ECR source. The perveance of the extracted beam is a key parameter of source design and several empirical results for the dependence of source properties on this parameter [482,483] are used in providing user input guidance. The perveance of the extracted beam is given by

$$P_{ext} = (q/A_{eff})^{-1} I_{ext} / (E_{ext})^{3/2}$$
 , (1.1)

where q is the particle charge (a Global Parameter) and A_{eff} is effective atomic mass of the extracted beam. The effective mass of the extracted ion beam is give by:

$$A_{eff} = [R_{proton} + 1.8333(1 - R_{proton})]A$$
 , (1.2)

where A is the atomic mass of the desired beam ion (a Global Parameter, 1 or 2 corresponding to either H⁺ or D⁺) and R_{proton} is the fraction of that component in the beam (the remainder of the beam are molecular ions). Systematic studies of the Chalk River ECR source for $A_{eff} = 1.1$ to 1.3 (90 to 60% protons) have characterizied its performance for perveance values between 0.20 and 0.45 mA/(keV)^{3/2}. These limit values for the perveance are used to provide user guidance limits for the extracted beam current. Specifically:

$$I_{ext,min} = 6.32 \ (q/A_{eff})(E_{ext})^{3/2} \ (Amps) ,$$
 (1.3)

and

$$I_{ext,max} = 14.2 \ (q/A_{eff})(E_{ext})^{3/2} \ (Amps)$$
 (1.4)

The default value for the extraction current is taken to be approximately the average of the upper and lower limits, using the default values for the extraction energy (0.050 MeV) and mono-atomic ion fraction (0.8):

$$I_{ext,default} = 10.3 (1/1.167)(0.05)^{3/2} = 0.0985$$
 (Amps) . (1.5)

Studies of the divergence and emittance of the Chalk River ECR source for proton beams have shown that the best, i.e. lowest, emittance obtained for a variety of beam currents and energies is nearly a linear function of the perveance [482]. Consequently a lower limit for the emittance of that ECR source can be written as:

$$\varepsilon_{min,protons} = a + bP_{ext}$$
 (1.6)

The empirical constants a and b have been fit to the minimum emittance data of reference [482] yielding:

$$a = 0.00857$$
 (π -cm-mrad), (1.7)

and

$$b = 0.008096 \quad (\pi\text{-cm-mrad-(keV})^{3/2}/\text{mA}).$$
 (1.8)

Comparable data for deuterium are not available. If one assumes that the emittance is due simply to an effective temperature, and that the temperature is independent of the mass of the beam ion, then the emittance would be expected to scale with the inverse of the square root of the mass. The lower limit for the emittance is thus taken to be:

$$\varepsilon_{rms,min} = [a + bP_{ext}]/(A)^{1/2} \quad (\pi\text{-cm-mrad}) \quad . \tag{1.9}$$

Note that since the perveance, given by equation (1.1), depends on the effective mass of the beam ions, equation (1.9) does not give a strict inverse square root dependence on A. The upper limit for the emittance is somewhat arbitrary. The value used here is taken to be twice the largest reported in reference [483]:

$$\varepsilon_{rms.max} = 0.04 \quad (\pi\text{-cm-mrad}) \quad .$$
 (1.10)

The default value for the emittance is taken to be approximately 33% higher than the minimum value given by equation (1.9) for the default values of the beam current, energy, and mono-atomic mass fraction. Specifically:

$$\varepsilon_{rms.default} = 1.33(0.0105) = 0.014 \quad (\pi\text{-cm-mrad})$$
 (1.11)

Several useful parameters can be derived from the ECR Piece Data inputs and are used in the modeling of the Beam Vector and/or Engineering Vector. One, the perveance, has been described above. The others calculated by the ECR model in ASM are described below.

An important parameter often used to characterize an ion source is the matched perveance, P_m . Matched is used in this context to describe the minimum emittance, which for the ECR source corresponds very closely to minimum divergence [483]. This matched perveance is, in general, a property of the geometry of the extraction optics and the acceptance of the accelerator. Keller [494] has given an expression for P_m in terms of the ratio S of the extraction aperture radius, a, to the extraction gap distance, d, which is approximately valid for two-gap (triode) extraction systems of the type used by Chalk River for their ECR source:

$$P_m = P_{mo} \left[S^2 / (1 + \alpha S^2) \right] . \tag{1.12}$$

The values of two constants appearing in (1.12) were determined by Keller to be

$$P_{m,o} = 1.9 \text{ mA/(keV)}^{3/2} ,$$
 (1.13)

and

$$\alpha = 1.7 \quad . \tag{1.14}$$

The limiting form of equation (1.12) when $\alpha = 0$ corresponds to the Child-Langmuir law for the space-charge limited perveance of a planar diode. However, the numerical coefficient,

 $P_{m,o}$ given by equation (1.13), is below the Child-Langmuir value. The α term effectively describes aberration limits to the perveance. Taylor and Wills [483] have shown that their minimum emittance perveance is accurately given by Keller's formula for the matched emittance. Equation (1.12) is inverted here in order to predict the value of S necessary to match the perveance of the extracted beam so that the minimum emittance, given by equation (1.9), should be realizable with an ECR source. This value of S is given by

$$S = [P_{ext} / (P_{mo} - \alpha P_{ext})]^{1/2} . {(1.15)}$$

In addition to the ratio S, the individual values of the extraction gap d and the extraction aperture a (or plasma electrode aperture) are also important source design parameters. The extraction gap is limited by breakdown and a reasonable estimate of a suitable value of d can be made using this limit. The dc Kilpatrick field limit could be used for this, but a somewhat more conservative practical limit has been suggested by Keller [494]:

$$d > 0.001414 (E_{ext})^{3/2}$$
 , (1.16)

where d is in centimeters when E_{ext} is in keV. To estimate a value for the extraction gap, we assume that it scales with the extraction energy according to Keller's minimum value, but use a value approximately 40% larger value than his limit in equation (1.16) suggests. Specifically:

$$d = 0.002 (E_{ext})^{3/2}$$
 (cm) . (1.17)

The radius a of the plasma (extraction) electrode can be computed from the values of d and S:

$$a = S d \quad \text{(cm)} \quad . \tag{1.18}$$

The extraction current density is also an important design parameter and can be computed from:

$$J_{ext} = I_{ext} / (\pi a^2)$$
 (mA/cm) . (1.19)

A number of these are output from ASM as ECR model diagnostic parameters (see Section 1.4).

1.2 ECR Source Beam Vector (BV) Model.

The ECR source model produces a Beam Vector which may be written as

$$(BV)_{ECRsource} = \begin{bmatrix} E \\ I \\ < x^{2} > | \\ \varepsilon_{t,rms}^{2} \\ < \Delta p^{2} > | \\ | \varepsilon_{t,rms}^{2} \\ | \alpha_{t} \\ | \alpha_{t} \end{bmatrix}$$

$$(1.20)$$

The beam energy, E in MeV, is taken directly from the corresponding value for the extraction energy in the Piece Data (Table 1.1):

$$E = E_{ext} . (1.21)$$

The beam current, I in Amperes, is given by

$$I = R_{proton} I_{ext} . (1.22)$$

The normalized, rms, transverse emittance is also taken directly from the Piece Data input:

$$\varepsilon_{t,rms} = \varepsilon_{rms}$$
 (1.23)

The value of $< r^2 >$, the mean square radius of the beam, is taken to be one-half of the square of the extraction (plasma electrode) aperture radius:

$$\langle r^2 \rangle = 0.5 \, a^2$$
 , (1.24)

where a is given by equation (1.18). This corresponds to the assumption of a uniform current density at the extraction aperture. Since a circular beam at the extraction aperture is also implied in this assumption, i.e. $\langle x^2 \rangle = \langle y^2 \rangle$, then

$$\langle x^2 \rangle = 0.5 \langle r^2 \rangle = 0.25 \ a^2$$
 , (1.25)

Data for the transverse Twiss parameter, α_t , at the ion source are not reported in the studies used in developing the ECR source model. However, TRASNOPTR modeling of the CRNL direction extraction LEBT reported in [485] gives an emittance diagram for the beam at the exit of the LEBT. This has been used, together with a TRACE 3-D model of the LEBT, to estimate α_t at the ion source. The results are consistent with a value of zero, consequently:

$$\alpha_t = 0 \quad . \tag{1.26}$$

The momentum spread and longitudinal emittance of the extracted beam are assumed to be negligible:

$$\langle \Delta p^2 \rangle = 0 \quad , \tag{1.27}$$

$$\varepsilon_{l,rms} = 0 \quad . \tag{1.28}$$

Likewise the longitudinal Twiss parameter, α_i , is taken to be zero:

$$\alpha_I = 0 \quad . \tag{1.29}$$

This completes the model for the BV of the ECR ion source. The next section deals with the modeling of the Engineering Vector.

1.3 ECR Source Engineering Vector (EV) Model.

The Engineering Vector (EV) for the ECR ion source is

$$\begin{bmatrix} L \\ | V \\ | M \\ | M \\ | P \\ | x \\ | y \\ | Conf \\ | Cost \end{bmatrix}$$
(1.30)

The ECR source is divided into three components or assemblies for the purposes of discussion here. These are (1) the ion source plasma chamber with solenoids and extraction electrodes, (2) the input waveguide with tuner, directional coupler and circulator and (3) the microwave generator. The length L of the ECR source is taken to be the sum of the lengths of these three components:

$$L = L_{source} + L_{waveguide} + L_{generator} , (1.31)$$

The length of the ion source including plasma chamber, solenoids, extraction electrodes and waveguide flange section, is taken from the scaled drawing in Reference [484].

$$L_{source} = 0.35 \quad \text{(meters)}. \tag{1.32}$$

The length of the waveguide line is taken to be a multiple of the microwave wavelength, λ_{ECR} , which is given by

$$\lambda_{FCR} = 0.299729 \cdot f_{FCR}$$
 (m), (1.34)

where the microwave frequency is in GHz. This frequency is taken to be 2.45 GHz, the value used for the Chalk River ECR source, so that the corresponding value of λ_{ECR} is about 0.122 meters. The stub tuners, directional coupler, circulator and connecting waveguide sections are included in the waveguide length. The overall length of the waveguide line is then:

$$L_{wavequide} = 8\lambda_{ECR} , \qquad (1.35)$$

The length of the microwave generator is based on a 1 kW magnetron and is taken to be:

$$L_{generator} = 0.25 \text{ (meters)}, \qquad (1.36)$$

The two maximum transverse dimensions, x and y, are taken to be the largest of the corresponding dimensions of the source, waveguide line, and microwave generator sections, as measured from the center of the beam line. The largest value of the horizontal (x) dimension is taken to be that of the dummy load:

$$x = 0.25$$
 (m) . (1.37)

The largest dimension in the vertical (y) direction is taken to be 5 cm larger than the solenoid coils:

$$y = r_i + a + 0.05$$
 (m), (1.38)

where r_i and a are given by Equations (1.65) and (1.66) below. The volume is then given by

$$V = 4 xy L \text{ (m)}$$
 (1.39)

The total mass is taken to be the sum of two terms, each corresponding roughly to the electrical components ($M_{electrical}$) and the mechanical components ($M_{mechanical}$):

$$M = M_{electrical} + M_{mechanical}$$
 (1.40)

The electrical components include the power supplies and rack mounted electronics. The solenoid power supplies for the ECR source are among the heaviest items and are about 150 lbs each [484a]. The mass of the remainder of the electrical components is taken to be 50 lbs. Thus:

$$M_{electrical} = 90 \text{ (kg)} , \qquad (1.41)$$

The ECR ion source is a CW source, so that except for hardware associated with the cooling requirements, the masses are taken to be independent of the duty factor. The total mechanical mass is given by the sum:

$$M_{mechanical} = M_{source} + M_1 + M_2 + M_{waveguide} + M_{generator} + M_{cooling}$$
, (1.42)

where the individual masses are those associated with the corresponding lengths, except the solenoid masses, M_1 and M_2 , and the mass of cooling system, $M_{cooling}$, are separately indicated. The mass of the source assembly, including the extractor components, is taken to be:

$$M_{source} = (kg) . (1.43)$$

The mass, M_i , of each solenoid is given in kilograms by the sum of the wire mass and the winding mechanical support mass. This is computed as:

$$M_{i} = l_{i} \left\{ \left[\pi (r_{i} + a)^{2} - r_{i}^{2} \right] \rho_{Cu} + \left[2\pi (y) \Delta R_{s} \right] \rho_{linac} \right\} , \qquad (1.44)$$

where r_i , a, and y are described above, l_i is the length of the solenoid given by Equation (1.66), ρ_{Cu} is the denisty of copper (2.7·10⁺³ Kg/m³) assumed for the wire, ρ_{linac} is the density of the structural material used for the linear accelerator (a Global Parameter) and ΔR_s is the assumed thickness of the linac structural components. The mass of the waveguide section includes that of the stub tuners, coupler, circulator and dummy load, as well as of the waveguide itself. The waveguide is assumed to be WR-284 and this mass is estimated as

$$M_{WR-284} = (4.3 \cdot 10^{-5}) \rho_{Cu} L_{waveguide} \text{ (kg)}$$
 (1.45)

The total mass of the stub tuners, coupler, circulator and dummy load is estimated as 30 kg, so that the mass of the waveguide section is given by:

$$M_{waveguide} = 30 + M_{WR-284}$$
 (kg) . (1.46)

The mass of the microwave generator is taken as

$$M_{generator} = 15 \text{ (kg)} . \tag{1.47}$$

The cooling system mass is assumed to depend linearly on the duty factor, df, an ASM Global Parameter. For df expressed as a fraction:

$$M_{cooling} = m_1 + m_2 df , \qquad (1.48)$$

where the values of m_1 and m_2 have been tentatively set as 5 kg and 100 kg, respectively.

The total dc power required by the ECR ion source is the sum of contributions from the microwave generator, the plasma chamber solenoids, the auxiliary electronics and the extractor. It is assumed that the electronics and solenoids are on continuously and that the microwave generator and extractor are pulsed at the same duty factor, df, as the rest of the accelerator (df is an ASM Global Parameter). The average power is thus given by:

$$P = [P_{oux} + P_{sol}] + df \cdot [P_{ext} + P_{get}/\eta] \quad . \tag{1.50}$$

The required microwave generator power, P_{gen} , is a function of the extracted beam current [484]; the efficiency factor η is for the conversion to microwave power. Two stable operating regimes for the CRNL ECR source have been described and are referred to as the on-resonance and off-resonance modes. Higher beam currents are associated with the on-resonance mode, lower beam currents with the off-resonance mode. The two modes are distinguished in ASM by introducing a binary parameter, K_r . For the high current (on-resonance) mode $K_r = 1$ and for the low current mode $K_r = 0$. An extraction current of 70 mA is taken as the transition point:

$$K_r = 0 \text{ if } I_{ext} < 70 \text{ (mA)},$$
 (1.51)

and

$$K_r = 1 \text{ if } I_{ext} \ge 70 \text{ (mA)}$$
 (1.52)

The data in Ref [484], relating the total extracted current to P_{gen} and the gas flow rate, \hat{u} , has been parameterized as:

$$I = a + bK_r + c[e^{-(\hat{u}/\hat{u}_o)}] + dP_{een} , \qquad (1.53)$$

where a = 1.13 mA, b = 31.33 mA, c = 37.33 mA, d = 37.78·10⁺³ mA/MW and $\hat{\mathbf{u}}_0$ = 3.8925 secm. The region of validity for this fit is roughly for $1 \le \hat{\mathbf{u}} \le 5$ (secm) and $0.2 \le P_{gen} \le 1.1$ (kW). It is assumed that lower mass flow rates are preferable and take as an initial estimate:

$$\hat{\mathbf{u}} = 1 \quad (\text{sccm}) \quad . \tag{1.54}$$

An estimate of the required generator power is then computed from:

$$P_{est} = \left\{ I_{ext} - a - bK_r - c[e^{-(\hat{u}/\hat{u}_o)}] \right\} / d \quad (MW) \quad . \tag{1.55}$$

The value for the required generator power, P_{gen} , is then taken to be the larger of P_{est} or 0.0002 MW, the lower range of validity of the data fit:

$$P_{gen} = \max[0.0002, P_{est}] \quad . \tag{1.56}$$

For the defaults inputs this yields a microwave generator power of 0.984 kW. If P_{gen} is at the lower limit, which may occur for extracted beam currents less than 30 mA or so, the mass flow rate is recomputed for this value of I_{ext} and P_{gen} :

$$\hat{\mathbf{u}} = \hat{\mathbf{u}}_{o} \ln \left\{ c / \left[I_{ext} - a - b K_{r} - d P_{gen} \right] \right\}$$
 (1.57)

The efficiency factor for the 2.45 GHz generator, η appearing in (1.50), is taken to be:

$$\eta = 0.7 \tag{1.58}$$

The contribution to the power for the extractor, P_{ext} in MW, is given by:

$$P_{ext} = 10^{-6} E_{ext} I_{ext} \quad . \tag{1.59}$$

For the default input values this yields 4.925 kW for the extractor power.

The power (in MW) for the two solenoids is computed as described for the electromagnetic solenoid (EMS) LEBT model of ASM. Specifically

$$P_{sol} = 2.10^{-6}P_i = 2.10^{-6}I_i^2 R \quad , \tag{1.60}$$

where R is the resistance of each solenoid winding and I_i is the current (in amperes) in each winding. These are modeled as:

$$R = 0.05[(r_i + a/2)/(0.05 + a/2)] \text{ ohms,}$$
 (1.61)

and

$$I_i = 71.1 B_i (kG) / g(r_i / l_i)$$
 , (1.62)

where

$$g(r_i / l_i) = [1 + 1.84 \cdot (r_i / l_i)^2]^{-1/2}$$
 (1.63)

For the ECR source solenoids the value of the on-axis magnetic induction is taken as

$$B_i(kG) = 0.82 + 0.10K$$
, (1.64)

again based on the data in Ref [484]. The values for the inner radius, coil height and length of the solenoid are also from Ref [484]:

$$r_i = 0.090 \text{ (m)}$$
 , (1.65)

$$a = 0.060 \text{ (m)}$$
 (1.66)

and

$$l_i = 0.050$$
 (m) . (1.67)

For $K_r = 1$ (on-resonance mode) this yields 2.234 kW for each solenoid.

The power for the auxiliary electronics is taken to be a constant:

$$P_{aux} = 0.001 \text{ (MW)}$$
 (1.68)

Several considerations are used in developing the confidence factor for the ECR ion source. The modeling of the Beam Vector is based on empirical fits to experimental data and, to the extent that the inputs to the model fall within certain limits, the confidence in the model output is high. This suggests that Conf > 0.95 for the model. The Engineering Vector data is based upon the ECR source built and run on the Chalk River CW RFQ beam line, also suggesting that Conf > 0.95. For Piece Data input parameters within the limits indicated in Table 1.1, the baseline (default) value for the confidence factor is assigned to be:

$$Conf_d = 0.95$$
 . (1.70)

For inputs to the model which are outside the limits specified in Table 1.1, this confidence factor is not useful.

1.4 ECR Diagnostic Parameters.

ASM provides additional guidance to the user on the reliability of the computer model through the use of diagnostic parameters. Table 1.2 summarizes the ECR source diagnostic parameters together with approximate model validity ranges for each parameter, i.e. for which data on the Chalk River ECR source is available.

Table 1.2. Diagnostic Parameters for the ECR Source Model.

Diagnostic Parameters Symbol (Equation)	Value for Default Inputs	Default Units	Range for l Lower	Model Validity Upper
Beam Perveance P_{ext} (1.1)	0.2388	mA/(keV) ^{3/2}	0.2	0.45
Aperture to Gap Ratio S (1.15)	0.3998	(none)	0.35	0.625
Extraction Gap d (1.17)	0.7071	cm	0.56	0.76
Plasma (Extraction) Radi a (1.18)	us 0.2827	cm	0.20	0.35
Extraction Current Densit $J_{\rm ext}$ (1.19)	392.2	mA/cm ²	tbd	tbd
Source Output Twiss Para β_T (1.71)	ameter 0.2246	m/rad	tbd	tbd
Gas Flow Rate from Sou dV/dt (1.72)	633	liters/sec	126	64,000

Most of the diagnostic parameters appearing in Table 1.2 have already been described. The phase-space ellipse diagnostic parameter β_T , one of the output beam Twiss (or Courant Synder) parameters, may be obtained directly from the third and fourth elements of the Beam Vector, together with relativistic velocity β and energy γ parameters for the beam. Specifically:

$$\beta_T = \beta \gamma \ 10^{+1} < x^2 > / (\epsilon_{t,rms}) \quad , \tag{1.71}$$

where the factor of 10⁺¹ converts the units to mm/mrad (or m/rad).

The gas flow rate from the ion source, in liters per second, is taken from the mass flow rate û estimated in Equation (1.57):

$$dV/dt = (760/60) \hat{\mathbf{u}}/P_{lebt} , \qquad (1.72)$$

where is the LEBT pressure in millitorr.

1.5 Interface Parameters To and From Other ASM Models.

Aside from the Beam Vector and Engineering Vector there is only one ECR source parameter that is needed by other models in ASM. This parameter is the gas flow rate, dV/dt given by Equation (1.72) above, used to estimate the pumping requirements in the ASM LEBT models. The pressure in the LEBT, in mtorr, is needed from the LEBT model following the ion source. If no LEBT is present, the value is defaulted to 0.02 mtorr.

- 1.6 References for ECR ion source model.
- [480] "Emittance and Matching of ECR Sources," W. Krauss-Vogt, H. Beuscher, H. Hagedoorn, J. Reich and P. Wucherer, Nuclear Instruments and Methods in Physics Research, Vol. A268, pp. 5-9, 1988.
- [481] "A High-Current Low-Emittance dc ECR Proton Source," W. Krauss-Vogt, H. Beuscher, H. Hagedoorn, J. Reich and P. Wucherer, Nuclear Instruments and Methods in Physics Research, Vol. A309, pp. 37-42, 1991.
- [482] "Design Recommendations for Low-Energy Components of ESNIT and OMEGA," T. Taylor, B. Chidley and G. McMichael, 1992 Linear Accelerator Conference, pp.651-653, Jan. 1993.
- [483] "Extraction of High-Current Low-Emittance Proton Beams From An ECR Plasma Generator," T. Taylor and J. S. Wills, 1992 Linear Accelerator Conference, pp.347-349, Jan. 1993.
- [484] "Enhanced High-Current ECR Proton Source," T. Taylor and J. S. Wills, 1992 Linear Accelerator Conference, pp.350-352, Jan. 1993.
- [484a] T. Taylor, personal communications, 1993.
- [485] "High-Current Direct Injection to a CW RFQ Using An ECR Proton Source," G. M. Arbique, T. Taylor, A. D. Davidson and J. S. Wills, 1992 Linear Accelerator Conference Proceedings, pp.52-54, Vol. 1, 1992.
- [486] "Beam Parameter Measurements on the CW RFQ1-1250 Accelerator," G. M. Arbique, B. G. Chidley, G. E. McMichael and J. Y. Sheikh, 1992 Linear Accelerator Conference Proceedings, pp.55-57, Vol. 1, 1992.
- [487] "Optical Beam Sensors for RFQ1-1250," G. M. Arbique, B. G. Chidley, W. L. Michel and B. H. Smith, 1992 Linear Accelerator Conference Proceedings, pp.654-656, Vol. 2, 1992.
- [488] "Development of a High Brightness Ion Source for the Proton Linear Accelerator (BTA) at JAERI," Y. Okumura, T. Inoue, H. Oguri and H. Tanaka, 1992 Linear Accelerator Conference Proceedings, pp.645-647, Vol. 2, 1992.
- [489] "Multi-Beamlet Injection to the RFQ1 Accelerator A Comparison of ECR and Duopigatron Proton Sources," G. M. Arbique, T. Taylor, M. H. Thrasher and J. S. Wills, 1991 IEEE Particle Accelerator Conference, pp.842-844, Vol. 2, 1991.
- [490] "Beam Transmission and Emittance Measurements on the RFQ1 Accelerator," G. M. Arbique, T. Taylor, M. H. Thrasher and J. S. Wills, 1991 IEEE Particle Accelerator Conference, pp.845-847, Vol. 2, 1991.
- [494] "High-Brightness, High-Current Ion Sources," R. Keller, American Institute of Physics Conference Proceedings No.139, pp. 1-15, 1986.

EMS

2. Electromagnetic Solenoid (EMS) Low Energy Beam Transport (LEBT) Model.

2.0 EMS LEBT Model Overview.

The EMS LEBT model is based on the neutralized transport of the beam, with solenoid magnetic focusing to match the beam into a radiofrequency quadrupole (RFQ) accelerator. Both positive and negative ion beam transport are modeled, utilizing data from the Chalk River direct injection proton LEBT [485,487] and several negative ion LEBTs developed for the NPB program. Not all of the physical phenomena associated with neutralized beam transport are quantitatively understood. The ASM solenoid model incorporates several of the physical phenomena known to affect LEBT performance, using mathematical models which are well defined even though it is recognized that they are only approximate. The user may selectively "turn-off" some of these mathematical models in order to make some quantitative assessment of how important these phenomena are for a given LEBT configuration, or for downstream accelerator system components. This is accomplished by using certain values of input parameters (selecting a particular guidance limit value).

The ASM solenoid LEBT model includes:

- "Parallel-to-point" optics with one solenoid, or
- "Point-to-point" optics with two solenoids,
- For the neutralized transport of both positive and negative ions, an effective transverse emittance growth model due to the oscillations in the phase ellipse as a result of beam current fluctuations, which the user may selectively turn-off,
- In addition, for the neutralized transport of negative ions:

Different options for neutralizing background gas
Stripping losses due to collisions with background gas
Transverse emittance growth calculated for plasma instabilities,
the user may selectively turn-off this growth mechanism,

- Reliable prediction of LEBT Beam Vector properties predicted for both positive and negative ions when input parameters are within guidance limits,
- Engineering Vector for a solenoid LEBT which can produce the predicted Beam Vector.

2.1 EMS LEBT Input Data

Data input for the EMS LEBT is accomplished using the Piece Data Window for the EMS LEBT. This is accessed by double clicking an EMS Piece Icon on either the Model Pane or the Workspace Pane of an ASM Document Window. Table 2.1 summarizes the user input for the electromagnet solenoid (EMS) low energy beam transport (LEBT) model. Figure 2-2 shows the Piece Window used to input this data. The remainder of this section describes the expert rules developed to assist the user in setting up the input for this component. Section 2.2 describes how the inputs are used in modeling the Beam Vector for the ECR source. Section 2.3 describes the modeling of the Engineering Vector for the EMS LEBT. Section 2.4 provides the EMS model diagnostic parameters, which are output to the ASM Diagnostics file.

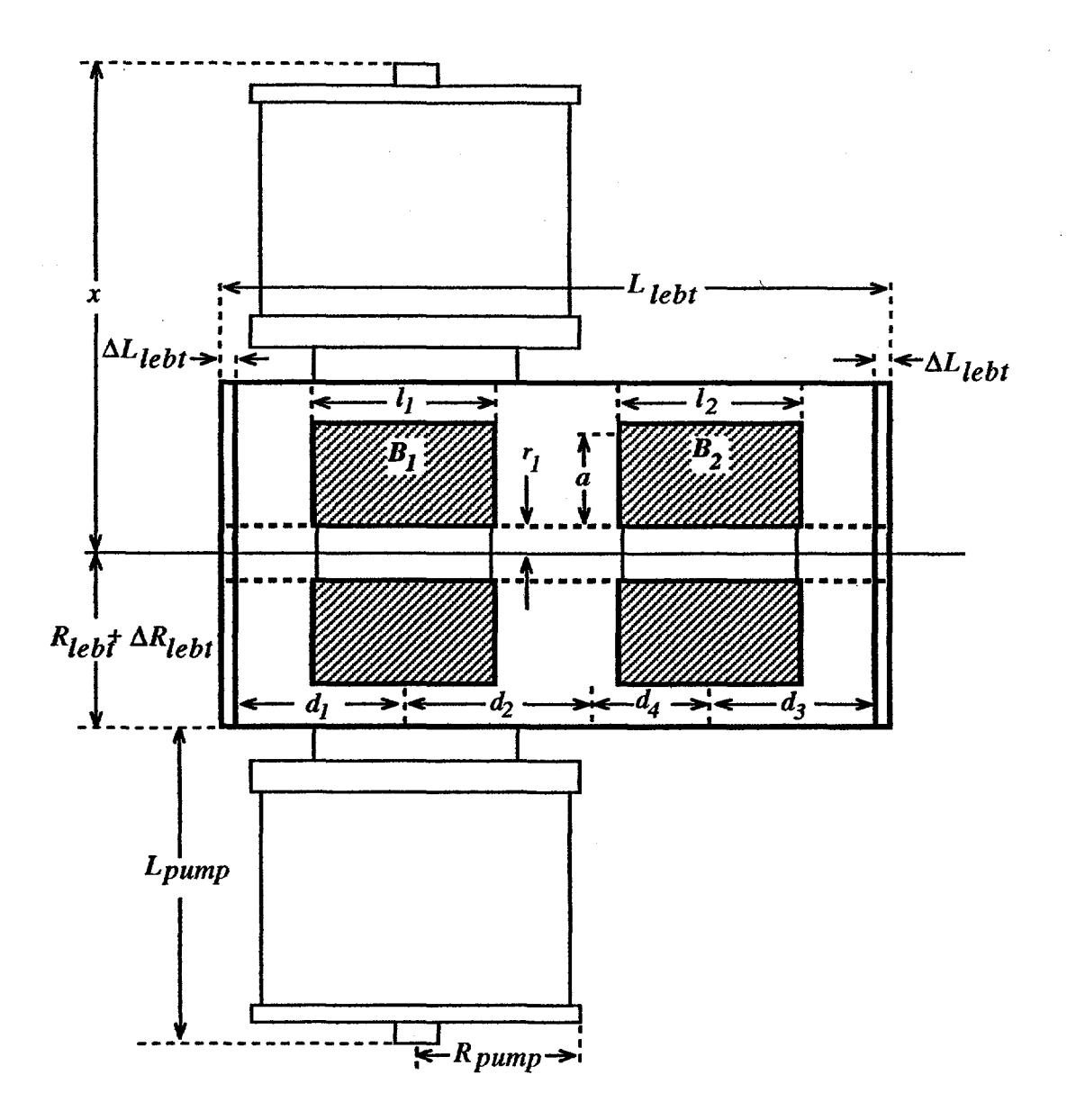


Figure 2-1. Electromagnetic solenoid (EMS) LEBT concept used for the modeling in ASM. Dimensions and major components used in the modeling of the size, mass and power are indicated. Either one or two solenoids may be included in the LEBT configuration, depending on the input beam Twiss parameters.

The first four input parameters for the EMS LEBT are largely self-explanatory. The transport channel radius, r_1 , is the smallest aperture for the beam inside the LEBT. This parameter can affect the transmission through the LEBT and other transport properties. The default value is set, somewhat arbitrarily, to 2 cm. The LEBT upper length goal, l_{lebr} is used by ASM as a starting point for the maximum LEBT length. As discussed in Section 2.2, this length goal is used to estimate whether the desired LEBT output beam matching parameters (the last two user inputs in Table 2-1) can be met with just one solenoid within this length, or if two solenoids will be needed. If the matching requirements can be met with one solenoid, then the final LEBT length will generally be less than this goal. If two solenoids are required to meet the matching requirements,

the spacing of the solenoids is adjusted to produce a final LEBT length the same as the goal. The default value for l_{lebt} is one-half meter, which usually results in adequate performance for either negative or positive ion beams. The lower guidance limit, 0.3 meters, is based on the minimum length necessary to fit two solenoids of the type discussed in Section 2.3. The upper guidance limit has been set to 1.5 meters. For the default parameters of the ion sources, this is the point at which emittance growth can be significant and, for negative ions in particularly, where beam transmission degrades. This upper guidance limit may not be appropriate for other beam parameters.

Table 2.1 Piece Data Inputs for the Electromagnet Solenoidal (EMS) Low Energy Beam Transport (LEBT) Model.

Element Parameters (Symbol)	Default Value*	Default Units	User Guidar Lower	nce Limits Upper
Transport Channel Radius	4	cm	1	5
LEBT Upper Length Goal l_{lebt}	0.5	m	0.3	1.5
Neutralizing Gas Species N_{gas}	1*	(none)	1	7
Neutralizing Gas Pressure P_{lebt}	0.02*	mTorr	0.001	0.1
Instability Threshold Factor Th_{gas}	0*	(none)	0 if $Q \ge 0$ 0.62 for $Q < 0$	$0 \text{ if } Q \ge 0$ $1 \text{ for } Q < 0$
Beam Current Fluctuation $\Delta I/I$	0.001	(fraction)	0.0	0.1
Matched RFQ Alpha Goal α_{To}	2.5	(none)	1.7	3.3
Matched RFQ Beta Goal β_{To}	0.04	meter/radian	0.030	0.054

^{*}Indicates a Piece Parameter whose default input can be scaled from Global Parameters and user preferences.

There are two parameters for describing the gas used in the LEBT for beam space charge neutralization. One is the gas species, which is selected by the user from a pop-up menu in the EMS LEBT Piece Window. The default value for the neutralizing gas is taken to be hydrogen. This assumes that the predominant gas in the LEBT arises from the gas flowing out of the ion source. For negative ion systems other gases may provide better transport properties with lower

other than hydrogen may also be desirable to avoid condensation on cryogenic linac surfaces. ASM provides for seven different neutralizing gases which sets the limits for this input parameter. Various properties of these gases used by ASM are given in Tables 2.2 and 2.3.

	EM	s E		
Element Parameters	Value Units		Limits	
Transport Channel Radius	4.0000	em	1.0000	5.0000
LEBT Length Goal	0.5000	m	0.3000	1.5000
Neutralizing Gas Species	Hydrogen 2	<u> </u>]	
Neutralizing Gas Pressure	0.0200	mTorr	0.0010	0.1000
Instability Threshold Factor	0.0000		0.0000	0.0000
Beam Current Fluctuation	0.0010	% Percent	0.0000	0.1000
Matched RFQ Alpha Goal	2.5000		2.0000	3.0000
Matched RFQ Beta Goal	0.0400	m/rad	0.0200	0.080.0

Figure 2-2. Piece Window for EMS LEBT parameter input

The LEBT gas pressure is an important parameter in the modeling of negative ion beams, but is not as critical for modeling proton beams. The Chalk River direct injection LEBT has been generally operated at a pressure of less than 0.05 mTorr [485]. The default value for P_{lebt} has been set at 40% of this value, 0.02 mTorr. The upper guidance limit has been set to twice the default value, i.e. 0.1 mTorr.

The instability threshold factor Th_{gas} is used in the modeling of emittance growth for negative ion beams. The limits for this parameter depended on the sign of the ion charge, Q, a Global Parameter. For negative ions (Q<0) the significance of the limits is discussed in Section 2.2.4.(a). For positive ions, which includes the default Global Parameter case of Q=1, Th_{gas} should be zero. To turn off the instability emittance growth mechanism, for any value of Q, simply set:

$$Th_{gas} = 0 . (2.1)$$

For the Global Parameter default selection of positive ions, the default value for this parameter, and both limits, are set to zero.

The beam current fluctuation, $\Delta I/I$, is used to model emittance growth for both positive and negative ions. This parameter is associated with the current fluctuations in the ion source and will result, when propagated through the LEBT focusing channel, in effective emittance growth due to oscillations in the phase space ellipse orientations. The default value and limits are estimates for the ECR positive ion source. Other values may be more appropriate for negative ion sources. For either positive or negative ions, the user may turn off this emittance growth mechanism by setting this parameter to zero:

$$\Delta I / I = 0 \quad . \tag{2.2}$$

The last two user inputs for the EMS LEBT are the goals for the two output beam Twiss parameters, α_{To} and β_{To} . These parameters are associated with the accelerator structure which follows the LEBT, usually an RFQ. The defaults are based on the GTA RFQ design, and if these goals are achieved the match into the RFQ models will be perfect (mismatch factor of zero). The limits correspond to mismatch factors of just under 0.5. This generally results in a transmissions losses in the RFQ of less than 10%.

The goal values for the Twiss parameters will usually be closely achieved by the EMS LEBT model in ASM, if the emittance grow in the LEBT is not too severe. The actual LEBT output value of the α_t parameter is given by the seventh element of the Beam Vector and the result may be compared to the goal value. The achieved value of β_t may be obtained from the third and fourth elements of the output Beam Vector:

$$\beta_{tout} = 10^{+1} (\beta \gamma) \langle x^2 \rangle_{out} / (\varepsilon_{tout}) . \qquad (2.3)$$

This is one of the diagnostic parameters for the EMS LEBT model (see Section 2.4) and is printed to the ASM Diagnostic file. (All the diagnostic parameters for the ASM LEBT model are summarized in Section 2.4.) Another diagnostic parameter is the LEBT background gas density. This gas density is determined from the pressure, P_{lebv} which is a user input.

$$n_{gas} = P_{lebt} / (k_B T) \quad , \tag{2.4}$$

where k_B is Boltzmann's constant ($k_B = 1.03551 \times 10^{-19}$ torr-cm³/°K) and T is the gas temperature in °K. It is assumed in ASM that the background gas is at room temperature (T = 300 K). For the LEBT pressure, P_{lebt} in milli-torr (mTorr) this gives

$$n_{eas}(\text{cm}^{-3}) = 3.2190 \cdot 10^{+13} [P_{leht}(\text{mTorr})]$$
 (2.5)

2.2 Beam Vector Model for the EMS Low Energy Beam Transport (LEBT).

The beam dynamics for the EMS LEBT model is described in term of the ASM matrix formalism. The Beam Vector is advanced through the LEBT according to Equation (2.10).

$$\begin{bmatrix}
E_{out} \\
I_{out} \\
< x^{2} >_{out}
\end{bmatrix}
\begin{bmatrix}
1 & 0 & 0 & 0 & 0 & 0 & 0 & 0 \\
0 & g_{22} & 0 & 0 & 0 & 0 & 0 \\
0 & 0 & g_{33} & g_{34} & 0 & 0 & g_{37} & 0 \\
0 & 0 & g_{33} & g_{34} & 0 & 0 & 0 & 0 \\
0 & 0 & 0 & g_{44} & 0 & 0 & 0 & 0 \\
0 & 0 & 0 & 0 & 1 & 0 & 0 & 0 \\
0 & 0 & 0 & 0 & 0 & 1 & 0 & 0
\end{bmatrix}
\begin{bmatrix}
E_{in} \\
I_{in} \\
0 \\
< x^{2} >_{in}
\end{bmatrix}
\begin{bmatrix}
0 \\
0 \\
0 \\
0
\end{bmatrix}$$

$$\begin{bmatrix}
E_{in} \\
0 \\
0
\end{bmatrix}
\begin{bmatrix}
0 \\
0 \\
0
\end{bmatrix}$$

$$\begin{bmatrix}
E_{in} \\
0 \\
0
\end{bmatrix}
\begin{bmatrix}
0 \\
0
\end{bmatrix}$$

$$\begin{bmatrix}
E_{in} \\
0
\end{bmatrix}
\begin{bmatrix}
0 \\
0
\end{bmatrix}$$

$$\begin{bmatrix}
E_{in} \\
0
\end{bmatrix}
\begin{bmatrix}
0 \\
0
\end{bmatrix}$$

$$\begin{bmatrix}
E_{in} \\
0
\end{bmatrix}
\begin{bmatrix}
0 \\
0
\end{bmatrix}$$

$$\begin{bmatrix}
E_{in} \\
0
\end{bmatrix}
\begin{bmatrix}
0 \\
0
\end{bmatrix}$$

$$\begin{bmatrix}
E_{in} \\
0
\end{bmatrix}
\begin{bmatrix}
0 \\
0
\end{bmatrix}
\begin{bmatrix}
0 \\
0
\end{bmatrix}$$

$$\begin{bmatrix}
E_{in} \\
0
\end{bmatrix}
\begin{bmatrix}
0 \\
0
\end{bmatrix}
\begin{bmatrix}
0 \\
0
\end{bmatrix}$$

$$\begin{bmatrix}
E_{in} \\
0
\end{bmatrix}
\begin{bmatrix}
0 \\
0
\end{bmatrix}
\begin{bmatrix}
0 \\
0
\end{bmatrix}$$

$$\begin{bmatrix}
E_{in} \\
0
\end{bmatrix}
\begin{bmatrix}
0 \\
0
\end{bmatrix}
\begin{bmatrix}
0 \\
0
\end{bmatrix}$$

$$\begin{bmatrix}
E_{in} \\
0
\end{bmatrix}
\begin{bmatrix}
0 \\
0
\end{bmatrix}
\begin{bmatrix}
0 \\
0
\end{bmatrix}$$

$$\begin{bmatrix}
E_{in} \\
0
\end{bmatrix}
\begin{bmatrix}
0 \\
0
\end{bmatrix}
\begin{bmatrix}
0 \\
0
\end{bmatrix}$$

$$\begin{bmatrix}
E_{in} \\
0
\end{bmatrix}
\begin{bmatrix}
0 \\
0
\end{bmatrix}
\begin{bmatrix}
0 \\
0
\end{bmatrix}$$

$$\begin{bmatrix}
0 \\
0
\end{bmatrix}$$

$$\begin{bmatrix}
0 \\
0 \\
0 \\
0
\end{bmatrix}$$

$$\begin{bmatrix}
0 \\
0 \\
0 \\
0
\end{bmatrix}$$

$$\begin{bmatrix}
0 \\
0 \\
0 \\
0
\end{bmatrix}$$

$$\begin{bmatrix}
0 \\
0 \\
0 \\
0
\end{bmatrix}$$

$$\begin{bmatrix}
0 \\
0 \\
0 \\
0
\end{bmatrix}$$

$$\begin{bmatrix}
0 \\
0 \\
0 \\
0
\end{bmatrix}$$

$$\begin{bmatrix}
0 \\
0 \\
0 \\
0
\end{bmatrix}$$

$$\begin{bmatrix}
0 \\
0 \\
0 \\
0
\end{bmatrix}$$

$$\begin{bmatrix}
0 \\
0 \\
0 \\
0
\end{bmatrix}$$

$$\begin{bmatrix}
0 \\
0 \\
0 \\
0 \\
0
\end{bmatrix}$$

$$\begin{bmatrix}
0 \\
0 \\
0 \\
0 \\
0
\end{bmatrix}$$

The subscripts in refer to the input BV, which is from the preceding ion source model, while the subscripts out refer to the output BV which will be passed to the next element of the beam line.

2.2.1. Stripping and Aperture Losses.

The matrix element g_{22} in Equation (2.10) describes the attenuation of beam current in the LEBT. The beam current through the LEBT is attenuated by stripping (for negative ions) and aperture losses. This is modeled by a LEBT transmission efficiency $g_{22} = \eta$:

$$I_{out} = \eta I_{in} \quad , \tag{2.11}$$

where

$$\eta = f_s f_a . ag{2.12}$$

The fractions f_s and f_a describe the losses due to stripping and the physical aperture limits respectively. Aperture losses are discussed first since they are computed in the same way for both positive and negative ions. Stripping losses are only computed for negative ions ($f_s = 1$ for positive ions).

Aperture losses are computed according to

$$f_a = [1 - \exp(-r_1^2 / 2r_{max}^2)]$$
 , (2.13)

where r_{max} is the maximum rms radius of the beam inside any solenoid in the LEBT, and r_1 is the LEBT transport channel radius which is a user input. The value for r_{max} is computed by assuming that the maximum beam radius occurs in the middle of the first solenoid, i.e. at a distance into the LEBT given by d_1 (see Figure 2-1). The value of d_1 is determined by the transport and matching requirements of the LEBT whose computation is described in Sections 2.2.2 and 2.2.3. The transport through this distance is approximated as a pure drift. This gives for r_{max} :

$$r_{max}^{2} = \langle x^{2} \rangle_{in} + 10^{-2} \left[(d_{1})^{2} (1 + \alpha_{t,in}^{2}) (\epsilon_{t,in}/\beta \gamma)^{2} \right] / \langle x^{2} \rangle_{in} - 2 \cdot 10^{-1} (d_{1}) (\epsilon_{t,in}/\beta \gamma) \alpha_{t,in}$$
(2.14)

The powers of 10 convert the units to cm². The values of $\alpha_{t,in}$, $\epsilon_{t,in}$ and $\langle x^2 \rangle_{in}$ come, respectively, from the from the seventh, fourth, and third elements of the input BV. The relativistic velocity (β) and energy (γ) parameters are computed from the first element of the input BV (the beam energy E_{in}) and the particle mass (a Global Parameter).

Magnetic focusing LEBTs must generally be operated with a background gas to neutralized the beam space charge forces. For negative ions this can result in the collisional stripping of electrons from the ions and a loss of beam current. For hydrogenic positive ions this is not a problem so:

$$f_{\rm s} = 1$$
 , if $Q > 0$, (2.15)

where Q is the ion charge (a Global Parameter).

For negative ions, the stripping attenuation through the LEBT is given by:

$$f_s = \exp(-10^{+2}n_{gas}\sigma_{-1.0}L_{lebt})$$
, if $Q < 0$, (2.16)

where L_{lebt} (in meters) is the length of the LEBT, $\sigma_{-1,0}$ is the stripping cross section (in cm²) and n_{gas} is the LEBT gas density (in cm⁻³). The length L_{lebt} is calculated as part of the EMS LEBT Engineering Vector which is discussed in Section 2.3. The factor of 10^{+2} is to convert the units of L_{lebt} to cm. The stripping cross section, $\sigma_{-1,0}$ appearing in Equation (2.16), utilizes a parametric fit to experimental data of the form:

$$\sigma_{-1,0} = (8\pi \ a_o^2) \frac{\alpha^2}{\beta^2} I_{-1,0} / \left[1 + a_{-1,0} (\alpha / \beta) + b_{-1,0} (\alpha / \beta)^2 \right]$$
 (2.19)

The parameter $I_{-1,0}$, which establishes the high energy cross section (> 1 MeV), is taken from Born approximation calculations and $a_{-1,0}$ and $b_{-1,0}$ are determined from fits to cross section data over a wide range of energies above 10 keV [106]. The energy dependence is in the relativistic β (= v/c) parameter which is a function of the beam energy E_{in} in the LEBT. The constant a_o is the Bohr radius (so $8\pi a_o^2 = 7.04 \times 10^{-16} \, \mathrm{cm}^2$) and $\alpha = (137.037)^{-1}$ is the fine structure constant. The data base available for these calculations includes hydrogen, deuterium, helium, nitrogen, neon, argon, and xenon. The gas species is determined by the choice of N_{gas} , a user input (Table 2.1). Table 2.2 gives the stripping cross section parameters for the different neutralizing background gas species.

Table 2.2. Cross section parameters for $\sigma_{.1,0}$ to be used in Equation (2.19) for determining stripping losses in the LEBT according to Equation (2.16). Also shown for reference is the value for $\sigma_{.1,0}$ from Equation (2.19) at a beam energy of 30 keV. (For positive ions $\sigma_{.1,0}$ is zero.)

Gas Species (Atomic No)	N_{gas}	<i>I</i> _{-1,0}	<i>a</i> _{-1,0}	b _{-1,0}	$\sigma_{-1,0} (10^{-16} \mathrm{cm}^2)$
H ₂ (1)	1	4.11	0.85	2.00	7.00
$D_2(1)$	1	4.11	0.85	2.00	7.00
He(2)	3	2.80	1.24	2.59	3.83
N ₂ (7)	4	35.56	4.30	14.67	12.2
Ne(10)	5	19.90	3.28	22.84	5.07
Ar(18)	6	62.40	11.85	18.07	13.6
Xe(54)	7	315.0	98.67	-25.	26.3

2.2.2. Beam Transport Equations.

The matrix elements g_{33} , g_{34} , g_{37} , g_{73} , and g_{77} , and the vector element $\Delta \alpha$, appearing in Equation (2.10) depend upon the transport (R) matrix for the EMS LEBT configuration. The R-matrix values for the EMS LEBT are computed below. The values of g_{33} , g_{34} and g_{35} are given by:

$$g_{33} = R_{11}^2 {,} {(2.19)}$$

$$g_{34} = 10^{-6} \left[(\beta \gamma)^{-2} (1 + \alpha_{t,in}^2) R_{12}^2 \right] / \langle x^2 \rangle_{in}$$
, (2.20)

and

$$g_{37} = 2 \cdot 10^{-3} \left[(\beta \gamma)^{-1} R_{11} R_{12} \varepsilon_{t,in} \right]$$
 (2.21)

Here R_{12} , the (1,2) element of the transport (R) matrix, is in units of meters/radian. The factor of 10^{-6} in (2.20) converts to the units used for $< x^2 > (\text{cm}^2)$ and ε_t^2 (π -cm-mrad)². Similarly, the factor of 10^{-3} in (2.21) converts to the units used for $\varepsilon_{t,in}$ (π -cm-mrad). In both (2.20) and (2.21) β and γ are the usual relativistic parameters for the LEBT input energy E_{in} .

The elements g_{73} , g_{77} and $\Delta \alpha$ are given by:

$$g_{73} = -10^{+?} [(\beta \gamma) R_{11} R_{21}] / \varepsilon_{t,in}$$
, (2.20)

$$g_{77} = R_{11}R_{22} + R_{12}R_{21} \quad , \tag{2.23}$$

and

$$\Delta \alpha = -10^{+7} \left[R_{12} R_{22} \left(1 + \alpha_{t,in}^{2} \right) (\beta \gamma)^{-1} \varepsilon_{t,in}^{2} \right] / \langle x^{2} \rangle_{in} . \qquad (2.24)$$

2.2.3. R-Matrix Equations.

The R matrix used in Equations (2.19)-(2.24) is determined by the LEBT matching requirements. The optics design is that of either (a) the "point-to-point" type using two solenoids, shown schematically in Figure 2-2, or (b) the "parallel-to-point" type using one solenoid.

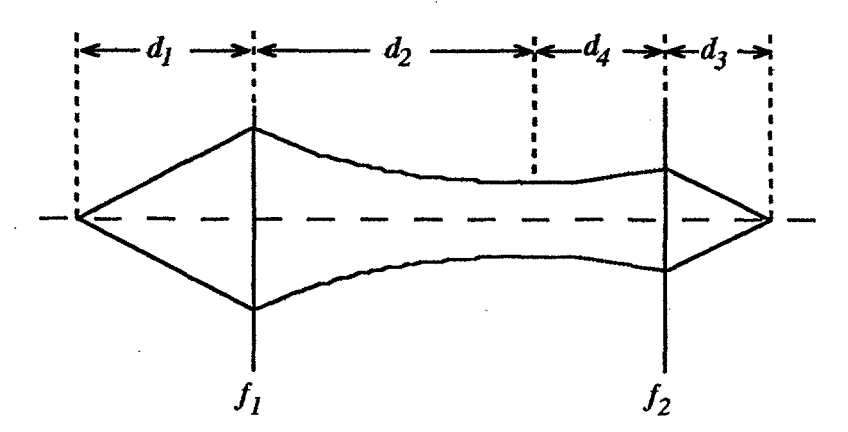


Figure 2-2. Schematic of the point-to-point solenoid LEBT matching concept, assuming a thin lens approximation for both solenoids.

The selection of which type of optics, point-to-point or parallel-to-point, to be used is based upon two criteria: good transmission through the LEBT and meeting the LEBT length goal. These criteria are discussed further below.

The remainder of this section presents the formulas for determining the positions (d_i) and strengths (f_i) of the solenoids used in the LEBT. These values are determined by the matching requirements imposed by the (goal) LEBT output Twiss parameters (i.e. those needed by the RFQ) and the Twiss parameters input to the LEBT by the ion source. As the schematic of Figure 2-2 indicates, a thin lens model is used for determining the solenoid strengths as effective focal lengths. The final results used in the BV calculation are given by Equations (2.19)-(2.24) above. The rest of this section discusses the derivation of the R matrix elements to be used in those equations.

Two equations can be used to describe the transformation of Twiss parameters in terms of the R matrix. For two input Twiss parameters $\alpha_{t,in}$ and $\beta_{t,in}$, the output Twiss parameters, $\alpha_{t,out}$ and $\beta_{t,out}$ after the beam passes through a transport channel described by an R matrix are given by:

$$\beta_{t,out} = R_{11}^2 \beta_{t,in} - 2R_{11}R_{12} \alpha_{t,in} - R_{12}^2 (1 + \alpha_{t,in}^2)/\beta_{t,in} , \qquad (2.25)$$

and

$$\alpha_{t,out} = -R_{11}R_{21}\beta_{t,in} + (R_{11}R_{22} + R_{12}R_{21})\alpha_{t,in} - R_{12}R_{22}(1 + \alpha_{t,in}^2)/\beta_{t,in} . (2.26)$$

Here $\alpha_{t,in}$ and $\alpha_{t,out}$ are the seventh elements of the input and output Beam Vectors, and $\beta_{t,in}$ and $\beta_{t,out}$ are related to first, third and fourth elements of the respective Beam Vectors by:

$$\beta_{i,j} = 10^{+1} (\beta \gamma)_j [\langle x^2 \rangle_j / (\epsilon_{i,j})] ,$$
 (2.27)

 10^{+1} is to convert the units of $\beta_{i,j}$ to meters/radian. The factor $(\beta \gamma)_j$ contains the usual relativistic parameters for either the input energy E_{in} , or output energy E_{out} , respectively. There is no energy gain in the EMS LEBT so $E_{in} = E_{out}$ and the $(\beta \gamma)$ input and output factors are the same.

The objective of the LEBT optics is to provide a beam which is matched into the RFQ. Good RFQ performance requires particular values of the Twiss parameters output from the LEBT. These particular Twiss parameters are referred to as goals, α_{To} and β_{To} . The solenoid strengths and drift distances are adjusted to produce a LEBT output beam which has Twiss parameters close to these goals.

The selection of which type of optics, (a) point-to-point or (b) parallel-to-point, to be used is based upon the two criteria mentioned above: achieving the LEBT maximum length goal and good transmission. The input Twiss parameters, $\alpha_{l,in}$ and $\beta_{l,in}$, the goal output Twiss parameters, α_{To} and β_{To} , the LEBT length goal, l_{lebt} and the LEBT transport channel radius, r_1 , are used in estimating if these two criteria can be met.

A LEBT length less than the maximum length goal can generally be met with the point-to-point optics, but not with parallel-to-point optics. It is shown later in Section 2.3.2.(b) that for the case of parallel-to-point optics, the LEBT length will be less than the goal l_{lebt} if:

$$l_{lebt} \ge 2[\beta_{To} \ \beta_{t.in}]^{1/2} + \alpha_{To} \ \beta_{t.in}$$
 (2.28)

Consequently, the inequality of Equation (2.28) must be satisfied for a single solenoid, parallel-to-point optics LEBT to be used.

The second criteria uses an estimate of the aperture losses to see if good transmission can be achieved. The calculation of aperture losses is the same for both positive and negative ions. However, for negative ions there will be additional losses due to stripping. Those losses are computed for the EMS LEBT, but are not included in the initial transmission estimate used for selecting the optics. The first step in estimating the aperture transmission losses is to estimate the maximum value of the beam radius. The first drift distance for the parallel-to-point optics is derived in Section 2.3.2.(b) and is given by Equations (2.47) and (2.46). Combining those and substituting $d_1 = [\beta_{To}\beta_{t,in}]^{1/2} + \alpha_{To}\beta_{t,in}$ into (2.14) yields an estimate for this maximum radius squared, r_m^2 .

$$r_{m}^{2} = \langle x^{2} \rangle_{in} + 10^{-2} \left[([\beta_{To} \beta_{t,in}]^{1/2} + \alpha_{To} \beta_{t,in})^{2} (1 + \alpha_{t,in}^{2}) (\epsilon_{t,in}/\beta \gamma)^{2} \right] / \langle x^{2} \rangle_{in}$$

$$- 2 \cdot 10^{-1} \left([\beta_{To} \beta_{t,in}]^{1/2} + \alpha_{To} \beta_{t,in} \right) (\epsilon_{t,in}/\beta \gamma) \alpha_{t,in} .$$
(2.29)

A maximum 10% beam loss criteria due to aperture scrapping is then used to estimate if a single solenoid LEBT with an initial drift length of $[\beta_{T_0}\beta_{t,in}]^{1/2} + \alpha_{T_0}\beta_{t,in}$ would be acceptable. Using $f_a = 0.9$ and $r_{max}^2 = r_m^2$ in Equation (2.13) then gives the criteria that if

$$r_1^2 / (2r_m^2) \ge -\ln(0.1) = 2.302585$$
 , (2.30)

then a single solenoid, parallel-to-point optics LEBT should be acceptable.

then a single solenoid, parallel-to-point optics LEBT should be acceptable.

In summary, both inequalities (2.28) and (2.30) must be met for ASM to select the parallel-to-point LEBT optics design with a single solenoid. The two LEBT designs are discussed separately below.

2.2.3.(a) Point-to-Point Optics (Two Solenoids)

The beam propagation from the source through the first solenoid and drifting a distance d_2 can be expressed through the matrix for a drift-focus-drift as

$$M_{1} = \begin{pmatrix} 1 - \frac{d_{2}}{f_{1}} & d_{1} + d_{2} - \frac{d_{1}d_{2}}{f_{1}} \\ -\frac{1}{f_{1}} & 1 - \frac{d_{1}}{f_{1}} \end{pmatrix}$$
(2.31)

The distance d_1 is chosen to be close to the focal length f_1 so that $d_1/f_1 = 1 + \varepsilon$ where ε is small. The distance d_2 is that to where the beam is at a waist, for which the Twiss parameter $\alpha = 0$. Substituting the above M matrix into (2.25) and (2.26) for the R matrix, solving for $\alpha_{t,out} = 0$, and dropping small terms gives

$$d_{2} = d_{1} - \left(\alpha_{in} / \beta_{in}\right) d_{1}^{2} , \qquad (2.32)$$

where we have simply used subscripts in for the input Twiss parameters. Similarly the region of drift-focus-drift through d_4 , f_2 and d_3 can be expressed as

$$M_{2} = \begin{pmatrix} 1 - \frac{d_{3}}{f_{2}} & d_{3} + d_{4} - \frac{d_{3}d_{4}}{f_{2}} \\ -\frac{1}{f_{2}} & 1 - \frac{d_{4}}{f_{2}} \end{pmatrix}$$
(2.33)

Again with the same approximations for $d_3/f_2 = 1 + \varepsilon$, equations analogous to (2.25) and (2.26) can be solved to give

$$d_{4} = d_{3} + \frac{\alpha_{out} d_{1}^{2}}{\beta_{in}}$$
 (2.34)

and

$$d_{3}^{2} = d_{1}^{2} \left(\beta_{out} / \beta_{in} \right)$$
 (2.35)

Equations (2.34), and (2.35) can be solved in terms of d_1 :

$$d_{3} = \left(\beta_{out}/\beta_{in}\right)^{1/2} d_{1} \qquad (2.36)$$

and

$$d_{4} = \left(\beta_{out} / \beta_{in}\right)^{1/2} d_{1} + \left(\alpha_{out} / \beta_{in}\right) d_{1}^{2}$$
(2.37)

The length d_1 can then be solved for in terms of the total length using the goal $L = l_{lebt}$:

$$L = d_1 + d_2 + d_3 + d_4 (2.38)$$

to give

$$d_{1} = \frac{-b + (b^{2} + 4aL)^{1/2}}{2a}$$
(2.39)

where

$$b = 2 \left[1 + \left(\frac{\beta_{out}}{\beta_{in}} \right)^{1/2} \right] , \qquad (2.40)$$

and

$$a = (\alpha_{out} - \alpha_{in}) / \beta_{in} \qquad (2.41)$$

Equations (2.39), (2.32), (2.36) and (2.37) specify the lengths d_1 through d_0 , respectively, for the EMS LEBT. The focal lengths are determined from

$$\frac{d_1}{f_1} = 1$$
 (2.42)

and

$$\frac{d_{3}f_{2}}{f_{2}} = 1 {(2.43)}$$

The values of d_i and f_i are then substituted into the matrices M_1 and M_2 and the final R matrix is given by the matrix product:

$$R = M_2 \cdot M_1 \quad . \tag{2.44}$$

2.2.3.(b) Parallel-to-Point Optics (One Solenoid)

The beam propagation from the source through the drift distance d_1 , the solenoid, and the drift distance d_2 has a drift-focus-drift matrix given by:

$$M_{1} = \begin{pmatrix} 1 - \frac{d_{2}}{f_{1}} & d_{1} + d_{2} - \frac{d_{1}d_{2}}{f_{1}} \\ -\frac{1}{f_{1}} & 1 - \frac{d_{1}}{f_{1}} \end{pmatrix}$$
(2.45)

The basic assumption for the parallel-to-point LEBT is that $\alpha_{t,in}$ is negligibly small. Setting $\alpha_{t,in}$ = 0 in Equations (2.25) and (2.26) and choosing the distance d_2 to be close to the focal length f_1 (i.e. $d_2/f_1 = 1 + \varepsilon$ where ε is small), yields for the two drift distances (in meters):

$$d_2 = [\beta_{To} \ \beta_{t,in}]^{1/2} , \qquad (2.46)$$
 and
$$d_1 = d_2 + \alpha_{To} \ \beta_{t,in} . \qquad (2.47)$$

The thin lens equivalent solenoid strength is then

$$f_1 = d_2 . (2.48)$$

Using the values of d_i and f_1 are in the matrix M_1 of Equation (2.45) then gives the final R matrix:

$$R = M_1 . (2.49)$$

Note that for the single solenoid, parallel-to-point optics, the LEBT length goal cannot, in general, be met. From (2.46) and (2.47) it can be seen that the LEBT length, d_1+d_2 , will be less than or equal to the length goal if:

$$l_{lebt} \ge 2[\beta_{To} \ \beta_{t.in}]^{1/2} + \alpha_{To} \ \beta_{t.in}$$
 (2.50)

This result is the first criteria discussed previously, Equation (2.28), used by ASM in selecting between the parallel-to-point and point-to-point optics options.

2.2.4. Emittance Growth Modeling.

Transverse emittance growth in the EMS LEBT due to two phenomena are included. These are (a) emittance growth due to plasma instabilities and (b) effective transverse emittance growth due to the oscillation in the phase ellipse as a result of beam current fluctuations. For negative ions the modeling of (a), the plasma instability emittance growth, is based on the scaling of experimental data [235,236]. For positive ions this emittance growth mechanism should be turned off (through the user input parameter $Th_{\rm gas}=0$). The beam current fluctuation emittance growth, mechanism (b), is based on the model by Allison [227] and is the same for both positive and negative ions. For either positive or negative ions the user may selectively adjust either of these emittance growth mechanisms, if desired, by adjusting the user inputs ($\Delta I/I$) or $Th_{\rm gas}$, respectively. Setting either of these to zero effectively turns off that emittance growth mechanism. We first discuss the modeling of the instability driven emittance growth, followed by the Allison model implementation.

2.2.4.(a) Negative Ion Beam Instability Emittance Growth.

Experimental data [235,236] relating the gas density of xenon to beam emittance growth has been parametrized and included in the model. This data is for a 20 keV beam in a LEBT channel with a xenon (Xe) density varied from 0 to 7.5 x 10¹² cm⁻³. The emittance data has been fit by:

$$\left[\Delta\varepsilon \left(\pi \, cm \, -mrad\right)\right]^{2} = 10.4 \times 10^{-4} \exp\left(-8.2 \times 10^{-12} \, \rho\right) + 4.6 \times 10^{-4} \exp\left(-0.67 \times 10^{-12} \, \rho\right)$$
(2.51)

where ρ is the xenon density given in cm⁻³. Little data exists for other gases or energies, so this fit is scaled in the model according to results obtained from theoretical analyses and computer simulations [185,194,205]. These results are summarized briefly below. The basic result is that

together with the assumption that the emittance growth increases linearly with the length of the LEBT. Specifically the emittance growth term $\Delta \varepsilon^2$ appearing on the right hand side of Equation (2.10) is given by:

$$\Delta \varepsilon^{2} = \left[10.4 \times 10^{-4} \exp\left(-A_{\rho} \frac{n_{gas}}{n_{th}}\right) + 4.6 \times 10^{-4} \exp\left(-B_{\rho} \frac{n_{gas}}{n_{th}}\right)\right] \left[\frac{L_{LEBT}}{L_{norm}}\right] , (2.52)$$

where L_{lebt} is the length of the LEBT and L_{norm} is the length of the transport line used in the experiment of Reference [235,236]:

$$L_{norm} = 0.6 \text{ (meters)} , \qquad (2.53)$$

Detailed numerical simulations [205] for transport in argon (Ar) at 10^{-5} torr show that for beam currents falling below a line given by I (mA) = $0.8 \ V^{3/2}$, where V is the beam voltage in kilovolts, the beam transport is stable. The instability is seen for beam currents above the line I (mA) = $1.3 \ V^{3/2}$. Because of the limited number of simulations done to generate the data base, the intermediate region is uncertain. Nevertheless this suggests that one can define a quenching threshold constant, k, which determines when little or no emittance growth due to this instability should occur, i.e. when

$$I_{in}$$
 (mA) $< k E_{in}^{3/2}$ (2.54)

Quenching of the instability, identified as being due to electrons, occurs when the ratio of electron density to beam density exceeds the ratio of electron energy to beam energy [383],

$$\frac{n_{\epsilon}}{n_{b}} \ge \frac{E_{\epsilon}}{E_{b}} \tag{2.55}$$

Expressing the beam density in terms of the beam current and energy gives the condition determining stable propagation as

$$I_{ext} < k_1 n_e r^2 E_b^{3/2} \tag{2.56}$$

where r is the beam radius. The necessary electron density is generated by ionizing the gas, so this density is proportional to the product of the ionization cross section σ_i and the density of gas available to be ionized. The gas density is proportional to the pressure, which is a user input. Finally, maintaining this electron density depends on the diffusion of the gas ions. The diffusion time and the density go as the square root of the plasma ion mass $M_{gas}^{1/2}$. This analysis suggests we scale the factor k appearing in (2.54) as:

$$k = \kappa \left(\frac{P \ (m \ torr)}{10^{-2}} \right) \left(\frac{\sigma_i}{\sigma_i \ (Ar)} \right) \left(\frac{M}{M_{Ar}} \right)^{1/2} \left(\frac{r \ (cm)}{.643} \right)^2 \left[mA \ / \ (keV)^{3/2} \right]$$
(2.57)

where the value of κ is between 0.8 and 1.3. The rms beam radius, r, is scaled by the effective rms radius used in the simulations (i.e. 0.91 cm/ $\{2\}^{1/2} = 0.643$ cm). The criteria used in the model

 $V^{3/2}$ as being in the stable regime, i.e. $\kappa = 0.8$. Equations (2.54) and (2.57) can be combined to define a threshold pressure, for assuring that the ion-ion instability is quenched:

$$P \ge P_{th} (m torr) = \frac{10^{-2}}{\kappa} \left(\frac{\sigma_i (Ar)}{\sigma_i} \right) \left(\frac{M_{Ar}}{M_{gas}} \right)^{1/2} \left(\frac{.643}{r_{in}} \right)^2 I_{in} E_{in}^{-3/2} , (2.58)$$

Here I_{in} is in mA, and E_{in} is in keV. The corresponding threshold density is given by

$$n_{th} (cm^{-3}) = Th_{gas} \frac{P_{th}}{kT} = Th_{gas} \frac{9.6571 \times 10^{13}}{\kappa T (^{\circ}K)} \left(\frac{\sigma_i (Ar)}{\sigma_i (N_{gas})} \right) \left(\frac{M_{Ar}}{M_{gas}} \right)^{1/2} \left(\frac{.643}{r_{in}} \right)^2 I_{in} E_{in}^{-3/2}$$
,(2.59)

where the instability threshold factor Th_{gas} has been included. The default value for this parameter (a user input) is set to zero, but the user may adjust this emittance growth mechanism in the calculations by increasing Th_{gas} up to unity. The cross section σ_i (N_{gas}) and the molecular mass M_{gas} of the LEBT gas are determined from a look-up table (Table 2.4). The instability driven emittance growth, given by Equation (2.52), is then obtained from the scaling of equation (2.51), with the additional assumption that magnitude (in quadrature) of the emittance growth increases with the length of the LEBT. The parameters A_{ρ} and B_{ρ} appearing in Equation (2.52) are determined by the threshold density for Xe gas:

$$A_{\rho} = 8.2 \times 10^{-12} n_{th} \text{ (Xe)}$$

and

$$B_{\rho} = 0.67 \times 10^{-12} n_{th} \text{ (Xe)}$$
 (2.61)

Here n_{th} (Xe) is calculated for the experimental conditions given in references [235,236], i.e. for a 20 keV, 100 mA beam with an rms radius of 0.707 cm:

$$n_{th}(Xe) = \frac{9.6571 \times 10^{13}}{\kappa \ 300 \ \kappa} \left(\frac{\sigma_i (Ar)}{\sigma_i (Xe)} \right) \left(\frac{M_{Ar}}{M_{Xe}} \right)^{1/2} \left(\frac{.643}{.707} \right)^2 (100) (20)^{-3/2}$$
$$= \frac{3.29 \times 10^{11}}{\kappa} \left[\frac{4.5}{5.5} \right] \left[\frac{40}{131} \right]^{1/2} (.828) (1.118) = \frac{13.8 \times 10^{10}}{\kappa} cm^{-3}$$
(2.62)

This gives:

$$A_0 = 1.132/\kappa$$
 , (2.63)

and

$$B_0 = 0.0925/\kappa$$
 (2.64)

Note that setting the (user input) instability threshold factor $Th_{gas} = 0.8/1.3 = 0.62$ is equivalent to selecting the criteria $\kappa = 1.3$ for determining the stable region. This is used to set the lower limit for this user input for negative ions.

A useful parameter for assessing the beam propagation in the LEBT is the Gabovich critical density n_c . This is the density required to achieve complete space-charge neutralization of the beam. It is given by [354]:

$$n_c = [2 / (r \sigma_i)] (v_{gas} / v_{beam})$$
, (2.65)

where v_{gas} is the mean velocity of the ions in the neutralizing gas, $v_{beam} = \beta c$ is the beam velocity and r is the rms beam radius, taken to be given by the value of r_{max} from Equation (2.14). Using the value $v_{gas} = (8kT / \pi M_{gas})^{1/2}$ with kT = (1/40) eV corresponding to the assumption of room temperature (300 K), then n_c can be written as:

$$n_c = 3.63 \cdot 10^{-3} \left[(r_{max} \sigma_i)^{-1} \right] \left(A / M_{gas} \right)^{1/2} E_{in}^{-1/2} ,$$
 (2.66)

where E_{in} is the beam energy (in MeV). While this critical density is not used directly in the EMS LEBT modeling, it is available to the user as a model diagnostic parameter (see Section 2.4).

Table 2.3 Parameters of Background Gases Used for Neutralized Transport in Magnetic LEBTs. The Cross Sections σ_i are from Reference [317] at 20 keV.

Neutralizing Back- ground Gas Species (Atomic Number)	N _{gas}	M _{gas} (amu)	σ_i (cm ²)	Critical Temperature (° K)	Vapor Pressure near 30 K (mTorr)
H ₂ (1)	1 .	2.016	8x10 ⁻¹⁷	33	$6.2x10^6$
D ₂ (1)	2	4.000	8x10 ⁻¹⁷	38	~10+7
He (2)	3	4.003	$5x10^{-17}$	5.2	N/A
N ₂ (7)	4	28.02	4x10 ⁻¹⁶	126	4.8x10 ⁻²
Ne (10)	5	20.18	$7x10^{-17}$	44	$1.7x10^6$
Ar (18)	6	39.94	4.5x10 ⁻¹⁶	151	9.3x10 ⁻⁴
Xe (54)	7	131.3	5.5x10 ⁻¹⁶	290	5.6x10 ⁻¹⁷

2.2.4.(b) Beam Current Fluctuation Emittance Growth.

The non-instability emittance growth factor, element g_{44} of Equation (2.10) above, is due to beam current fluctuations ΔI . Beam current fluctuations result in a fluctuation of the orientation of the transverse phase-space ellipse for the beam and a larger effective emittance ellipse is then required to describe the bulk of the beam. These fluctuations "smear out" the phase space ellipses resulting in an effective emittance growth. The calculation of this contribution to the emittance growth is based upon the model due to Allison [227]. From Allison's model, the emittance growth is:

$$\varepsilon_{t,out}^2 = g_{44} \varepsilon_{t,in}^2 , \qquad (2.67)$$

where

$$g_{44} = 1 + \frac{\Delta}{2} + \left(\Delta + \frac{\Delta^2}{4}\right)^{1/2}$$
 (2.68)

Allison's expression for Δ , which is zero for no emittance growth, depends on the net beam current, I, and the fluctuations in the current ΔI . Specifically,

$$\Delta = (1+x/R)^2 + (1+x/R)^{-2} + (\beta \gamma R^2/\varepsilon_B)^2 (x^1/R)^2 - 2 \qquad (2.69)$$

where

$$\frac{x}{R} = \frac{r(\Delta I)K^2}{2[1+r(I)/2]},$$
(2.70)

and

$$\frac{x^{-1}}{R} = \frac{r(\Delta I)(k_2/100)K(1-K^{-2})^{1/2}}{2[1+r(I)/2]}$$
(2.71)

The function r(I) describes the beam current dependence. It is the ratio of the space-charge force to the effective emittance force:

$$r(I) = \frac{2R^2}{\beta \gamma \varepsilon_B^2} \frac{I}{I_m} , \qquad (2.72)$$

with

$$I_m = 4\pi\epsilon_0 A (m_p c^3/e) = A \cdot 3.124 \times 10^7 \text{ Amps}$$
 (2.73)

 I_m is the Alfven current for an ion of the atomic mass A (in amu). The parameters β and γ are the usual relativistic parameters corresponding to a beam with energy E_{in} (first element of the Beam Vector input to this module). R is the radius of the transport channel and ε_B (π -cm-rad) is the normalized emittance corresponding to the boundary of the beam. These appear in both Equations (2.69) and (2.72). The transport channel radius is given by r_1 , a user input:

$$R = r_1 (2.74)$$

The normalized boundary emittance is computed by assuming a Gaussian beam distribution. The boundary emittance enclosing a fraction f_R of the total beam, is related to the rms transverse

emittance ε_{in} (which is input to this module via the fourth element of the Beam Vector) by

$$\varepsilon_B (\pi - cm - rad) = 2 \cdot 10^{-3} \ln \left[1 / (1 - f_B) \right] \varepsilon_{in} (\pi - cm - mrad)$$
 , (2.75)

where the factor of 10^{-3} converts the units of emittance to π -cm-rad from π -cm-mrad. We pick $f_B = 0.9$, corresponding to 90% of the beam, so that $\varepsilon_B = 4.605 \cdot 10^{-3} \varepsilon_{in}$.

The current I is the net current after adding a background gas (such as Xe) to achieve space-charge neutralization, i.e. $I = (1 - f_N) I_{in}$ where f_N represents the fractional neutralization. For any reasonable transport of negative ions in a magnetically focused LEBT (i.e. EMS or PMQ) f_N must be very close to unity. Without loss of any significance, we take $f_N = 1$, so that the net current I = 0. Only the function $r(\Delta I)$ need be evaluated for Equations (2.70) and (2.71) since r(I) = r(0) = 0. The factor K appearing in Equations (2.70) and (2.71) is given by:

$$K = \sin(k_2 L_{leht}/2) \quad , \tag{2.76}$$

where k_2 is the wave number, in (meters)-1, characteristic of the (matched) transport channel and L_{lebt} is the length (in meters) of the LEBT, which is from the LEBT Engineering Vector given in the next section. The wave number, k_2 , is given by Allison; in units of (meters)-1 it is:

$$k_2 = 2 \cdot 10^{-2} \varepsilon_B (\pi\text{-cm-rad})/(\beta \gamma R^2)$$
 , (2.77)

where ε_B (π -cm-rad), β , γ , and R have been defined above. As in the case of the instability emittance growth, the user may "turn-off" this emittance growth mechanism by setting (via the user input) the beam current fluctuation to zero, i.e.($\Delta I/I$) = 0.

2.3 EMS LEBT Engineering Vector (EV) Model.

The Engineering Vector for the EMS LEBT is of the form:

$$\begin{bmatrix} L \\ | V | \\ | M | \\ | P | \\ | EV = | x \\ | | y \\ | Conf \\ | Cost \end{bmatrix}$$
(2.81)

The EMS engineering model is based primarily on the GTA LEBT, data from the BEAR and CRNL LEBTs, and conceptual designs for NPB flight injectors. The general concept used for

2.3.1 LEBT Length Calculation.

The length, L, depends on the drift distances (d_i) given Section 2.3.2. Specifically

$$L = L_{lebt} (2.82)$$

where

$$L_{lebi} = \sum (d_i) \quad . \tag{2.83}$$

For a two solenoid LEBT the value of L_{lebt} should be the same as the user input for the LEBT length goal, l_{lebt} . However, for a single solenoid LEBT, L_{lebt} will generally be less than the goal value.

2.3.2 LEBT Volume Calculation.

The LEBT volume, V in meters³, is calculated from

$$V = \pi L_{lebt} R_{lebt}^{2} + N_{p} \left(\pi L_{pump} R_{pump}^{2} \right)$$
 (2.84)

Here R_{lebt} is the radius of the LEBT transport vacuum enclosure, assumed to be cylindrical and referred to as the LEBT transport "pipe" below. N_p is the number of vacuum pumps required and L_{pump} and R_{pump} are the length and radius, respectively, of a single pump. These parameters are discussed below. This model for the LEBT volume calculation assumes a geometry as illustrated in Figure 2-1.

The radius, R_{lebt} , of the LEBT transport pipe is taken to be 20% more than the value necessary to enclose the solenoids. Hence, in units of meters:

$$R_{lebt} = 1.2 \cdot R_{solenoid} , \qquad (2.85)$$

where $R_{solenoid}$ (in meters) is the outer radius of the solenoid. This is taken to be the sum of the aperture, r_1 , the effective radial extent of the wire used in the windings, a (in meters), and the thickness of the mechanical support upon which the wire is wound, ΔR_s (in meters):

$$R_{solenoid} = 10^{-2}r_1 + a + \Delta R_s$$
 , (2.86)

where the factor of 10^{-2} converts the units of r_1 (a user input in centimeters) to meters. We take $\Delta R_s = \Delta R_{linac}$, a User Definition Parameter, and the value of a is based on the GTA solenoid designs [231]. Specifically:

$$a = 0.14 \text{ meter}$$
 (2.87)

The number and dimensions of the vacuum pumps are the final numbers required for the volume calculation. The vacuum pumps are sized according to the gas flow coming from the ion source. The peak gas flow rate, dV / dt, is computed by the ion source models and is passed to the LEBT

which are Global Parameters. These are

$$\langle dV / dt \rangle = df \frac{dV}{dt} \qquad (2.88)$$

and

$$V_{total} = \langle dV / d t \rangle t_{oper} \tag{2.89}$$

ASM is intended to provide users with different options for vacuum pumps. The present version only has pumps based on the BEAR getter pumps [369], which are modified versions of a commercially available pump. These pumps have a pumping speed of 0.2 torr-liters/second, and a maximum capacity of 1300 torr-liters between regeneration (activations). The number of pumps required is taken to be the larger of the two limiting cases, i.e.:

$$N_p = \max(N_{p1}, N_{p2})$$
 , (2.90)

where

$$N_{P}I = 10^{-3}P_{Ioh} < dV / dt > / (0.2)$$
 , (2.91)

and

$$N_{p2} = 10^{-3} P_{lebt} V_{total} / (1300) (2.92)$$

The individual pump length and radius, L_{pump} and R_{pump} , are taken to be the values for the BEAR getter pump:

$$L_{nump} = 0.265 \text{ meters}$$
 , (2.93)

and

$$R_{pump} = 0.117 \text{ meters}$$
 (2.94)

2.3.3 LEBT Mass Calculation.

The EMS LEBT mass, M, is described by

$$M = \sum_{i=1}^{N_T} M_i + M + M_{pipe} + N_p M_{pump}$$
(2.95)

The mass, M_i , of each solenoid is given in kilograms by the sum of the wire mass and the winding mechanical support mass. This is computed as:

$$M_i = l_i \left\{ \left[2\pi (10^{-2} r_1 + a/2) a \rho_{Cu} \right] + \left[2\pi \left(R_{solenoid} \right) \Delta R_s \rho_{linac} \right] \right\} \ , \ (2.96)$$

where l_i is the length of the solenoid, ρ_{Cu} is the density of copper (2.7·10⁺³ Kg/m³) assumed for the wire, and ρ_{linac} is the density of the structural material used for the linear accelerator (a Global Parameter). We use for a the value given by Equation (2.87). For the solenoid lengths we use the GTA design values [231]:

$$l_1 = l_2 = 0.14$$
 meters . (2.97)

 M_{pipe} in kilograms, is given by

$$M_{pipe} = 2\pi \rho_{pipe} L_{lebt} R_{lebt} \Delta R_{lebt} + \pi \rho_{pipe} R_{lebt}^2 \Delta L_{lebt} , \qquad (2.98)$$

where ΔR_{lebt} is the thickness (in meters) of the vacuum pipe, ΔL_{lebt} is the thickness (in meters) of the end walls, and ρ_{pipe} is the density (in kg/m³) of the vacuum pipe material and end walls. The density of the vacuum pipe and end wall material is set by the structural density Global Parameter:

$$\rho_{pipe} = \rho_{linac} \quad . \tag{2.99}$$

The thicknesses of the vacuum pipe and end walls are taken given by:

$$\Delta R_{lebt} = \Delta L_{lebt} = \Delta R_{linac} , \qquad (2.100)$$

where ΔR_{linac} is the thickness of the structural walls for the linac components (ΔR_{linac} is a FORTRAN data parameter).

The mass of a single pump, M_{pump} , is taken to be the mass of a BEAR getter pump:

$$M_{pump} = 12.25 \quad \text{kilograms.} \tag{2.101}$$

2.3.4 LEBT Power Requirements.

The EMS LEBT power requirements are taken to be the sum of the power required for the solenoids and for the vacuum pumps:

$$P = P_S + P_D \quad . \tag{2.102}$$

Getter pumps do not require power during operation, so their contribution to the power is taken to be zero:

$$P_p = 0$$
 . (2.103)

The solenoid power requirements are determined by the effective focal lengths f_i required to achieve the match conditions. The connection between focal lengths f_i and magnetic induction B_i of the solenoid is given by:

$$f_i l_i = 4(r_{ion})^2$$
 , (2.104)

where l_i is the effective length of the solenoid and r_{ion} is the gyro radius (in meters) of the beam ions:

$$r_{ion} = [(m_p c^2/|Q|)/30][A \beta \gamma / B_i]$$
, (2.105)

where B_i is in kiloGauss (kG) and $m_p c^{-2}$ is one atomic mass unit (in MeV). A is the atomic mass

(in amu) and Q the net charge of the beam ions (both Global Parameters). β and γ are the relativistic velocity and energy parameters associated with the beam input energy, E_{in} . Rewriting (2.104) and (2.105) gives

$$B_i(kG) = [(m_p c^{-2}/|Q|)/15][A \beta \gamma] / [f_i l_i]^{1/2}$$
, (2.106)

when the lengths f_i and l_i are in meters. From Ampere's Law the magnetic induction of a solenoid on axis is

$$B_i(kG) = 4\pi \cdot 10^{-6} n I_i g(r_1/l_i)$$
, (2.107)

where n is the number of turns/m, I_i is the solenoid current in amperes, and $g(r_1 / l_i)$ is a geometric factor taken to be a function of the aspect ratio of the solenoid. Using the GTA value $n = 1.12 \cdot 10^{+3}$ turns/m, gives $B_i(kG) = 0.0141I g(r_1 / l_i)$. For the $r_1 = 5$ cm GTA solenoid [231] the value of g is 0.9; which is used to parametrize g as:

$$g(r_1/l_i) = [1+1.84\cdot10^{-4}(r_1/l_i)^2]^{-1/2}$$
, (2.108)

where the factor 10^{-4} accounts for the different units of r_1 and l_i . The current required in each solenoid (in amperes) is then given by:

$$I_i = 71.1 B_i (kG) / g(r_1 / l_i)$$
, (2.109)

From Ohm's Law the power dissipated is

$$P_i = I_i^2 R , (2.110)$$

where R is the resistance. The resistance is proportional to the effective length of the windings which is expected to scale linearly with the aperture. The resistance is calculated as:

$$R = 0.05[(10^{-2}r_1 + a/2)/(0.05 + a/2)]$$
 ohms, (2.111)

where the GTA values of $R = 0.05 \Omega$ and $r_1 = 5$ centimeters have been used [231] for normalization. The value of a is given by Equation (2.87). The power for each solenoid (in Megawatts) is

$$P_i = 10^{-6} (I_i)^2 R (2.112)$$

The final power requirement for the LEBT solenoids is given by the sum

$$P_{S} = P_1 + P_2 \quad , \tag{2.113}$$

where P_1 and P_2 are computed for the two LEBT solenoids as described above, using the values of f_1 and f_2 given in Section 2.3.2.

2.3.5 LEBT Transverse Dimensions.

There a two transverse dimensions of the LEBT, the horizontal (x) and vertical (y) extensions from the centerline of the LEBT structure. In this version of ASM these two dimensions are taken to be the same:

$$y = x \quad , \tag{2.114}$$

The (horizontal) transverse dimension (with respect to the centerline) is given by:

$$x = R_{lebt} + \Delta R_{lebt} + L_{pump} \quad , \tag{2.115}$$

where R_{lebt} , ΔR_{lebt} and L_{pump} have been defined previously. The above formula is valid if the number of pumps required is not too large. An estimate of the maximum number of pumps that can be supported by a LEBT of the type shown in Figure 2-1 is discussed in Section 2.5.

2.3.6 EMS LEBT Model Confidence Factor.

Several considerations are used in developing the confidence factor for the EMS LEBT model. The modeling of the Beam Vector is based on empirical fits to experimental data and theoretical analyses which are in agreement with experiments. The engineering data are based upon existing hardware and a simple conceptual design. One drawback to the engineering model, however, is that only getter pumps of the type used for the BEAR are included. There is no model for cryogenic vacuum pumps, for example. However, to the extent that the inputs to the model fall within the guidance limits, the confidence in the model output is good. This suggests that $Conf \ge 0.9$ for the model. For the input parameters within the user guidance limits we have assigned:

$$Conf = 0.90$$
 . (2.120)

For inputs to the model which are outside the limits specified in Table 2.1 this confidence factor may not be not useful.

2.3.7 EMS LEBT Cost Estimate.

There are no cost estimates in this version of ASM.

2.4 Electromagnetic Solenoid Diagnostic Parameters

Most of the EMS LEBT model output is contained in the Beam and Engineering Vectors. There are certain parameters calculated for internal use in the model which may also be useful for assessing results, particularly when input parameters out of the limit ranges are being used. Table 2.4 summarizes the EMS LEBT Diagnostics together with approximate model validity ranges for each parameter.

Table 2.4. Diagnostic Parameters for the EMS Model.

Diagnostic Parameters Symbol (Equation)	Value for Default* Inputs	Default Units	Range* for Lower	Model Validity Upper
LEBT Gas Density $n_{gas} \ (2.5)$	6.438·10+11	cm ⁻³	3.219·10+10	3.219 10+12
Maximum Ream Radius r_{max} (2.14)	in LEBT 0.19 7 8	cm	tbd	tbd
Aperture Scraping Surviv f_a (2.13)	val Fraction tbd	(fraction)	tbd	1.0
Stripping Survival Fracti f_s (2.15) or (2.16)		(fraction)	tbd	1.0
Instability Threshold Den n_{th} (2.59)	nsity 0.0	cm ⁻³	tbd	tbd
Gabovich Critical Densit n_c (2.66)	y 7.25·10 ⁺¹⁴	cm ⁻³	tbd	tbd
Instability Contribution t $\Delta \epsilon$ (2.52)	o Emittance 0.0	π-cm-mrad	tbd	tbd
Achieved Output Twiss I $\beta_{t,out}$ (2.3)	Parameter 0.04	m/rad	tbd	tbd
No. of BEAR Type Vacua N_p (2.90)	uum Pumps 1	(none)	tbd	tbd
First Solenoid Power P_1 (2.112)	0.0129	MW	tbd	tbd
Second Solenoid Power P_2 (2.112)	0.0305	MW	tbd	tbd

^{*}Default values and ranges for model validity are for an H⁺ beam. Default values and ranges for model validity will be different for an H⁻ beam.

2.4.1 Additional "Rules of Thumb" for the EMS LEBT Model Validity Checks.

2.4.1.(a) Maximum Pump Capacity.

The maximum number of pumps that can be supported by a LEBT of length L_{lebt} and radius R_{lebt} + ΔR_{lebt} is approximately determined by amount of surface area available for attaching pumps each of radius R_{pump} . Assuming the geometry of Figure 2-1, the limit on the number of vacuum pumps will be approximately given by:

$$N_p < 2 (R_{lebt} + \Delta R_{lebt}) L_{lebt} / (\pi R_{pump}^2)$$
 (2.121)

This practical constraint on the packaging of adequate pumping capacity is checked in ASM. If this condition is not satisfied then a comment is written to the Diagnostics file. Note that increasing the LEBT length goal (a user input) may alleviate this problem.

2.4.1(b) Geometric Aberration Check.

For good optics (low geometric aberrations) it is desirable to have the maximum rms beam radius, r_{max} , to be significantly smaller than the transport channel radius, r_1 . If r_1 is at least 3 times r_{max} , i.e. if

$$r_1^2 > 9r_{max}^2$$
 , (2.122)

then it is assumed that the geometric aberrations are negligible and their neglect in the modeling is acceptable. If this condition is not satisfied then a comment is written to the Diagnostics file.

2.5 Interface Parameters To and From Other ASM Models.

Aside from the Beam Vector and Engineering Vector there is only one other EMS LEBT parameter needed by other models in ASM. The LEBT pressure, P_{lebt} in mtorr, is used in the two negative ion source models of ASM Verison 1.0. This pressure is a user input to the EMS model (Table 2.1). One parameter from the ASM ion source models is needed by the EMS LEBT model; this the gas flow rate, in liters per second, used to estimate the LEBT vacuum pump requirements.

2.6 References for EMS LEBT Model

- [106] "Task Assignment Final Report, Subtask B: NPB Technology Computer Code Development, Analysis and Assessment of Neutralizer Concepts," George H. Gillespie, Yu-Yun Kuo, Charles E. Eminhizer, Anna Porto and Thomas Roberts, Physical Dynamics Report No. PD-LJ-86-357R, 1986.
- [145] "CWDD Injector and Ion Source Studies, Injector Development for Block One Specification," G. Proudfoot, Neutral Particle Beam Injector Workshop Proceedings, February 1990.
- [185] "Preliminary Studies of Low Energy H⁻ Beam Transport in a Gas for White Horse," M. M. Campbell and L. A. Wright, Mission Research Corporation Report No. AMRC-R-780, February 1986.
- [194] "IVORY PIC Model of Low Energy Beam Transport: Final Report," M. M. Campbell and L. A. Wright, Mission Research Corporation Report No. AMRC-R-969, August 1987.
- [205] "LANL Beam Plasma Studies: Simulation of the GTA LEBT," M. M. Campbell, R. M. Clark and L. A. Wright, Mission Research Corporation Report No. MRC/ABQ-R-1113, November 1988.
- [211] "Conditions for Stabilizing the Ion-Ion Instability of a Negative-Ion Beam," V. P. Goretskii and A. P. Naida, Soviet Journal of Plasma Physics, 11, 394-399, 1985
- [227] "Emittance Growth Caused by Current Variation in a Beam Transport Channel," P. Allison, IEEE Transactions on Nuclear Science NS-32, 2556-2558, 1985.
- [231] "GTA Single Beam Injector Design Review," GTA Injector Team, Preliminary/Final Design Review, Los Alamos National Laboratory, January 1989.
- [235] "A High-Brightness Negative Hydrogen Linear Accelerator," E. A. Wadlinger, J. A. Farrell and H. O. Dogliani, Presented at the Seventh Conference on the Application of Accelerators in Research and Industry, LA-UR-82-3267, November 1982.
- [236] "Operating Experience with a 100 keV, 100 mA H⁻ Injector," P. Allison and J. D. Sherman, Third International Symposium on the Production and Neutralization of Negative Ions and Beams (Brookhaven), AIP Conference Proceedings No. 111, 511-519, 1983.
- [317] "Ionization of Gases by Negative Ions," Y. Fogel, A. Koval and Y. Levchenko, Soviet Physics JETP, 11, 760-762, 1960.
- [354] "Space Charge Neutralization of an Intense Negative Ion Beam," M. D. Gabovich, L. S. Simonenko and I.A. Soloshenko, Soviet Physics Technical Physics, 23, 783-785, 1978.

- [364] "Pop-Up Injector, A Summary of Status and Issues," L. Hansborough and GTA Injector Team, Presented at ACDTI In Progress Review at Grumman Aerospace Corporation, March 14, 1991.
- [369] "BEAR Project Final Report, Volume I: Project Summary," BEAR Project Staff, Los Alamos National Laboratory Report No. LA-11737-MS, Vol 1., BEAR-DT-7-1, January 1990.
- [383] "I. G. Technologies, Inc. Technical Data, Properties Table," I. G. Technologies, Inc. Staff, October 1990.
- [485] "High-Current Direct Injection to a CW RFQ Using an ECR Proton Source," G. M. Arbique, T. Taylor, A. D. Davidson and J. S. C. Wills, 1992 Linear Accelerator Conference Proceedings, 52-54, 1992.
- [487] "Optical Beam Sensors for RFQ1-1250," G. M. Arbique, B. G. Chidley, W. T. Michel and B. H. Smith, 1992 Linear Accelerator Conference Proceedings, 654-656, 1992.

3. Radiofrequency Quadrupole Two (RFQ-2) Model

RFQ 2

3.0 Radiofrequency Quadrupole (RFO-2) Model Overview.

The ASM RFQ-2 model for the radiofrequency quadrupole is similar to that of the RFQ-1 model but utilizes a somewhat different prescription for the vane modulations and for the engineering design. Both the RFQ-1 and RFQ-2 models for the radiofrequency quadrupole are based on the technology which has been developed in the latter half-decade of the 1980's. Many vane RFQs have been design in the U.S, since the proof-of-principal and accelerator test stand (ATS) devices were built at LANL in the early eighties. Two CW RFQs operating at room temperature (FMIT and CRNL), two RFOs operating pulsed at cryogenic temperatures (GTA and CWDD), and well as a space qualified RFQ (BEAR) are representative of the spectrum of designs developed. These provide a strong data base for modeling this technology and the engineering model for the RFQ-2 module in ASM is based primarily upon these machines. Figure 3-1 shows a schematic of an RFQ which indicates selected dimensions and other elements used in developing the RFQ-2 Engineering Vector. The beam dynamics scaling, especially the emittance growth, is based largely upon the work of Wangler, Mills, and Crandall. The scaled default parameters include: (a) a current limit scaling given by Krejick, (b) Kilpatrick limit scaling for the vane potential, (c) and front aperture scaling proportional to the initial $\beta\lambda$. This essentially determines all of the critical parameters so that the RFQ-2 model can cover a wide range of RFQ designs. Key features of this model are:

- Transverse emittance model based on the work of Wangler, Mills, and Crandall,
- Longitudinal emittance model based on envelope equation and energy separatrix,
- Transmission efficiency computed from mismatch factor and user input current limit,
- Power requirements scaled from BEAR RFQ with provision for cryogenic cooling,
- Default values of key input parameters may be scaled from Kilpatrick factor, rf wavelength and injection energy,
- User may select structural material (core tank, end walls and vanes) used in model,
- Reliable RFO-2 Beam Vector for input parameters within guidance limits, and
- Engineering Vector for an RFQ which can produce the predicted Beam Vector.

3.1 RFQ-2 Input Data

RFQ-2 parameter data is input using the Piece Window for the RFQ-2 model, accessed by double clicking the Piece Icon on either the Model Pane or the Workspace Pane of an ASM Document Window. Table 3-1 summarizes the user input for the ASM RFQ-2 model. Figure 3-2 shows the Piece Window used to input this data. "User input" here means either input from the human user, or input (including defaults) generated by ASM when the Use Parameter Scaling option has been selected. The remainder of this section describes the expert rules developed to assist the user in setting up the input for this component. Section 3.2 describes how the inputs are used in compute the Beam Vector for the RFQ-2 model. Section 3.3 describes the modeling of the Engineering Vector for the RFQ. Section 3.4 provides the RFQ-2 model diagnostic parameters, which are

output to the ASM Diagnostics file.

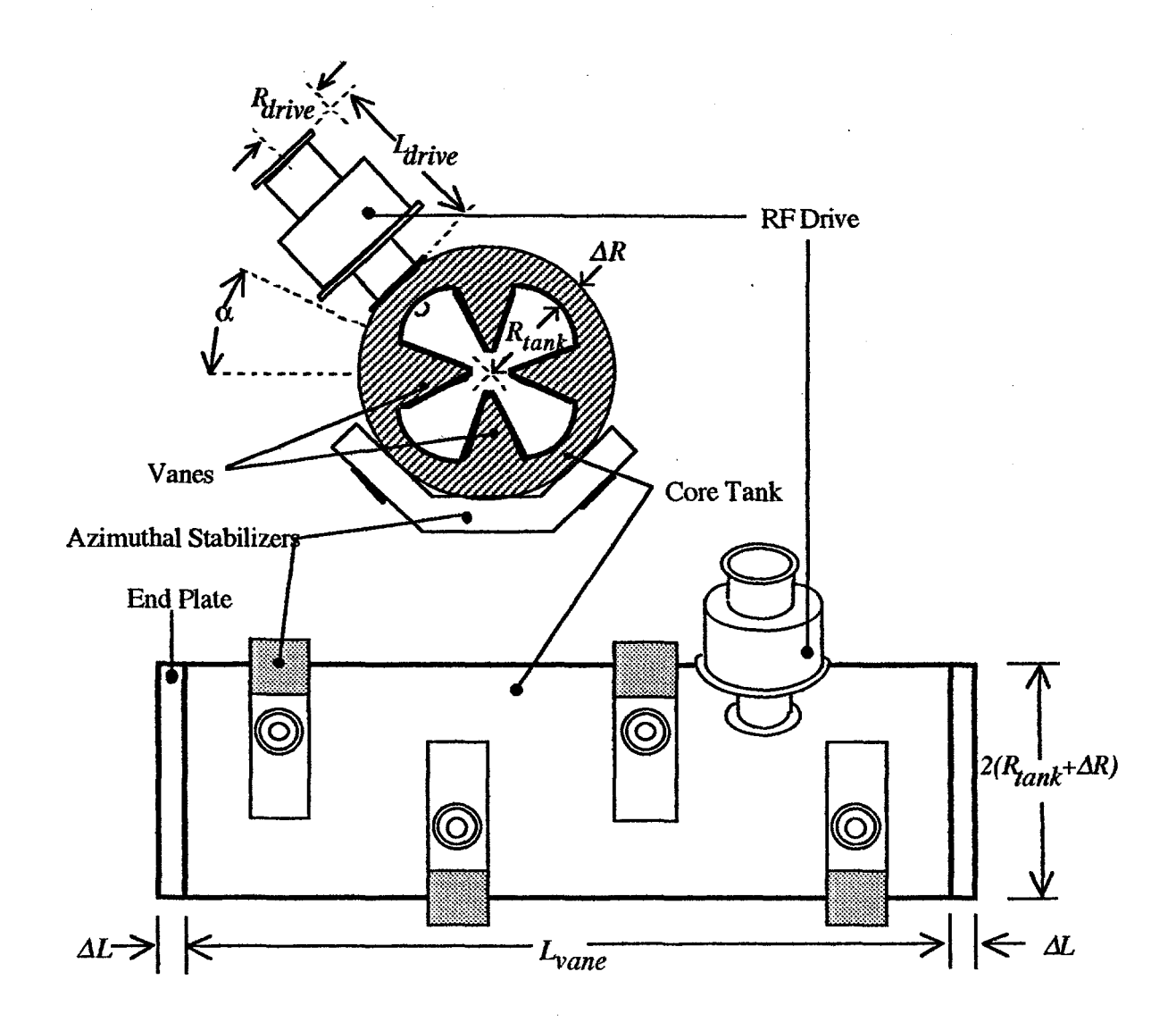


Figure 3-1. Schematic end (top) and side (bottom) views of the concept used for the ASM radiofrequency quadrupole model, RFQ-2. This shows key components and dimensions for computing engineering vector elements.

The first RFQ-2 user input is the RFQ final energy. The default value is 2.5 MeV, based on the 425 MHz GTA RFQ [476]. The lower limit is set to 500 keV and the upper limit is set to 3.5 MeV. The BNL RFQ has a final energy of 750 keV [372] and an RFQ built by ITEP [246,417] has a final energy of 3.0 MeV, so these guidance limits are modest extrapolations beyond RFQs in use on existing accelerators.

Table 3.1 Piece Data Inputs for the Radiofrequency Quadrupole (RFQ-2) Model.

Element Parameters (Symbol)	Default Value*	Default Units	User Guidance Limits Lower Upper		
Output Energy E_{RFQ}	2.5	MeV	0.5	3.5	
Intervane Voltage V_o	1.23×10+5*	volts	1.0×10+4	$1.56 (K_p) E_k(f_1) a_1$	
Final Synchronous Phase ϕ_f	-30	degrees	-45	-20	
Average Aperture Radius (a_1	front) 0.0026*	m	$(\beta_{in}\lambda)/3.8$	$(\beta_{in}\lambda)/1.8$	
Final Vane Modulation Fac m	etor 1.9	(none)	1.2	3.0	
Design Current Limit I_{lim}	0.118*	amps	$0.5c_4(K_p)^2\beta_{in}\lambda$	$1.5c_4(K_p)^2\beta_{in}\lambda$	
Kilpatrick Guidance Limit K_p	1.8	(none)	1.0	3.0 for $df < 0.02$ 2.1 for $df \ge 0.02$	
Quality Enhancement Factor $Q_{e\!f}$	or 1.0*	(none)	0.9 (ambient) 2.0 (cryogenic) 10 (superconducting)	1.1 (ambient) 6.0 (cryogenic) 10 ¹⁰ (superconducting)	
Single Drive Loop Power P_{drive}	100	kW	10	500 for $df < 0.02$ 250 for $df \ge 0.02$	
Structural Material SM_{RFQ}	4 (Cu)	(none)	1 (Be)	5 (Nb)	
Max Coolant Temperature ΔT	Rise (note: 10	this param	neter is not used in ASM 5	version 1.0) 15	

^{*}Denotes an input parameter that can be scaled by ASM with Use Parameter Value Scaling option.

The intervane voltage, and several other RFQ-2 model user inputs, have defaults based on scaling with three key parameters. When the Use Parameter Value Scaling option is selected from the user

guidance limits also scale with these key parameters. The three parameters which drive the scaling are:

- the rf wavelength λ,
- the beam velocity at injection into the RFQ β_{in} , and
- the Kilpatrick factor guidance limit K_p .

The rf wavelength comes from the fundamental frequency f_1 , a Global Parameter:

$$\lambda = c / f_1 = 2.99792 / f_1$$
, (3.1)

The rf wavelength will be in meters since f_1 is in MHz.

The injected beam velocity β_{in} comes from the injection energy of the beam, E_{in} and the particle mass, a Global Parameter. This is given by the first element of the input Beam Vector assigned in the FORTRAN side of ASM, but the FORTRAN may not have been called when this parameter is needed for the Piece Window data. The ASM interface examines the beam line elements preceding the RFQ to determine the injection energy. If the injection energy can not be determined (e.g. no preceding elements on the beam line) then this energy is defaulted to 50 keV.

The Kilpatrick factor guidance limit K_p is itself a user input to the RFQ-2 model. It is discussed further below.

	RFC	12		
Element Parameters	Value Units (Limits	
Output Energy	2.5000	MeV	0.5000	3.5000
Intervane Voltage	1.23E+05	V	10000.0000	1.48E+05
Final Synchronized Phase	-30.0000	deg	-45.0000	-20.0000
Avg. Aperture Radius, front	0.0026	m	0.0019	0.0040
Final Vane Modulation Factor	1.9000		1.2000	3.0000
Design Current Limit	0.1180	Amps	0.0590	0.1770
Kilpatrick Factor	1.8000		1.0000	2.1000
Q-Enhancement Factor	1.0000		0.9000	1.1000
Max. Power of Drive Loop	100.0000	k¥	10.0000	250.0000
Structural Material	Cu 8.92 gm	/cubic cm]	
Max. Coolant Temp. Rise	10.0000	°K	5.0000	15.0000

Figure 3-2. Piece Window for RFQ-2 parameter input

The intervane voltage (V_o) is the second user input. The default value is set in terms of the Kilpatrick field limit:

$$V_o = \kappa(K_p) E_k(f_1) a_1$$
 (3.2)

The Kilpatrick field limit depends on the frequency f_1 and for f_1 in MHz is given by the approximate expression

$$E_k(f_1) = 15.0 (f_1/209.76)^{0.427} \text{ (MV/m)}$$
 (3.3)

In equation (3.2) a_1 is the RFQ front average aperture (after the radial matching section) which is often referred to as r_o . This parameter is also a user input and is discussed below. The scaling coefficient κ appearing in (3.2) is often referred to as the enhancement factor and depends on the details of the vane design. This factor is a function of the ratio of a_1 to the vane tip radius ρ , but in practice is usually restricted to a narrow range between 1.2 and 1.4. Typical results can be found in Ref. [253]. ASM uses the value

$$\kappa = 1.3 \quad , \tag{3.4}$$

so that default value for the intervane potential is

$$V_{o,default} = 1.3(K_p) E_k(f_1) a_1$$
 (3.5)

For the default Global Parameters and 50 keV injection, and the default values for K_p of 1.8 and for a_1 of 2.6 mm, then Equation (3.5) gives a default intervane potential of approximately 123 kV. When the Use Parameter Value Scaling option is selected from the user Preferences menu, and the Used Scaled Value box for the intervane voltage has been checked, the default value for V_o is calculated according to (3.5). Figure 3.4 illustrates the logic flow of the calculations of the default values for a_1, V_o and I_{lim} for the RFQ-2 Model, when the Use Parameter Value Scaling option is selected.

The upper guidance limit to V_o is taken to be 20% higher than the default value, corresponding to an enhancement factor of 1.56 (Table 3.1). The lower guidance limit has been set, somewhat arbitrarily, at 10 kV.

The default value for the final synchronous phase is set to a typical value

$$\phi_{f,default} = -30^{\circ} \quad . \tag{3.6}$$

The lower and upper guidance limits are set to -45° and -20° respectively. In the remainder of this discussion of the RFQ-2 model, it is frequently useful to express the synchronous phase in radians. The notation adopted uses ϕ_s , where $\phi_s = (\pi/180)\phi_f$.

that a_1 is after the radial matching section and is usually the same as r_o , the average aperture, often referred to in the literature. (For some RFQ designs the value of r_o may increase with distance along the RFQ.)

The RFQ-2 default and limit values of the initial average aperture a_1 are taken to be proportional to the basic RFQ cell length at injection which is $\beta_{in}\lambda/2$. A survey of data on RFQs was used to determine the proportionality constant. Selected results of this survey are shown in Figure 3-3. The solid line in the figure provides an estimate for the aperture of low-power RFQs. The coefficient determined from this line is used for the default value of front average aperture radius:

$$a_{1.default} = (\beta_{in}\lambda)/2.8 \quad , \tag{3.7}$$

All of the data displayed in Figure 3-3 fall within 36% of this value for a_1 . The dashed curve provides an estimate for the upper limit of the average aperture. Four RFQs built for the NPB program, which are not displayed in Figure 3.3 (GTA [476], CWDD [346], Boeing [312], and BEAR [366,369]), have values of initial apertures which are somewhat smaller than given by (3.7). These RFQs have points on or slightly above the solid line shown, but are generally within 36% of the value predicted by the solid line. The lower and upper guidance limits for a_1 are taken to be:

$$a_{1,lower} = (\beta_{in}\lambda)/3.8 \quad , \tag{3.8}$$

and

$$a_{1,upper} = (\beta_{in}\lambda)/1.8 \quad . \tag{3.9}$$

It is worth noting that the data shown in Figure 3.3 are for RFQs which span a large spread in frequency, from 25.5 MHz [500] to 473 MHz [499]. These include machines which accelerate ions heavier than those of the hydrogen isotopes. The limit guidelines given by (3.8) and (3.9) should be useful over a broad range of parameters.

The fifth input parameter is the final value of the vane modulation factor, m. ASM uses the default value:

$$m_{default} = 1.9 . (3.10)$$

The lower and upper guidance limits are taken to be 1.2 and 3.0, respectively. The final minimum aperture radius, a_2 , is used in computations in the RFQ-2 model. (It is also a user input for the RFQ-1 model.) The value for final minimum aperture radius, a_2 , is given by Equation (2.216) of Reference [286]:

$$a_2 = 2 a_1 / (m+1)$$
 (3.11)

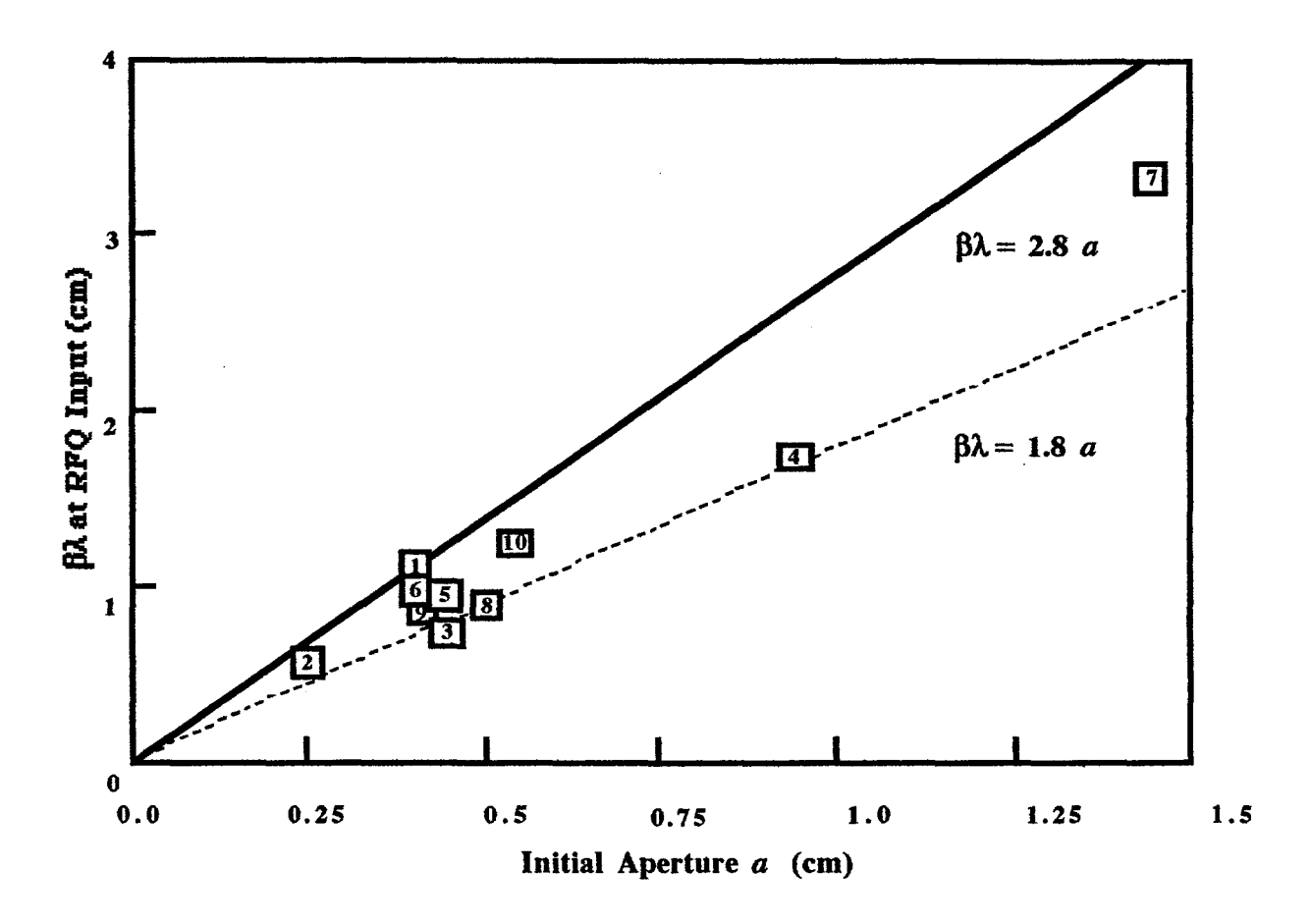


Figure 3-3. Scaling of RFQ initial aperture (a_1) with injection energy (via β) and rf wavelength (λ). Representative data for ten RFQs are shown together the linear fits for the lower aperture limit to the data (solid line) and to the upper aperture limit (dashed lines). Data are for RFQs from: (1) CRNL [253], (2) TAC [499], (3) GSI [498], (4) INS-JHP [500], (5) BNL [372], (6) LANL-ATS [371], (7) LANL-FMIT [393,315], (8) HERA [392], (9) INS-LITL [397], and (10) INS-TALL [397].

The design current limit (I_{lim}) input for the RFQ-2 is used by ASM in modeling beam current transmission. The default and guidance values are based on scaling suggested by Krejcik [340]. He writes the current limit dependence of an RFQ as:

$$I_{lim} \propto (K_p)^2 \lambda (E_{in})^{1/2}$$
 (3.12)

This injection energy (E_{in}) scaling may be rewritten in terms of the corresponding injection velocity (β_{in}) and the default value used for I_{lim} is given by:

$$I_{lim,default} = c_4 (K_p)^2 \beta_{in} \lambda . \qquad (3.13)$$

The value for c_4 is estimated for the GTA RFQ [476]. This gives:

$$c_4 = 5 \text{ Amperes/m} = 5 \times 10^{-3} \text{ Amperes/mm}$$
 (3.14)

The upper guidance limit for I_{lim} is based on an RFQ designed by ITEP. The value for c_4 obtained from the current limit (240 mA) for the ITEP RFQ design [417], together with the Kilpatrick factor estimate of 1.1 for this machine at 185 kV intervane potential [269], is $c_4 = 7$ Amperes/meter. This estimate is 40% above the value given by (3.14). A 50% increase in the value of c_4 is used for the upper guidance limit. The lower guidance limit is set at 50% below the value given by (3.14).

The Kilpatrick factor input K_p is used by the ASM interface to provide user guidance limits for other RFQ-2 input parameter and, as discussed above, for setting the default values for I_{lim} and V_o when the Use Parameter Value Scaling option is selected. The default value for the K_p is set conservatively:

$$K_{p,default} = 1.8 \quad . \tag{3.15}$$

The lower guidance limits for the Kilpatrick factor is taken to be 1.0. The upper guidance limit for K_p depends upon the duty factor, df, a Global Parameter. Specifically:

$$K_{p,upper} = 3.0 \text{ if } df < 0.02 ,$$
 (3.16)

and

$$K_{p,upper} = 2.1$$
 if $df \ge 0.02$. (3.17)

The Q-enhancement factor is used to model RF power efficiency improvements for the RFQ. The default value corresponds to ambient (room temperature) and

$$Q_{ef,default} = 1. (3.18)$$

If the Use Parameter Value Scaling option is selected, this default value depend on the operating temperature regime of the RF accelerator, a Global Parameter. If the Global Parameter corresponding to cryogenic (liquid hydrogen) operation is set, then $Q_{ef,default} = 4$. For the superconducting choice $Q_{ef,default} = 10^9$. The guidance limits for Q_{ef} also depend on the operating temperature regime. The numbers used are given in Table 3.1.

The default value for the maximum power that can be supplied by a single drive loop, P_{drive} , is set to 100 kW, independent of the accelerator duty factor:

$$P_{drive, default} = 100. (3.18)$$

The lower guidance limit has been set to 10 kW, also independent of the duty factor. The upper guidance limit, however, does depend on the duty-factor df (a Global Parameter) and is summarized in Table 3.1.

The last user input for the RFQ-2 model is the permissible temperature rise in the coolant flowing through the RFQ. The default value and limits are shown in Table 3.1 even though this parameter is not used in ASM Version 1.0. The purpose of the parameter is to permit some estimates of the cooling and thermal management system requirements for the RFQ. This parameter is available to user on the FORTRAN side of ASM.

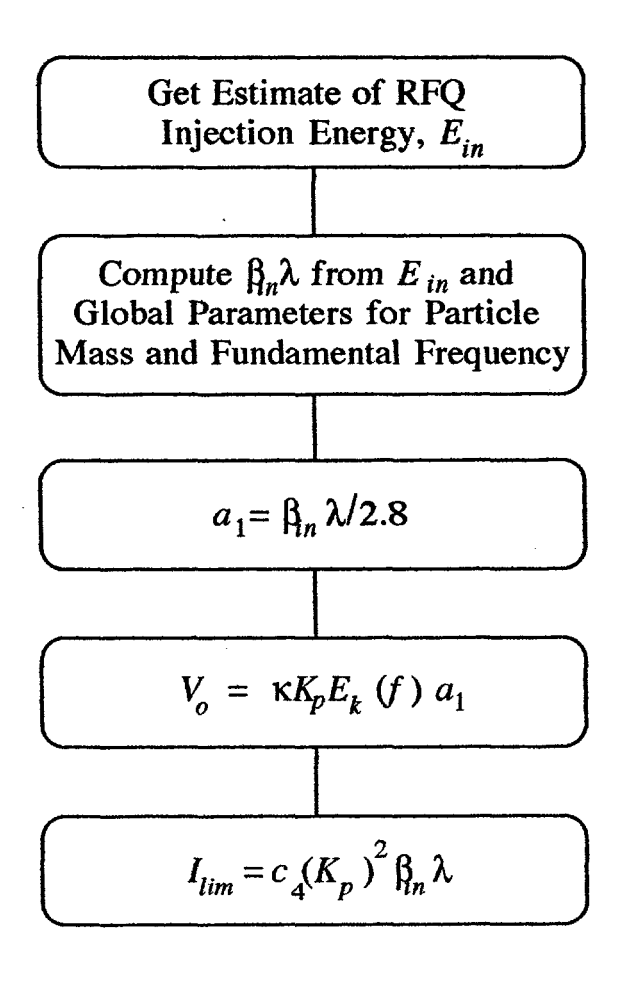


Figure 3-4. Flow Diagram for the Calculation of the Scaling Defaults for the Input Parameters a_1, V_o and I_{lim} for the RFQ-2 Model.

3.2 Beam Vector Model for RFQ-2.

The general form of the Beam Vector matrix equation for the RFQ-2 model is

$$\begin{bmatrix} E_{out} \\ I_{out} \\ < x^{2} >_{out} \\ \varepsilon_{t,out}^{2} \\ < \Delta p^{2} >_{out} \\ \varepsilon_{l,out}^{2} \\ \alpha_{t,out} \\ \alpha_{l,out} \end{bmatrix} = \begin{bmatrix} 1 & 0 & 0 & 0 & 0 & 0 & 0 & 0 \\ 0 & g_{22} & 0 & 0 & 0 & 0 & 0 & 0 \\ 0 & 0 & g_{33} & 0 & 0 & 0 & 0 & 0 \\ 0 & 0 & 0 & g_{44} & 0 & 0 & 0 & 0 \\ 0 & 0 & 0 & 0 & 1 & 0 & 0 & 0 \\ 0 & 0 & 0 & 0 & 0 & 1 & 0 & 0 & 0 \\ 0 & 0 & 0 & 0 & 0 & 0 & g_{77} & 0 \\ 0 & 0 & 0 & 0 & 0 & 0 & 0 & 0 & 1 \end{bmatrix} \begin{bmatrix} E_{in} \\ I_{in} \\ < x^{2} >_{in} \\ \varepsilon_{t,in} \\ < \Delta p^{2} >_{in} \\ \varepsilon_{l,in} \\ \alpha_{t,in} \\ \alpha_{t,in} \\ \alpha_{l,in} \end{bmatrix} + \begin{bmatrix} 0 \\ 0 \\ 0 \\ \Delta \varepsilon_{t}^{2} \\ \Delta \varepsilon_{2}^{2} \\ 0 \\ \Delta \alpha_{\ell} \end{bmatrix}$$

$$(3.22)$$

The subscripts in refer to the input BV, which is from the preceding (LEBT) model, while the subscripts out refer to the output BV which will be passed to the next element of the beam line, either a funnel or a drift tube linac (DTL).

3.2.1. Energy Gain and Beam Current Transmission

The value of g_{11} is simply determined by the RFQ output energy, E_{RFO} , which is a user input:

$$g_{11} = E_{RFQ} / E_{in} {3.23}$$

There is a lower limit to the value for E_{RFQ} , given by $\Delta E_{min} + E_{in}$, where ΔE_{min} is given by Equation (3.76). The matrix element g_{22} in Equation (3.22) describes the attenuation of beam current in the RFQ. The beam current through RFQ-2 is attenuated as a result of losses due to any beam mismatch at the entrance to the RFQ, as well as the inherent losses due to the imperfect bunching process. This is modeled by an effective RFQ transmission efficiency $g_{22} = \eta$:

$$I_{out} = \eta I_{in} \quad , \tag{3.24}$$

where

$$\eta = f_M f_B \quad . \tag{3.25}$$

The fractions f_M and f_B describe beam transmission efficiency after accounting for the losses due to mismatch and bunching respectively. The mismatch attenuation in RFQ-2 is modeled in terms of the mismatch factor, M, for the beam coming into the RFQ. The attenuation is modeled as a linear dependence on M, following the results of Sander's fit to simulations (for M < 3) for the GTA RFO:

$$f_M = 0.97918 - 0.14412M$$
, for $M < 3$. (3.26)

The mismatch factor M is computed from the actual LEBT Twiss parameters, (α_{LEBT} and β_{LEBT}) and the RFQ (design) acceptance Twiss parameters (α_{RFQ} and β_{RFQ}). Specifically (see appendix C of Ref. [168]):

$$M = \left[\frac{1}{2}R + \frac{1}{2}\sqrt{R^2 - 4}\right]^{1/2} - 1 \tag{3.27}$$

where

$$R = \frac{\beta_{RFQ}}{\beta_{LEBT}} \left(1 + \alpha_{LEBT}^{2} \right) + \frac{\beta_{LEBT}}{\beta_{RFQ}} \left(1 + \alpha_{RFQ}^{2} \right) - 2 \alpha_{RFQ} \alpha_{LEBT}$$
(3.28)

(This result uses the identity $\beta \gamma - \alpha^2 = 1$ to reduce R to an expression in terms of only independent Twiss parameters.) For the RFQ-2 model the (design) acceptance Twiss parameters are assigned values based on GTA, typical of high-brightness machines [231]:

$$\alpha_{RFQ} = 2.5 \quad , \tag{3.29}$$

and

$$\beta_{RFQ} = 0.04 \text{ (meters/radian)}$$
 (3.30)

Estimates of the matched Twiss parameters for the RFQ1-1250 of CRNL, from the acceptance diagram [485], give values of about 1.3 and 0.05 m/radian for α_{RFQ} and β_{RFQ} respectively. These Twiss parameters indicate a beam with lower convergence than the values given by (3.29) and (3.30) which may be easier to match in the LEBT. The user may adjust the RFQ match parameters on the FORTRAN side of ASM.

The input LEBT Twiss parameters, α_{LEBT} and β_{LEBT} , come directly from the BV for the preceding LEBT model. The value for α_{LEBT} is

$$\alpha_{LEBT} = \alpha_{t,in} \tag{3.31}$$

whereas β_{LEBT} is computed from using:

$$\beta_{LEBT} = 10^{+1} (\beta \gamma) \langle x^2 \rangle_{in} / (\epsilon_{t,in})$$
 , (3.32)

where the factor 10⁺¹ converts the units to meters/radian.

The expression for f_M predicts a negative value if M > 6.864, which is clearly unphysical. This is a large mismatch factor and the RFQ performance will be severely degraded although we do not have a quantitative prediction of how much. For the region beyond Neushaefer's simulations (for M > 3), we use an exponential dependence, which is matched in value and slope to the linear dependence of Equation (3.26):

$$f_M = 1.206 \exp(-M / 3.794)$$
 , for $M > 3$. (3.33)

The beam current attenuation due to imperfect bunching is anticipated to depend primarily on the ratio of the input beam current, I_{in} , to the RFQ current limit, I_{lim} . This is taken to be of the following form:

$$f_B = \exp(-[I_{in}, /2I_{lim}]^2)$$
 (3.34)

This model for the current attenuation predicts a 92% transmission efficiency for a perfectly matched beam when the input current is one-half of the design current limit. This is typical for the optimum (predicted) performance of vane-type RFQs.

The value for g_{33} appearing in Equation (3.22) is given by Equation (3.65) below.

3.2.2. Transverse Emittance Growth Modeling.

The emittance growth is based on the model of Wangler, Mills, and Crandall [86]. The basic equation describing the emittance growth is:

$$\varepsilon_{t,out}^2 = c_1 \varepsilon_{t,in}^2 + c_2 (\lambda / \sigma_{ot}^{1/3})^2 (I_{lim} / A)^{4/3} . \tag{3.35}$$

The transverse emittance growth terms, g_{44} and $\Delta \varepsilon_t^2$, are then given by:

$$g_{44} = c_1$$
 (3.36)

and

$$\Delta \varepsilon_t^2 = c_2 \left(\lambda / \sigma_{ot}^{1/3} \right)^2 \left(I_{tim} / A \right)^{4/3} \tag{3.37}$$

The constants c_1 and c_2 are taken directly from the work of Wangler, Mills and Crandall [86], noting that $c_2 = a_2/4$ of their work to correspond to the use of rms emittances in ASM:

$$c_1 = 0.95$$
 (3.38)

$$c_2 = 4.0 \times 10^{-3} \text{ (mrad)}^2 / \text{ (Amperes / amu)}^{4/3}$$
 (3.39)

The other parameters include: λ , the rf wavelength (in meters); σ_{or} the zero current transverse phase advance (in radians); I_{lim} , the (theoretical) current limit of the RFQ (a user input); and A, the atomic mass of the beam ions (a global parameter for the Beam Generator Subsystem). The zero-current transverse phase advance is given by [85]:

$$\sigma_{oi} = \left[\frac{\theta_o^4}{8\pi^2} + \Delta_{if} \right]^{1/2} , \qquad (3.40)$$

where

where

$$\theta_o^2 = (\lambda / a_1)^2 \left(eV_o \times 10^{-6} / \gamma_{\min} Am_p c^2 \right)$$
 (3.41)

and

$$\Delta_{rf} = (\pi^2/2) \left(eV_o \times 10^{-6} / \gamma_{\min}^3 Am_p c^2 \right) A_o \sin \phi_s / \beta_{out}^2$$
 (3.42)

Here V_o and ϕ_s are the intervane voltage and final synchronous phase (both user inputs); the factor of 10^{-6} converts the V_o to megavolts (MV). The RFQ acceleration efficiency, A_o , is given below and Am_pc^2 is particle mass (in megavolts), determined from the Global Parameters. The term given by Equation (3.41) corresponds to the rf electric quadrupole focusing, while that given by Equation (3.42) corresponds to the rf transverse defocusing force due to the acceleration (A_o) . The value of γ_{\min} is the usual relativistic energy parameter corresponding the minimum RFQ output energy, given by $\Delta E_{\min} + E_{in}$, where ΔE_{\min} is computed in (3.76). Since this minimum energy is generally less than 1 MeV, we may set $\gamma_{\min} = 1$ without any significant loss of accuracy. In the limit of small rf defocusing (A_o) or $\phi_s \to 0$, Equation (3.40) reduces the approximate result:

$$\sigma_{oi} \cong \frac{1}{\pi} (\lambda / a_1)^2 (eV_o \times 10^{-6} / Am_p c^2) / \sqrt{8}$$
 (3.43)

Note that this differs by a factor of π^1 from that given in [86]. There are constraints on σ_{ot} for stability and practical linac designs. These are discussed is Section 5.3.1.

The user inputs a_1 and m are directly related to the RFQ acceleration efficiency, A_o , and focusing efficiency, B, frequently discussed in the literature. Specifically A_o is given by $(4/\pi)T$ where T is given by Equation (2.215) of Reference [286]. Hence:

$$A_o = [m^2 - 1] / [m^2 I_o(ka_2) + I_o(mka_2)] . (3.44)$$

The wave number parameter k is given by

$$k = 2\pi / \left(\beta_{out}\lambda\right) \quad , \tag{3.45}$$

where β_{out} is final beam velocity (divided by c) at the end of the RFQ, and λ is the rf wavelength (in meters) given in Equation (3.1). A simple power series approximation for the Bessel function $I_o(ka_2)$ is adequate for the range of arguments encountered in the model:

$$I_o(ka_2) \cong 1 + \frac{1}{4}(ka_2)^2 + \frac{1}{64}(ka_2)^4$$
 (3.46)

The value for the acceleration efficiency parameter (A_o) given by Equation (3.44) is the final value at the exit of the RFQ. In the model for the Engineering Vector (RFQ length, etc.) the acceleration efficiency is ramped quadratically to this final value in the model; see Equations (3.73) and (3.76).

The focusing efficiency, B, is obtained by solving

$$(a_2)^2 [B /a^2] + A_o I_o (ka_2) - 1 = 0$$
 (3.47)

This gives for the final value of $B(a = a_2)$ at the exit of the RFQ:

$$B = 1 - A_0 I_0(ka_2) \quad , \tag{3.48}$$

where the value of A_o at the RFQ exit is given by Equation (3.44). This is the same as given by Equation (2.215) of Reference [286] noting that $\kappa = B$ and $A_o = (4/\pi)T$.

3.2.3. Longitudinal Emittance Calculation.

The calculation of the longitudinal emittance for the RFQ-2 model, $\Delta \varepsilon^2$ of equation (3.22), is based on an envelope equation treatment of the longitudinal motion. The RFQ rms longitudinal emittance (in π centimeter milliradians) is given by

$$\Delta \varepsilon_{I}^{2} = \begin{cases} 10^{+10} z^{-2} \left[C_{1} - C_{2} \right], & \text{if } \frac{C_{2}}{C_{1}} < (1 - K_{I}); \\ K_{I} 10^{+10} z^{-2} C_{1}, & \text{if } \frac{C_{2}}{C_{1}} \ge (1 - K_{I}). \end{cases}$$
(3.49)

where z is the rms half-length of the beam bunch (in meters) at the exit of the RFQ. C_1 and C_2 are in units of (radians)² and are discussed below. The C_2 is proportional to beam current, so that the longitudinal emittance decreases with increasing beam current, up to a point determined by K_I . This is consistent with RFQ simulations by Wangler; the value of K_I is based on those simulations:

$$K_I = 0.15$$
 (3.50)

 C_1 depends on the average longitudinal rf focusing at the end of the RFQ.

$$C_{1} = -\frac{3}{4} \left(\frac{eV_{o} \times 10^{-6}}{Am_{p}c^{2}} \right) A_{o} \sin \phi_{s} G (\theta)$$
(3.51)

with

$$G(\theta) = \frac{1}{\theta} \left[\left(\frac{3}{\theta^2} - 1 \right) \sin \theta - \frac{3 \cos \theta}{\theta} \right]$$
 (3.52)

For small values of θ , $G(\theta) = \theta^2 / 15$. The parameter θ is related to the half length of a beam bunch, b in meters, by

$$\theta = \frac{2\pi}{\beta_{out}\lambda} b \tag{3.53}$$

where β_{out} is the relativistic velocity corresponding to final (output) energy of the RFQ (E_{RFQ}). The full length of the beam bunch is taken to be a fraction of the corresponding physical length, z_b , of the separatrix. The fraction is based on comparison with numerical simulations and is taken to be 1/3:

$$b = \frac{1}{3}z_b \tag{3.54}$$

where z_b is given by [389]

$$z_b = \frac{\beta_{out} \lambda}{2\pi} \Phi \tag{3.55}$$

with Φ obtained by solving the transcendental equation [389]:

$$\tan \phi_s = \frac{\sin \Phi - \Phi}{1 - \cos \Phi} \tag{3.56}$$

Here ϕ_s is the final synchronous phase of the RFQ, a user input. When this value is within the acceptable range, a good initial estimate to the solution of (3.56) is $\Phi = -3 \phi_s$. (With this value of Φ , Equations (3.54) and (3.55) reduce to equation (30) of Reference [85].) Equations (3.53)-(3.55) can be combined to relate θ simply to Φ as

$$\theta = \frac{1}{3}\Phi \tag{3.57}$$

The term C_2 depends on the space-charge forces and is proportional to the beam current:

$$C_{2} = 3 \left(\frac{\lambda}{r_{b}}\right) pf\left(p\right) \left(\frac{I_{out}}{I_{m}}\right) , \qquad (3.58)$$

where r_b is the bunch radius, $p = r_b/b$ and f(p) is the ellipsoidal form factor. I_{out} is the output current, obtained from ηI_{in} given in Equation (3.24), and I_m is given by:

$$I_m = A \cdot 3.124 \times 10^7$$
 Amps (3.59)

The ellipsoidal form factor f(p) is [85]:

$$f(p) = \begin{cases} \frac{1}{1-p^2} - \frac{p}{1-p^{-\frac{3}{2}}} \cos^{-1}(p) & \text{, for } p < 1; \\ \frac{p \ln \left[p + \sqrt{p^2 - 1} \right]}{\left(p^2 - 1 \right)^{\frac{3}{2}}} - \frac{1}{p^2 - 1} & \text{, for } p > 1. \end{cases}$$
(3.60)

Near p = 1, $f(p) = (3 p)^{-1}$, so that the limiting value as $p \to 1$ is given by:

$$f(1) = \frac{1}{3} (3.61)$$

The value for the radius of the beam bunch, r_b , is also taken from equations (26)-(28) of Reference [85]:

$$r_{b} = \frac{\left[1 - \frac{\theta_{o}^{2}}{4\pi^{2}}\right]^{1/2}}{\left[1 + \frac{\theta_{o}^{2}}{4\pi^{2}}\right]^{1/2}} a_{2}$$
, (3.62)

where θ_o^2 is given by (3.41) and a_2 is the final aperture radius, a user input. The ratio $p = r_b/b$ is then obtained from (3.54) and (3.62). The value for z used in Equation (3.49) is based on the rms length for an elliptical bunch:

$$z^2 = \frac{1}{5}b^2 \tag{3.63}$$

Equation (3.62) is also used to compute the final rms beam radius out of the RFQ. The relation between the rms radius and the elliptical bunch radius (including the conversion to cm) is:

$$r_{out} = \frac{10^{+2}}{\sqrt{5}} r_b \tag{3.64}$$

so that g_{33} appearing in Equation (3.22) is given by:

T

$$g_{33} = \frac{10^{+4}}{5} \left(\frac{r_b^2}{r_{in}^2} \right) \tag{3.65}$$

h e v a l u e

o f

 Δp^2 , appearing in the Device Vector for the RFQ-2 given in Eq. (3.22), is given by:

$$\Delta p^{2} = 10^{-10} \left[\Delta \varepsilon_{\ell}^{2} / z^{2} \right] \left(A m_{p} c^{2} \right)^{2} . \tag{3.66}$$

The value of $\Delta \varepsilon_l$ (in π -cm-mrad) is given by Eq. (3.49), the value of z (in meters) is given by Eq. (3.63), and $m_p c$ is one amu divided by the speed of light (in MeV/c). The factor of 10^{-10} converts the units so that Δp^2 is (MeV/c)². The value of A appearing in Eq. (3.66) above is the atomic mass of the beam ions (in amu) which is a Global Parameter.

3.2.4. Transverse and Longitudinal α Twiss Parameters.

The seventh and eighth elements of the BV, α_l and α_l , were added to ASM to a provide a basis for enhanced modeling of the beam. This includes the future possibility of transferring data and component models between ASM and other accelerator modeling codes such as TRACE 3-D and PARMILA. Version 1.0 does have detailed modeling of the change in the Twiss parameters as the beam goes through the RFQ. With the exception of the LEBT models in ASM, which use the R-matrix formalism to advance the beam through the component, the α_l and α_l in ASM Version 1.0 are only place holders. Of course, the user may add modeling for the parameters to the FORTRAN part of ASM.

The output values of α_l and α_l for the RFQ-2 model are based on those obtained from TRACE 3-D matched beam calculations for the GTA RFQ. At an x-y symmetry point for the beam near the RFQ exit $\alpha_{l,out} = \alpha_y = -\alpha_x = 1.7$ and $\alpha_{l,out} = 0.04$. These are used to estimate the changes in α_l and α_l as the beam passes through the RFQ. Specifically, the parameters g_{77} and $\Delta\alpha_l$ appearing in Equation (3.22) are taken to be:

$$g_{77} = 1.7/2.5 = 0.68$$
 , (3.67)

and

$$\Delta \alpha_l = 0.04 \quad . \tag{3.68}$$

3.3 RFQ-2 Engineering Vector (EV) Model.

The Engineering Vector for RFQ-2 is of the standard form for ASM:

$$EV = \begin{bmatrix} L \\ V \\ M \\ P \\ x \\ y \\ Conf \\ Cost \end{bmatrix}$$
(3.70)

3.3.1 RFQ-2 Length Calculation

Dimensions and components of the RFQ-2 model are indicated in Figure 3-1. The length of the RFQ is given by:

$$L = L_{vane} + 2 \Delta L \quad . \tag{3.71}$$

The length of the RFQ vane can be calculated by summing the lengths $(\beta \lambda / 2)$ for each of the N cells in the RFQ. Specifically:

$$L_{vane} = \frac{\lambda}{2} \sum_{j=1}^{N} \beta(E_{j}) = \frac{\lambda}{2} N_{1} \beta(E_{in}) + \frac{\lambda}{2} \left[\sum_{j=N_{1}+1}^{N_{2}} \beta(E_{j}) + \sum_{j=N_{2}+1}^{N} \beta(E_{j}) \right]$$
(3.72)

where N is the total number of cells, λ is the wavelength, and E_j is the energy at the jth cell ($E_j = E_{in}$ for $j < N_1$). Here $\beta(E)$ is the relativistic velocity parameter associated with a given energy E. The

parameters N_1 and N_2 correspond approximately to the cell number at the start of the buncher section and the accelerator section, respectively. These two parameters are fixed in ASM, although the user may adjust them on the FORTRAN side of ASM. N_1 and N_2 are discussed further below. The energy E_i at the *j*th cell, for $N_1 \le j < N_2$, is given by

$$E_{j} = E_{in} + \frac{\pi}{4} A_{o} \left(eV_{o} \times 10^{-6} \right) \sum_{k=N_{1}}^{j} \left[\frac{\left(k - N_{1} \right)}{\left(N_{2} - N_{1} \right)} \right]^{2} \cos \phi_{k}$$
(3.73)

whereas for $N_2 \le j \le N$, it is given by

$$E_{j} = E_{in} + \Delta E_{\min} + (j - N_{2}) \frac{\pi}{4} A_{o} \left(eV_{o} \times 10^{-6} \right) \cos \phi_{s}$$
(3.74)

In Equation (3.73) ϕ_k is the synchronous phase. It is modeled as a linear ramp for RFQ cell numbers N_1 to N_2 , going from -90° (i.e. $-\pi/2$ radians) to the final value ϕ_s which is a user input (see Table 3.1). Specifically:

$$\phi_{k} = \begin{cases} -\pi / 2 & \text{for } 0 \le k \le N_{1} \\ -\pi / 2 + \frac{k - N_{1}}{(N_{2} - N_{1})} \left(\frac{\pi}{2} + \phi_{s}\right) & \text{for } N_{1} < k \le N_{2} \\ \phi_{s} & \text{for } k > N_{2} \end{cases}$$
(3.75)

The energy $E_{in} + \Delta E_{min}$ is the energy at the beginning of the acceleration section (cell number N_2); the energy gain to this cell is given by:

$$\Delta E_{\min} = \frac{\pi}{4} A_o \left(eV_o \times 10^{-6} \right) \sum_{k=N_1+1}^{N_2} \left[\frac{k-N_1}{N_2-N_1} \right]^2 \cos \phi_k$$
 (3.76)

The value of N (the last cell number) is then given by:

$$N = N_{2} + \frac{\left(E_{RFQ} - E_{in} - \Delta E_{min}\right)}{\frac{\pi}{4} A_{o} \left(eV_{o} \times 10^{-6}\right) \cos \phi_{s}}$$
(3.77)

In Equations (3.73), (3.74), (3.76) and (3.77) the factor of 10^{-6} multiplying eV_o converts the units to MeV. The minimum RFQ energy, $E_{in} + \Delta E_{min}$, should be less than the RFQ output energy (the user input E_{RFQ}). This minimum RFQ energy is a diagnostic parameter and is printed to the Diagnostic file (see Section 3.4). It should be noted that this model results in a minimum RFQ length, corresponding to the minimum RFQ energy $E_{in} + \Delta E_{min}$. This minimum length is given by:

$$L_{RFQ}(\min) = \frac{\lambda}{2} N_1 \beta(E_{in}) + \frac{\lambda}{2} \sum_{j=N_1+1}^{N_2} \beta(E_j)$$
(3.78)

While this length is not used explicitly in the model, it has been used to determine the fixed values of N_1 and N_2 used in ASM. These values are:

$$N_1 = 10$$
 , (3.79)

and

$$N_2 = 100. (3.80)$$

For RFQs which differ significantly from those used in developing the ASM model, the user may want to adjust the values of these two parameters. This may be the case when certain user inputs are outside the guidance limits indicated in Table 3.1. The values of N_1 and N_2 are set on the FORTRAN side of ASM.

The volume of the RFQ assumes that the core tank is cylindrical with tank radius R_{tank} scaled in proportion to the rf wavelength λ . An examination of a number of vane-type RFQs shows that to within \pm 20%, R_{tank} is given by:

$$R_{tank} = \frac{1}{86} \lambda \tag{3.81}$$

3.3.2 RFQ-2 Volume Calculation

The volume is then given by

$$V_{RFQ} = \pi \left(R_{tank} + \Delta R \right)^2 \left(L_{vane} + 2\Delta L \right) + N_{drive} V_{drive}$$
 (3.82)

where N_{drive} is the number of rf drive loops required and V_{drive} is volume of the drive loop interface to rf power line feeding the RFQ. These are given below.

3.3.3 RFQ-2 Mass Calculation

The mass of the RFQ is computed as the sum of the several individual components. Major elements common to all RFQs include: (a) core tank including two end plates, (b) vanes (four), and (c) RF drive feeds. These are included in the RFQ-2 mass model. In addition, elements such as RF manifolds, cryostats, cooling interfaces and tubing, and others may contribute. The mass for RFQ-2 is taken to be the sum:

$$M = M_{tank} + M_{vanes} + N_{drive} M_{drive} + M_{other} , \qquad (3.83)$$

with M_{tank} , M_{vanes} , M_{drive} and M_{stab} the corresponding component masses. Again N_{drive} is the number of rf drive loops.

For the core tank itself:

$$M_{tank} = \rho \pi L \left[\left(R_{tank} + \Delta R \right)^2 - R_{tank}^2 \right] + 2\rho \pi \left(R_{tank} + \Delta R \right)^2 \Delta L$$

$$\cong 2\pi \ \rho R_{tank} \left[L \ \Delta R \ + R_{tank} \ \Delta L \right] \tag{3.84}$$

where ΔR is this thickness of the core tank and ΔL is the thickness of each of the end plates. Both of these are taken to be equal to the linac structural thickness parameter, ΔR_{linac} , a FORTRAN data parameter. The density, ρ , of the material used in the construction of the core tank is based on the user input SM_{RFQ} (Table 3.1) and is obtained from the same look-up table as used for the Global Structural Material Parameter (Table 0.4). This input will override the ASM Global Parameter used for the linac Structural Material selection (see Table 0.1), so that the RFQ structural mass density can be different from the other components in the linac model.

For the four (4) RFQ vanes, each with a vane half-angle of α , the mass is given approximately by

$$M_{vanes} = 4\rho L_{vane} \left[\frac{1}{4} \left(R_{tank} - a \right)^2 \sin 2\alpha \right] \left[1 + \sec^2 \alpha \right]$$
 (3.85)

Here a is the average bore radius of the RFQ, which is usually small compared to R_{tank} . ODIN 2 uses the value $a = a_1$, the initial aperture radius (a user input). Note that $\alpha < 45^{\circ}$, by definition, and is typically 12-15°. This is a fixed constant in ASM and the value used is $\alpha = 15^{\circ}$.

The estimation of the mass of the core tank and vanes neglects many details in the design including the presence of cooling channels, which would reduce the dry weight of the components. This error in the mass is partially offset by the neglect of any contribution to the mass for other items such as manifolds, fittings and for the coolant input and output.

3.3.4 RFQ-2 Power Calculation

The power, P, required to drive the RFQ is the sum of the beam power and the (wall) losses in the RFO:

$$P = P_{beam} + P_{wall} (3.86)$$

The beam power is given by

$$P_{beam} = I_{out} \left(E_{out} - E_{in} \right) \tag{3.87}$$

where I_{out} , E_{out} and E_{in} are given by the corresponding elements of the RFQ model output and input Beam Vectors.

The resistive losses P_{wall} in the RFQ are computed from a scaling formula normalized to the wall power losses of the BEAR RFQ:

$$P_{wall} = \frac{P_{BEAR}}{Q_{ef}} \left(\frac{V_o}{V_{BEAR}} \right)^2 \left(\frac{\lambda_{BEAR}}{\lambda} \right)^{3/2} \left(\frac{L_{RFQ}}{L_{BEAR}} \right) \left(\frac{a_{BEAR}}{a_2} \right)^{0.3} \tag{3.88}$$

The dependence on the vane voltage, rf wavelength, and RFQ length are the same as discussed by Schempp [400] for the shunt impedance of a broad class of RFQs. Here Q_{ef} is the quality enhancement factor, which is a user input to the RFQ-2 model, and the aperture scaling is based on comparing several vane type RFQs. The BEAR values used for the normalization are given in Table 3.2. Selected examples are also given there showing the wall power losses predicted by Equation (3.88).

Table 3.2. BEAR RFQ Parameters (first line) Used in the RFQ-2 Model Power Calculation. Results Predicted by Equation (3.88), Pwail, for Other Selected RFQs are also Compared with Experimental Power Losses, Pexp.

Laboratory RFQ	Q_{ef}	V _o (volts)	λ (m)	L _{RFQ} (m)	a ₂ (m)	P _{wall} (MW)	P _{exp} (MW)	Ref
LANL BEAR	1	48 x 10 ³	0.7054	1.02	0.0012	0.07	0.07	[369]
LANL GTA	3.2	56 x 10 ³	0.7054	2.80	0.00163	0.075	0.062	[476]
CRNL RFQ1-1250	1	77.4 x 10 ³	1.123	1.47	.0026	0.104	0.135	[253]
GAC CWDD	4	92 x 10 ³	0.8351	3.96	.00257	0.154		[346]

The number of RF drive loops required to power the RFQ is determined by

$$N_{drive} = 10^{+3} \frac{P}{P_{drive}}$$
 (3.89)

where P_{drive} is the maximum power of a single drive loop and interface (window, transmission line, etc.). This is a user input (in kilowatts) and the factor of 10^{+3} is to reconcile the units to those of the total required RFQ power in megawatts from Equation (3.89). It is to be understood that N_{drive} is an integer value, in all cases rounded up to the next highest integer.

At high duty factors (df > .02), the RF drive is modeled after a CW system developed by Grumman Aerospace Corporation (GAC) for operation at 353 and 425 MHz. This is a nominal design for a 250 kW drive loop [319] which has operated successfully at over 100 kW. The dimensions of this drive-loop assembly are:

$$L_{drive} = 0.055 + 0.6df$$
 meters , (3.90)

and

$$R_{drive} = 0.159 \quad \text{meters}$$
 (3.91)

where we have assumed that the length has a linear dependence on df. The volume required by this drive loop assembly is taken to be

$$V_{drive} = \pi R_{drive}^2 L_{drive} \qquad (3.92)$$

This is to be used in Equation (3.82).

The mass of this drive-loop assembly is approximately 40 lbs. (20 kg). It is constructed primarily of copper and stainless steel. A space qualified version of this assembly could probably be light-weighted by using copper-plated aluminum and stainless (or possibly aluminum). ASM scales this mass according to the density of the linac structural material, ρ_{linac} , based on the SM_{linac} Global Parameter rather than the SM_{RFQ} parameter. For low-duty factors, the mass could drop significantly since much of the mass in this CW design is associated with the cooling requirements. A very low duty factor (df \approx .001), uncooled, space qualified aluminum design for the NPBSE is estimated to have a weight of only about 1/2 lb. (1/4 kg). Assuming a linear dependence on the duty factor, then the mass of drive-loop can be approximated as:

$$M_{drive} = \left(\frac{\rho_{linac}}{\rho_{cu}}\right) [1+19df]$$
 kilograms , (3.93)

where $\rho_{cu} = 8.92 \text{ x } 10^3 \text{ kg/m}^3$ is the density of copper.

3.3.5 RFQ-2 Transverse Dimensions

The maximum transverse dimensions from the center line, x and y, for the RFQ model are given by

$$x = R_{tank} + \Delta R \quad , \tag{3.94}$$

and

$$y = R_{tank} + \Delta R + L_{drive} . (3.95)$$

3.3.6 Model Confidence Factor

Several considerations are used in developing the confidence factor for the RFQ-2 model. The modeling of the beam dynamics is based on empirical fits to experimental data and theoretical analyses which are in agreement with simulations and experiments. The engineering data is based upon good conceptual designs and actual hardware. However, most existing RFQs are low duty factor devices. Only two CW machines have been operated. At cryogenic temperatures only the GTA RFQ as been demonstrated and no superconducting RFQs have been built for the parameter regime of interest. Nevertheless, to the extent that most of the inputs to the model fall within the guidance limits, the confidence in the model output is high and suggests that Conf > 0.90. For the input parameters within the specified ranges we have assigned:

$$Conf = 0.95$$
, if $df < 0.02$ and T_{linac} is ambient, and $2 \le SM_{RFQ} \le 4$; (3.96)

$$Conf = 0.90$$
, if $df \ge 0.02$ or T_{linac} is cryogenic, and $2 \le SM_{RFO} \le 4$; (3.97)

$$Conf = 0.50$$
 , if T_{linac} is superconducting or $SM_{RFQ} = 1$ or 5 . (3.98)

This last assignment simply reflects the uncertainty associated with Be or Nb construction. For Nb one is presumably interested in superconducting operation.

3.4 RFQ-2 Diagnostic Parameters

Most of the model output is contained in the Beam and Engineering Vectors. A few parameters are output to other ASM models (Section 3.5). There are certain parameters calculated for internal use in the model which may also be useful for assessing results. This is particularly true when inputs parameters out of the limit ranges are being used. These diagnostic parameters available to the user interface are listed in Table 3.3

3.4.1.(a) Zero-Current Phase Advance Checks.

There is a constraint on σ_{or} , for stable transverse focusing at low (zero) current in the RFQ:

$$\sigma_{ot} \le \pi / 2 \tag{3.100}$$

Since a_1 and/or V_o can be input by the user, this constraint is checked in ASM. If this condition is not satisfied then a comment is written to the Diagnostics file. Note that either a_1 can be increased, or V_o can be reduced, in order to satisfy this stability criterion.

 σ_{ot} is also an interface parameter to the next module (either a funnel or a DTL in ASM) and has a practical lower limit in order for the accelerator to handle high currents:

$$\sigma_{ot} > \pi/9 \quad , \tag{3.101}$$

If this condition is not satisfied then a comment is written to the Diagnostics file.

Similar constraints are checked for the longitudinal phase advance defined by

$$\sigma_{ol} = \left(-2\Delta_{rf}\right)^{1/2} \tag{3.102}$$

where Δ_{rf} is given by Equation (3.42). In this case the user is alerted if σ_{ol} is outside of the bounds given by

$$\pi/18 < \sigma_{ol} \le \pi/2$$
 , (3.103)

then a comment is written to the Diagnostics file.

3.4.1.(b) Length to RF Wavelength Ratio.

The model also computes the RFQ length to RF wavelength ratio (L/λ) . If this ratio exceeds 4 then some form of field stabilization may be required. These could be vane coupling rings, azimuthal stabilizers, or a longitudinal segmentation of the RFQ.

Table 3.3. Diagnostic Parameters for the RFQ-2 Model.

Diagnostic Parameters Symbol (Equation)	Value for Default* Inputs	Default Units	Range* for Lower	Model Validity Upper
LEBT - RFQ Mismatch Fa M (3.27)	ctor 0	(none)	0	3.0
Zero Current Transverse P $(180/\pi)\sigma_{ot}$ (3.40)	hase Advance 61.5	degrees	20	90
Zero Current Longitudinal $(180/\pi)\sigma_{ol}$ (3.102)	Phase Advance 14.9	degrees	10	90
Final Acceleration Efficien A_o (3.44)	cy 0.556	(none)	0.4	0.6
Power Dissipated in RFQ P_{wall} (3.88)	0.544	MW	0.05	1.0
Number of Drive Loop As N_{drive} (3.89)	semblies 8	degrees	1	16
Twice the Initial Cell Leng $(\beta_{in}\lambda)100$ (3.7)	th 0.731	cm	0.28	1.7
Twice the Final Cell Lengt $(\beta_{out}\lambda)100$ (3.55)	h 5.14	cm	1.15	12.9
Total Number of Cells N (3.77)	128	(none)	100	tbd
Length to RF Wavelength (L/λ) (3.72)	Ratio 1.92	(none)	0.5	4
Longitudinal Current Limi I ₁ (3.104)	t 0.162	Amps	tbd	tbd
Transverse Current Limit I_t (3.105)	5.03	Amps	tbd	tbd
Approximate Buncher Ene $E_{in} + \Delta E_{min}$ (3.76)	ergy 1.19	MeV	tbd	E_{RFQ}

^{*}Default values and ranges for model validity are for an H+ beam produced by the ECR source and EMS LEBT. Default values and ranges for model validity will be different for other beams.

3.4.1.(c) Transverse and Longitudinal Current Limit Checks.

There are different transverse and longitudinal current limits in the RFQ. Approximate formulas have been given by Crandall, Stokes, and Wangler [389] for these two limits. From equations (A-5) and (A-6) of Ref. [389]:

$$I_l(\text{Amps}) = (120)^{-1} A_o V_o (-\phi_s)^3 (r_b/\lambda)$$
, (3.104)

and

$$I_t({\rm Amps}) = (90)^{-1} \, \beta_{out}(-\phi_s) (r_b \, / \, \lambda)^2 (A \, 10^{+6} \, m_p c^2) [\sigma_{ot}^{\ 2}] \, / \, [1 - f(p)] \quad , (3.105)$$

where we have noted that $[B^2 + 8\pi^2\Delta]$ of Ref. [389] is the same as $8\pi^2\sigma_{ot}^2$ given by Equation (3.40) here. These values for I_l and I_t are compared with the user input for I_{lim} , and if either one is greater than I_{lim} then a comment is written to the Diagnostics file.

3.5 Interface parameters to and from other ASM models.

Aside from the Beam Vector and Engineering Vector there are only a few RFQ-2 parameters that are needed by other models in ASM. These are the transverse and longitudinal phase advances, σ_{ab} and σ_{ab} given by Equations (3.40) and (3.102), respectively.

3.6 References for the RFO-2 model.

- [85] "Space-Charge Limits in Linear Accelerators," T. Wangler, Los Alamos Technical Paper LA-8388, December 1980.
- [86] "Emittance Growth in Intense Beams," T. Wangler, 1987 IEEE Particle Accelerator Conference, Catalog Number 87CH2387-9, pp. 1006-1010, September 1987.
- [168] "Trace 3-D Documentation," K. Crandall, Los Alamos Document LA-11054-MS, August 1987.
- [231] "GTA Single Beam Injector Design Review," GTA Injector Team, Preliminary/Final Design Review, Los Alamos National Laboratory, January 1989.
- [246] "ISTRA-10 Linear Proton Accelerator Start-Up", by V. A. Andreev, N.V. Lazarev et. al., Proceedings of the 1990 Linear Accelerator Conference, Albuquerque NM, Sept 10-14, LA-12004-C, pp. 782-784, 1990.
- [253] "New Vanes for RFQ-1," B. G. Chidley, F. P. Adams, G. E. McMichael, T. Tran Ngoe and T. S. Bhatia, Proceeding of the 1990 Linac Conference (Albuquerque), LANL Report LA-12004-C, 42-44, 1990.
- [269] "The Launching of a 3 MeV Proton RFQ Linac", by I. M. Kapchinskiy et.al., IEEE Transactions in Nuclear Science NS-30, pp.3579-3581, 1983.

- [286] Theory of Resonance Linear Accelerators, I. M. Kapchinskiy, 398 pages, Harwood Academic Publishers, 1985, ISBN 3-7186-0233-4, [translated from Russian by S. J. Amoretty].
- [312] "Cryogenic Accelerator Development," T. Hayward, Boeing Aerospace Report, D564-10009-1 Revision A, September 1989.
- [315] "RFQ's for the NPB Program: Present and Planned," G. E. McMichael, Proceedings of the First Neutral Particle Beam Technical Symposium (U), Monterey, CA, July 1989.
- [319] "Application of RF Superconductivity to High-Brightness Ion Beam Accelerators," J. R. Delayen, C. L. Bohn and C. T. Roche, presented at the 1990 Linac Conference, Albuquerque, NM, September 10-1, 1990.
- [340] "A Cascaded RFQ Principle for High-Current Beams," P. Krejcik, AIP Conference Proceedings No. 139, pp. 179-183, 1986.
- [346] "Continuous Wave Deuterium Demonstrator Final Design Review," Grumman Space Systems, Grumman Final Design Review, Volume 1, V89-0659-112/RP, May 23-25, 1989.
- [366] "BEAR RFQ Beam Experiment Aboard a Rocket," D. L Schrange, L. M. Young, B. Campbell, J. H. Billen, J. Stovall, F. Martinez, W. Clark, G. Bolme, S. Gibbs, D. King, P. G. O'Shea, and T. Butler, Application of Accelerators in Research and Industry '88 Nuclear Instruments and Methods in Physics Research, B40/41, November 1988.
- [369] "BEAR Project Final Report, Volume 1: Project Summary," BEAR Project Staff, Los Alamos Report LA-11737-MS, Vol., 1, BEAR-DT-7-1, January 1990.
- [371] "Operational Parameters of a 2.0 MeV RFQ Linac," O. R. Sander, F. O. Purser and D. P. Rusthoi, Proceedings of the 1984 Linear Accelerator Conference, GSI-84-11, May 1984.
- [372] "Design, Fabrication, and Testing of the BNL Radio Frequency Quadrupole Accelerator," H. Brown, T. Clifford, S. Giordano, F. Khiari, R. McKenzie-Wilson, M. Puglisi and P. Warner, Proceedings of the 1984 Linear Accelerator Conference, GSI-84-11, May 1984.
- [389] "RF Quadrupole Beam Dynamics Design Studies," K. Crandall, R. Stokes and T. Wangler, Proceedings of the 1979 Linear Accelerator Conference, BNL-51134, September 1979.
- [391] "Accelerator Technology Development Program Status Report," J. Sredniawski, Grumman Space Systems Report MV89-0659-1001JS, May 1989.
- [392] "Status of the HERA-RFQ Injector," A. Schempp, H. Klein, P. Schastok, K. Pape and S. Wang, 1986 Linear Accelerator Conference Proceedings, SLAC-303, CONF-860629 UC-28(M), June 1986.
- [393] "CW Operation of the FMIT RFQ Accelerator," W. Cornelius, Nuclear Instruments and Methods in Physics Research, B10/11, November 1985.

- [397] "RFQ Work at INS," N. Tokuda, American Institute of Physics Conference Proceedings 139, High Current, High Brightness, and High Duty Factor Ion Injectors, ISBN 0-88318-338-2, 1986.
- [400] "Recent Progress in RFQs," A. Schempp, 1988 Linear Accelerator Conference Proceedings, Continuous Electron Beam Accelerating Facility, CEBAF-Report-89-001, June 1989.
- [417] "The Pulsed Proton Prototype of a High Current Ion Linac", by R. Vengrov, E. Daniltsev, I. Kapchinskij, A. Kozodaev, V. Kushin, N. Lazarev, A. Nikitin and I. Chuvilo, Proceedings of the 1981 Linear Accelerator Conference, LA-9234-C, pp.92-95, October 1981.
- [476] "Commissioning the GTA Accelerator," O. R. Sander, et al, Proceedings of the 1992 Linear Accelerator Conference, Ottawa, Canada, AECL-10728, Vol. 2, pp 535-539, 1992.
- [485] "High-Current Direct Injection to a CW RFQ Using an ECR Proton Source," G. M. Arbique, T. Taylor, A. D. Davidson and J. S. C. Wills, 1992 Linear Accelerator Conference Proceedings, 52-54, 1992.
- [498] "Properties of the GSI HLI-RFQ Structure," J. Friedrich, A. Schempp, H. Deitinghoff, U. Bessler, H. Klein and R. Veith, Proceedings of the IEEE Particle Accelerator Conference, San Francisco, CA, May 6-9, 1991, pp. 3044-3046, 1991.
- [499] "Progress of the 473 MHz Four-Rod RFQ," R. Kazimi, F. R. Huson and W. W. MacKay, Proceedings of the IEEE Particle Accelerator Conference, San Francisco, CA, May 6-9, 1991, pp. 3050-3052, 1991.
- [500] "RF Tests on the INS 25.5-MHz Split Coaxial RFQ," S. Shibuya, S. Arai, A. Imanishi, T. Morimoto, E. Tojyo and N. Tokuda, Proceedings of the 1990 Linear Accelerator Conference, Albuquerque, NM, LA-12004-C, pp 207-209, 1990.

4. ASM Electromagnetic Quadrupole (EMQ) Model (for use in TFE routines)

4.0. ASM EMQ Model Overview and Formulae

Figure 4-1 displays the geometry and identifies the parameters of a single EMQ lens as used in the ASM quadrupole lattice Transverse Focusing Element (TFE) module [1]. The EMQ model closely follows that developed by Liska [2,3].

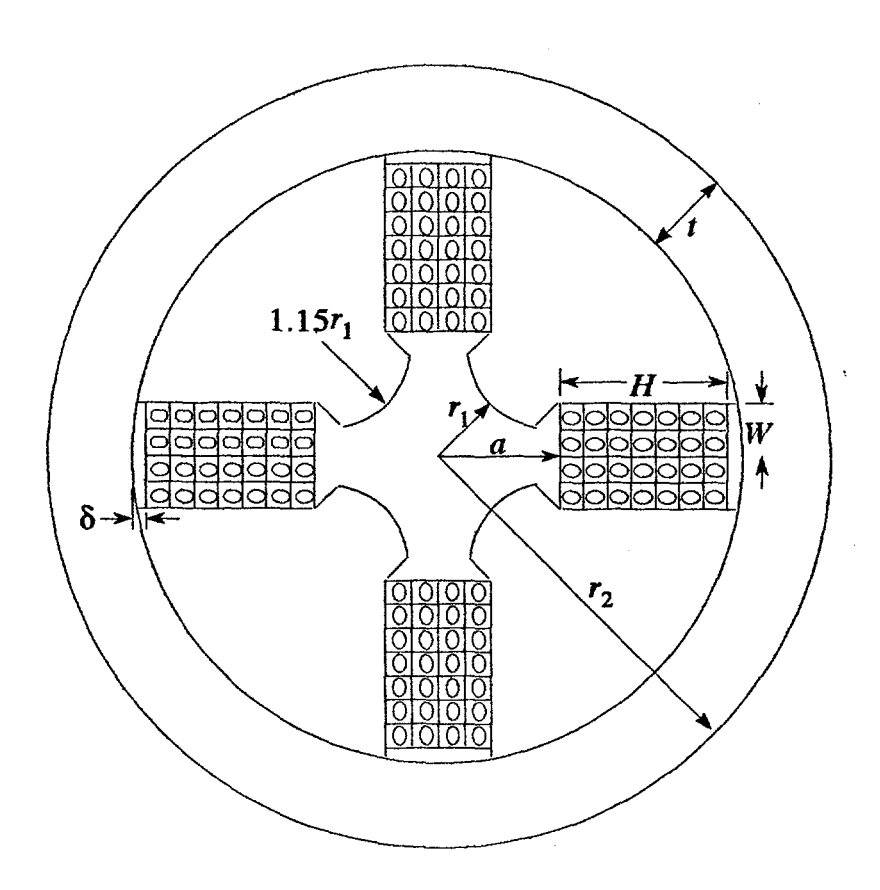


Figure 4-1. Cross sectional representation of the EMQ used in the ASM Quadrupole Lattice Transverse Focusing Element (TFE) Model.

Table III.12.1 of Reference [1] shows the inputs for the Transverse Focusing Element (TFE) module. For the EMQ model, only the quadrupole bore radius, r_1 , the quadrupole outer radius, r_2 , and the wavelength, λ , are used. The ASM TFE module calculates the individual quadrupole length, l. The value of l is used as well for the engineering model of the EMQ.

In order to calculate the maximum gradient, the EMQ can produce, the parameters associated with the coils must first be established. The coils that wrap the steel pole pieces are constrained to fit within the poles of the magnet. The size of the coil is approximated here to be the largest possible coil configuration. The coil dimensions are represented by the stack height,

ASM Electro-Magnetic Quadrupole (EMQ) GHGA-93-392-R

H, and the stack width, W. Figure 4-1 shows the coil dimensions. The shape of the pole tip are as prescribed. Table 4.1 shows the constants that are used in this model.

Constant	Value	Units	Definition
w_c	3.665x10 ⁻³	m	width of square coil wire
$ ho_{cu}$	8.90×10^3	kg/m ³	density of copper
$ ho_{H_2O}$	$1x10^{3}$	kg/m ³	density of water
j_{max}	$3x10^{7}$	A/m ²	maximum current density in wi
μ_o	$4\pi x 10^{-6}$	kGm/A	magnetic permeability
$ ho_{stl}$	2.88×10^3	kg/m ³	density of steel
ϕ_c	1.72x10 ⁻⁸	Ω m	resistivity of copper at 20° C

Table 4.1 Constants for EMQ Model

Halbach suggests that the radius of curvature be 1.15 times the aperture radius, and that the width of the pole be such that it subtends a ± 30 degree angle at the center of the aperture. The stack height can be approximated by subtracting the yolk thickness, t, the coil face to aperture center distance, a, and the gap space, δ , from the outer radius of the quadrupole. Such that

$$H = r_2 - t - a - \delta$$
 [m] (4.1)

The gap space, δ , can be expressed from the geometry as

$$\delta = (r_2 - t) - \sqrt{(r_2 - t)^2 - (N_w W_c)^2} \quad [m] \quad , \tag{4.2}$$

where N_w is the width number and W_c is the square wire dimension. Substitution into (4.1) leads to

$$H = \sqrt{(r_2 - t)^2 - (N_w W_c)^2} - a \quad [m]$$
 (4.3)

The distance from the center of the aperture to the coil face, a, is also a function of the stack width, or rather the width number, N_w . From geometric considerations of the pole shape, a can be given by

$$a = 1.14r_I + N_w W_c / \sqrt{2}$$
 [m] , (4.4)

Finally, the yolk thickness, t, can be determined by requiring the yolk thickness to be such that the flux density in the yolk is half of the flux density on the pole tips plus 50 percent for return flux from the end fields. Thus t can be expressed as

$$t = 1.18 B_{pt} r_1 / B_y$$
 [m], (4.5)

where B_{pt} is the pole tip field and B_y is the yolk field. B_y is generally assumed to be half of the maximum pole tip field, 5 kG.

The number of windings that will fit in the stack height, H, is defined as the height number, N_H . The height number is given by

$$N_H = H/W_c \quad . \tag{4.6}$$

The total number of windings around a single pole is N. N is given by

$$N = N_H N_w = \frac{N_w}{W_c} \sqrt{(r_2 - t)^2 - (N_w W_c)^2} - a$$
(4.7)

The pole tip field can be determined from

$$B_{pt} = \frac{2\mu_o NI_{\text{max}}}{r_1}$$
 [kG]

where μ_o is the magnetic permeability,

$$\mu_o = 4\pi \times 10^{-6} \text{ [kGmA}^{-1]}$$
 , (4.9)

and I_{max} is the maximum current that the coil conductor can carry. Based on an analysis of commercially available hollow copper wire by Liska, et al [3] at the Los Alamos National Laboratory, they concluded that the square 3.665 mm Anaconda wire was the best suited for small EMQ's. The cross sectional area of copper and cooling channel in this wire is approximately the same, hence the current carrying area, A_{cu} , of the wire is half of the wire's cross sectional area, $6.72 \times 10^{-6} \, \mathrm{m}^2$. The typical maximum allowable current density for water cooled copper wire, j_{max} , is $3 \times 10^{7} \, \mathrm{A/m}^2$. Thus the maximum current in the wire, I_{max} , is $j_{max}A_{cu} = 201 \, \mathrm{A}$.

Equations (4.7) and (4.8) give for the pole tip field for the EMQ

$$B_{pt} = \frac{2\mu_o I_{\text{max}}}{r_1} \left(\frac{N_w}{W_c} \sqrt{(r_2 - t)^2 - (N_w W_c)^2} - a \right) \quad \text{[kG]}$$
(4.10)

Substituting (4.4) and (4.5) for ta and t and solving for $B_{pt}(N_W)$ we find

$$B_{pl}(N_{w}) = \frac{-\theta + \sqrt{\theta^{2} - 4\Sigma\Gamma}}{2\Sigma} \quad [kG]$$
(4.11)

where

$$\Sigma = \left(\frac{w_c r_i}{2\mu_o I_{\text{max}} N_w}\right)^2 - \left(\frac{1.18 r_i}{B_y}\right)^2$$

$$\theta = \frac{\left(1.14 \, r_1 + N_w \, W_c / \sqrt{2}\right) \, W_c \, r_1}{\mu_o \, I_{\text{max}} N_w} + \frac{2.36 \, r_1 \, r_2}{B_y}$$

and

$$\Gamma = (1.14 r_1 + N_w W_c / \sqrt{2})^2 + (N_w W_c)^2 - r_2^2$$

If the gap distance, δ , is neglected in the derivation of $B_{nl}(N_W)$ then a simpler formula is achieved.

$$B_{pt}(N_w) = \frac{r_2 - 1.14r_1 - N_w W_c / \sqrt{2}}{\frac{W_c}{N_w} \frac{r_1}{2\mu_o I_{\text{max}}} + \frac{1.18 r_1}{B_y}}$$
 [kG]

This can be differentiated and solved for N_W when $dB_{pl}/dN_w = 0$. Solving for N_W gives the width number that will achieve the greatest pole tip field. The width number for the maximum pole tip field can be shown to be

$$N_{w \max} = \frac{\frac{-W_c}{2\mu_o I_{\max}} + \sqrt{\frac{W_c^2}{4\mu_o^2 I_{\max}^2} + \frac{1.18(r_2 - 1.14 r_1)}{B_y \sqrt{2} \mu_o I_{\max}}}}{\frac{1.18}{B_y}}$$
(4.13)

The pole tip field that is found by (4.11) is artificially large because when equation (4.7) was substituted into (4.8) the value for N_H from (4.6) was not an integer number. This allows for the winding height to be a fraction of a winding larger, thus allowing more ampere turns to encompass the pole and artificially enlarge the maximum pole tip field. Therefore, the magnetic field B_{pt} found in (4.11) is only used in (4.5) to calculate the yolk thickness. Once the yolk thickness, t, is found it can be used in (4.3) to find the stack height, H. With H known, division by the wire size and truncation of the decimal part yields the integer height number, N_H . The product of the height

ASM Electro-Magnetic Quadrupole (EMQ) GHGA-93-392-R

number, N_H , and the width number, N_W , is the total number of windings around the pole tip, N. Now the pole tip field, B_{pt} , may be determined by (4.8). Finally, the gradient can be calculated by

$$G = B_{pt} / r_1$$
. [kG/m] . (4.14)

This is the maximum gradient achievable in a magnet of given dimensions r_1 and r_2 .

4.1. EMQ Engineering Model

After the length, *l.*, has been determined by the quadrupole lattice TFE module in ASM, the engineering parameters of the EMQ can be calculated.

The total length of the wire required for the quadrupole and the feed wires to the quadrupole is

$$L_w = 4 N [2l. + \pi (a + H/2)] + \lambda + 0.6$$
 [m] . (4.15)

The wavelength, λ , is included in the equation for wire length to estimate the feed length and is calculated from the frequency (f in MHz) associated with the ASM component (Funnel, DTL, etc.) which is calling the TFE module:

$$\lambda = c/f \text{ [m]} , \qquad (4.16)$$

where $c = 299.792 \text{ m/}\mu\text{sec.}$

The total mass of the EMQ can be given by

$$M_Q = M_y + M_p + M_{cu} + M_w$$
 [kg] , (4.17)

where M_y is the mass of the yolk, M_p is the mass of the poles and M_{cu} is the mass of the copper windings and M_w is the mass of the water in the windings.

The mass of the yolk, M_{ν} can be determined by

$$M_{y} = \rho_{st} \pi \ell \left(2 r_{2} t - t^{2} \right) \quad [kg]$$

$$\tag{4.18}$$

The mass of the four poles is

$$M_{p} = \rho_{st} (\ell - 2N_{w}W_{c}) \pi (r_{2} - t - r_{1})^{2} \text{ [kg]}$$
(4.19)

and the mass of the windings is

$$M_{cu} = 0.5 \rho_{cu} L_w W_c^2$$
 [kg] . (4.20)

The mass of the water in the windings is

$$M_{w} = 0.5 \rho_{w} L_{w} W_{c}^{2}.$$
 [kg] . (4.21)

Knowing the length of the wire, L_w , then the power required for the EMQ can be determined. The Power, P, is from heating so the power loss is I^2R . Thus, the power may be determined by

$$P = \frac{\phi_c}{.5W_c^2} I_{\text{max}}^2 L_w \quad \text{[watts]}$$
, (4.22)

where ϕ_c is the resistivity of copper at 20° C, $\phi_c = 1.77 \times 10^{-8} \Omega m$.

The power supply for the quadrupole magnets is pulsed or DC (not RF), according to the duty factor of the accelerator. Equation (4.22) gives the peak power required; the duty factor dependence is modeled at the accelerator system model in ASM.

This completes the specification of the EMQ as implemented in ASM Version 1.0. However, formulas for other EMQ engineering parameters have been derived which would be useful for an improved ASM model. The formulas provide the voltage required for the power supply to drive an individual EMS and estimates of key parameters for the water cooling of the EMQs. These results are summarized below:

From Ohm's law, the voltage required for the EMQ is

$$V = P/I_{max}$$
.

or

$$V = \frac{\phi_c}{.5W_c^2} I_{\text{max}} L_w \quad \text{[volts]}$$
(4.23)

Once the power dissipation is calculated, the cooling requirements can be determined. The rate of water required to cool the windings can be determined from

$$\dot{m} = \frac{P}{c\Delta T} \tag{4.24}$$

where c is the specific heat of water. After unit conversion,

$$\dot{m} = 3.788 \times 10^{-3} - \frac{3P}{\Delta T}$$
 [gallons/min] (4.25)

where P is the power from (4.22) and ΔT is the temperature drop, typically 30° C.

ASM Electro-Magnetic Quadrupole (EMQ) GHGA-93-392-R

The velocity of water, ν , is given by

$$v = \frac{2.070 \times 10^{-4}}{N_F} \frac{\dot{m}}{.5 W_c}$$
 [ft/s] , (4.26)

where N_F is the number of feeds to the quadrupole which is normally 2.

The pressure drop given by Steffan [4], and modified for ASM parameters, is

$$\Delta_p = 7.9 \times 10^{-5} \frac{Lw}{N_F} \frac{(v)^{175}}{(.5 W_c)^{.625}} \quad [psi]$$
(4.27)

4.3. References for EMQ Model

- [1] "Physics and Engineering Models for the Beam Generator Subsystem of the ODIN 2 NPB Platform Scaling Code," George. H. Gillespie, Barrey W. Hill, John L. Orthel and Lawrence A. Wright, G. H. Gillespie Associates, Inc. Report No. GHGA-91-254-R, September 1991.
- [2] "Progress Toward Scaling and Optimization Criteria for High-Intensity, Low-Beam Loss RF Linacs," G. P. Boicourt, N. Bultman, R. W. Garnett, R. A. Jameson, T. H. Larkin, D. J. Liska, J. L. Merson, S. Nath, G. H. Neuschaefer, J. D. Sherman and T. P. Wangler, Los Alamos National Laboratory Report No. LA-CP-92-221, July 1992.
- [3] Personal communication, D. J. Liska, 1993.
- [4] High Energy Beam Optics, K. G. Steffan (Wiley, New York), 211 pages, 1965.